COMBINED BACTERICIDAL/BACTERIAL ADHESION-RESISTANT COATINGS THROUGH NITRIC OXIDE RELEASE

Wesley Langdon Storm

A dissertation submitted to the faculty of the University of North Carolina at Chapel Hill in partial fulfillment of the requirements for the degree of Doctor of Philosophy in the Department of Chemistry (Analytical Chemistry)

Chapel Hill
2013

Approved by:

Mark Schoenfisch

James Jorgenson

James Cahoon

Matthew Lockett

Alexander Miller

ABSTRACT

Wesley Langdon Storm: Combined Bactericidal/Bacterial Adhesion-Resistant Coatings through Nitric Oxide Release

(Under the direction of Mark H. Schoenfisch)

In response to the health and economic burdens associated with implant-related infections, researchers have developed coatings that resist bacterial adhesion and/or kill bacteria. Herein, the synthesis of coatings that release nitric oxide (NO) to inhibit bacterial adhesion and kill bacteria are described.

In order to expand the clinical utility of NO-releasing surfaces, xerogels were synthesized from *N*-diazeniumdiolate-modified silane precursors. Release kinetics and totals were tunable through careful selection of the silane precursor and its concentration, respectively. To demonstrate the versatility of this approach, NO-releasing xerogels were cast as outer membrane on glucose sensors. The sensors exhibited a linear response towards glucose and maintained glucose sensitivity in phosphate buffered saline for up to one week.

"Active" and "passive" antimicrobial surface approaches were combined by synthesizing NO-releasing superhydrophobic xerogels. These reduced viable adhesion of *Pseudomonas aeruginosa* by two orders of magnitude. Release of NO conferred biocidal properties to the coating, while superhydrophobicity reduced bacterial adhesion. Furthermore, the superhydrophobic coatings were also used to extend drug release rates.

The release of two antibacterial agents simultaneously (silver and NO) was pursued as a strategy for enhancing bacterial killing. To this end, xerogels were synthesized that released silver and NO at doses sufficient to kill *Pseudomonas aeruginosa* and *Staphylococcus aureus*. Confocal microscopy experiments revealed that NO primarily operated by reducing bacterial adhesion, while silver actively killed bacteria. Together, the two agents killed bacteria more effectively than either agent alone.

Poly(amido amine) dendrimers that release NO were used as dopants within polyurethane dispersions to make films and electrospun fibers. The NO flux from these materials could be tuned for antimicrobial or wound-healing purposes. Independent tuning of NO-release and hydrophobicity through multiple surface modifiers was used to minimize leaching of the dendrimers from polyurethane fibers while extending their NO-release duration.

To Tabitha and Tara,

for keeping my heart, mind, world and soul afloat.

ACKNOWLEDGEMENTS

The work presented in this dissertation was only possible with the help of many colleagues, friends, and family members. First, I'd like to thank my advisor, Mark Schoenfisch, for helping me grow as a scientist and person, for providing professional and personal support, and for always accommodating my unexpected fatherhood-related schedule changes without complaint.

I would also like to give special thanks to some particular graduate students in the Schoenfisch lab who have given much of their time and effort to help me succeed—Justin Johnson for synthesizing thousands of silver-releasing xerogels, Katey Reighard for carrying out countless bacteria assays in the superhydrophobic/NO project, Danielle Slomberg for helping with confocal microscopy, Robert Soto for synthesizing electrospun fibers, and Brittany Worley for doing—at some point over this final year—every conceivable laboratory task that I can possibly think of at the moment. I'm lucky to consider all of you friends as well as colleagues. I would also like to thank some of my other lab colleagues, namely Jonghae Youn and Professor Jae Ho Shin, for their help and guidance in the superhydrophobic/NO project.

The friends I've made in graduate school have made each day a little brighter: Peter Coneski, BJ Privett, Scott Nichols, Ahyeon Koh, Chris Backlund, Rebecca Hunter, and Angela Broadnax. Thank you all. I would like to give a special acknowledgement to Dan Riccio and Alexis Carpenter for not only being great friends, but for also being great

mentors. Both of you were a source of inspiration to me long after your defense dates. Most of all, I thank both of you for always believing in me.

I've also had the pleasure of working with a number of great undergraduate students. Hetali Lodaya developed many superhydrophobic materials that were not included in this dissertation, Shalini Chudasama helped in the early stages of the NO-releasing dendrimer/polyurethane project, and Chris Chouinard helped me operate the ICP-OES when it was first purchased. As the cliché goes, I learned more from each of you than you probably ever learned from me. Thank you for giving me the opportunity to work with you.

Most of all, I'd like to thank my family: my parents, for their unconditional love and encouragement, my wife Tabitha for her unending support, and my daughter Tara for always giving me a reason to smile. I love you all.

TABLE OF CONTENTS

LIST OF TABLES

LIST OF FIGURES

LIST OF SCHEMES

LIST OF ABBREVIATIONS AND SYMBOLS

^{o}C	degree(s) Celcius
~	approximately
%	percentage
[…]	concentration
ε	molar absorptivity
λ	wavelength
17FTMS	(heptadecafluoro-1,1,2,2-tetrahydrodecyl)-trimethoxysilane
3D	three-dimensional
μL	microliter(s)
μM	micromolar
ACN	acrylonitrile
AEAP	*N*-2-(aminoethyl)-aminopropyltrimethoxysilane
AEAP/NO	*N*-diazeniumdiolate-modified *N*-2-(aminoethyl)-aminopropyltrimethoxysilane
AFM	atomic force microscope
Ag^{+}	silver ion
$AgNO_3$	silver nitrate
AHAP	*N*-(6-aminohexyl) aminopropyltrimethoxysilane
BP	bandpass
BTMOS	isobutyltrimethoxysilane
cfu	colony forming units
d	day(s)
DMEM	Dulbecco's modified essential media
DMF	dimethylformamide

e.g.	*exemplia grata* (for example)
et al.	and others
EAiB	*N*-ethylaminoisobutyltrimethoxysilane
EAiB/NO	*N*-diazeniumdiolate-modified *N*-ethylaminoisobutyltrimethoxysilane
ED	1, 2-epoxy-9-decene
ETMOS	ethyltrimethoxysilane
FBS	fetal bovine serum
FDA	United States Food and Drug Administration
G4	generation 4
h	hour(s)
H_20	water
HCl	hydrochloric acid
i.e.	*id est* (in other words)
iNOS	inducible nitric oxide synthase
M	molar
MΩ	Megaohm(s)
MAP	*N*-methylaminopropyltrimethoxysilane
MAP/NO	*N*-diazeniumdiolate-modified *N*-methylaminopropyltrimethoxysilane
MTMOS	methyltrimethoxysilane
mM	millimolar
min	minute(s)
mg	milligram(s)
mL	milliliter(s)
mm	millimeter(s)
MTMOS	methyltrimethoxysilane

MTS	4,5-dimethylthiazol-2-yl)-5-(3-carboxymethoxyphenyl)-2-(4-sulfophenyl)-2H-tetrazolium
NaOMe	sodium methoxide
nm	nanometer(s)
NO	nitric oxide
N_2	nitrogen gas
O_3	ozone
P. aeruginosa	*Pseudomonas aeruginosa*
PBS	phosphate buffered saline
pH	-log of proton concentration
PI	propidium iodide
PMS	phenazine methosulfate
ppb	parts per billion
ppm	parts per million
PTMOS	propyltrimethoxysilane
PMMA	poly (methyl methacrylate)
PROLI/NO	disodium 1-[2-(Carboxylato)pyrrolidin-1-yl]diazen-1-ium-1,2-diolate (1)
PVC	poly (vinyl chloride)
rpm	revolutions per minute
s	second(s)
S. aureus	*Staphylococcus aureus*
S. epidermidis	*Staphylococcus epidermidis*
SSD	silver sulfadiazene
SEM	scanning electron microscope
SN-38	7-Ethyl-10-hydroxy-camptothecin

SO	styrene oxide
t	time
THF	tetrahydrofuran
TP470	tecoplast tp-470-00
TPU	tecophilic sg-80a
TSA	tryptic soy agar
TSB	tryptic soy broth
UV	ultraviolet

Chapter 1:

The Development of Antifouling and Biocidal Coatings for Biomedical Implants

The advent of modern biomaterials research began when clinicians serendipitously discovered that certain polymers (e.g., poly(methyl methacrylate) canopies "implanted" into the eyes of fighter jet pilots via machinegun fire) evoked a favorable healing response when compared to other materials.[1] As the scientific understanding of molecular biology and materials science has grown, researchers have studied the processes governing the tissue biocompatibility of implants. Given the seemingly endless combination of polymer chemistries, 3D-architectures and mechanical properties that have been developed, it is best to categorize these materials by their function rather than their form. A clear delineation in function appears between two types of biomaterials: 1) implantable *devices*, where the material in-and-of-itself is the purpose of the implant (e.g., prosthetic joints, catheters, stints, engineered tissue scaffolds, drug-release reservoirs, etc.); and, 2) device *coatings*, where the biomaterial serves as a companion to an existing implant to improve its utility. This introductory chapter focuses on the latter, specifically coatings that reduce bacterial adhesion or kill bacteria on implanted materials.

1.1 Microbial colonization on medical devices

Implanted medical devices are widespread in clinical care. Unfortunately, many devices cause infections which result in massive economic and health costs. Urinary and central venous catheters, pacemakers, and prosthetics are all prone to bacterial colonization,

with infection rates ranging from 1—20% depending on the implant type as well as the expertise of the surgical staff performing the procedure.[2, 3] At worst, bacterial colonization on an implanted material may lead to life-threatening infections.[4] In milder cases, the presence of bacteria on a surface discourages successful integration of the device into native tissue, necessitating device removal.[5,6] These episodes are costly; for instance, the expense of arthoplasty infections exceed >$50,000 per case and extend average hospital stays by an average of 11 days.[3,7] Mechanisms to reduce the incidence of infection on implanted devices are greatly needed.

The critical density of bacteria required to infect an implant is much lower than the amount required when an implant is absent.[2] This discrepancy arises from bacteria's ability to adhere readily to surfaces. Furthermore, surgical implantation procedures themselves cause inflammation and a localized immuno-incompetent zone, weakening the natural response of the host to microbes introduced during surgery.[5] The weakened host response is evident from the vast number of implant infections caused by *Staphylococcus epidermidis;* in normal tissue, *S. epidermidis* is virtually avirulent.[5,8] Following implantation, localized inflammatory responses produce reactive oxygen intermediates such as superoxide, while production of interferon-γ and interleukin-1 are inhibited.[9] As a result, macrophages (immune cells that combat bacteria) become less effective and the activity of other immune cells such as lympochytes, monocytes and neutrophils is depleted.[8] Moreover, some immune cells (e.g., leukocytes) are not adept at killing surface-adhered bacteria due to shear stresses at the fluid-solid interface.[10]

To compensate for the weakened host immune response, antibiotics are typically administered before/following surgery.[6] However, some bacteria on surfaces form "biofilms"

that render conventional antibiotic treatments ineffective.[11,12] Biofilms are extremely common and implicated in at least 90% of catheter related infections.[13] Biofilm bacteria are thus best considered the norm rather than the exception. Biofilms form when bacteria adhere to a surface and secrete a thick polysaccharide matrix. Bacteria within biofilms also occupy a broad range of phenotypes and metabolic states, many of which are less susceptible to antibiotics.[12] The environmental heterogeneity within biofilms causes broad variations in nutrient concentrations, oxygen levels and pH that interfere with the action of many antibiotics.[12, 14-17] While still not fully understood, cells in biofilms utilize quorum sensing (e.g., cell-to-cell communication) to rapidly change gene expression patterns within the colony.[18] This form of communication may control biofilm dispersal, where bacteria within the sessile biofilm are "released" into the local environment in their planktonic form to colonize new surfaces.[19] As a result, biofilms on clinical devices cause repeated incidents of acute infection (Figure 1.1).

Complicating matters further, most biofilms are polymicrobial.[20] Polymicrobial biofilms are even less susceptible to antibiotics. Harriott et al. examined the efficacy of vancomycin against polymicrobial biofilms containing *Staphylococcus aureus* and *Candida albicans*, finding that *C. albicans* caused *S. aureus* to become highly resistant to treament.[21] Polymicrobial biofilms can also grow faster; for example, Peters et al. found that polymicrobial biofilms of *C. albicans* and *S. aureus* grew synergistically.[22]

In summary, nosocomial infections emerge from the practicalities of clinical procedures and the highly evolved survival mechanisms of bacteria. Infection and implant damage that results from biofilm formation is best treated by preventing (or limiting) viable

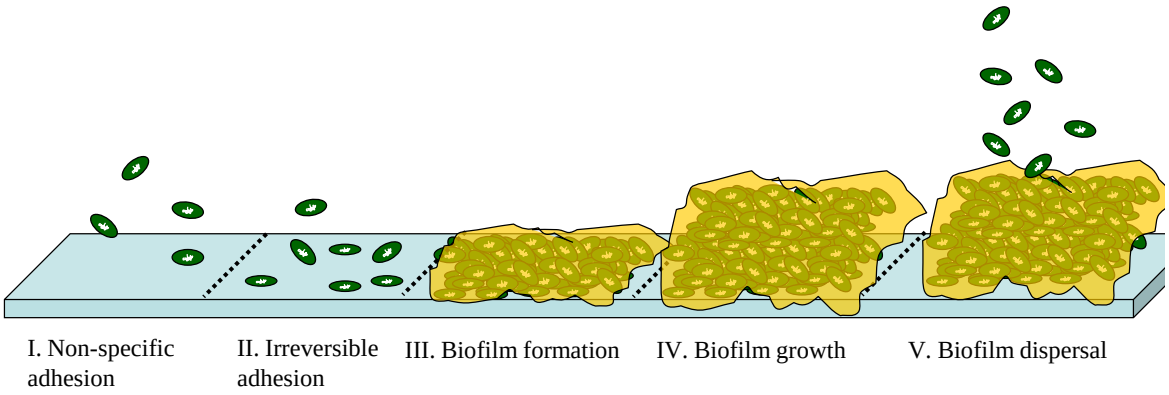

Figure 1.1 The stages of biofilm formation that occur when bacteria interact with surfaces. After adhering to a surface, bacteria excrete a protective exopolysaccharide matrix (represented in the graphic as a yellow film), multiply, and disperse into planktonic bacteria.

microbial adhesion from the start.[23] To this end, researchers have developed antimicrobial materials that quell the adhesion of bacteria to surfaces and/or kill bacteria that do adhere. The two major branches of antifouling/antimicrobial materials, *passive* and *active*, are discussed in sections 1.3 and 1.4.

1.2 Passive surface modifications for reducing infection

A number of coatings feature topographies or covalently bound chemical moieties that reduce bacterial adhesion or kill bacteria. Coatings of this type ("passive") rely on mechanisms intrinsic to the surface itself (Figure 1.2) to combat infection. In this section, the strengths and limitations of such surfaces as they relate to clinical applications are discussed.

1.2.1 Non-fouling surfaces

Surfaces that resist fouling (i.e., adherence of proteins and bacteria) represent perhaps the simplest route towards antimicrobial coatings.[24] Perhaps the most thoroughly studied antifouling interface utilizes poly(ethylene glycol) (PEG) to resist protein adhesion.[25] The PEG macromolecule is easily grafted onto a number of existing surfaces ("PEGylation"), including polyurethanes,[26] silicon,[27] silica,[28] and stainless steel.[29] Not limited to grafting, PEG can also comprise 3-dimensional scaffolds such as hydrogels.[30]

The protein-resistant capabilities of PEGylated materials arise from its hydrophilic nature. When proteins in solution come in contact with these surfaces, the hydrated PEG chains become compressed, forcing steric interactions that are not energetically favorable.[31, 32] Sheth et al. found that repulsive forces between proteins in solution and PEG-grafted surfaces dominate over short distances.[33] However, attractive forces begin to emerge if

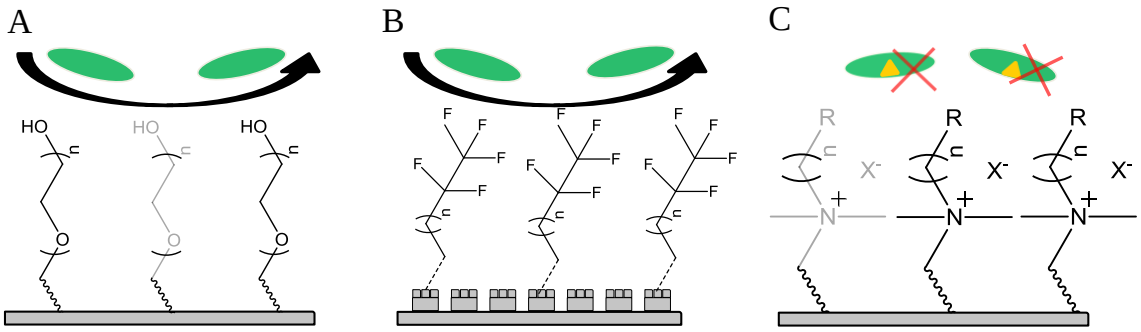

Figure 1.2 Passive strategies for reducing bacterial adhesion and viability on a surface. (A) Poly (ethylene glycol) and (B) superhydrophobic modifications prevent bacterial adhesion, while (C) polycationic quaternary ammonium surfaces kill adhered bacteria via membrane disruption.

proteins are forced into the PEGylated layer. As such, it was concluded that steric hindrance alone does not fully account for the antifouling properties of PEG.[33] A second, more likely mechanism involves competition between the adhesion of water molecules and the adhesion of larger macromolecules to the PEG chains.[33]

Despite a proven ability to resist protein adhesion, the ability for PEGylated surfaces to resist bacterial adhesion is less promising. Whitesides and coworkers found that a resistance to protein adhesion does not correlate with a resistance to bacterial adhesion,[34] owing to mechanisms of bacterial adhesion that do not rely on proteins. Likewise, PEG surfaces on stainless steel that were highly resistant to protein showed very little resistance in adhesion to *Pseudomonas sp.* and *Listeria monocytogenes.*[29] These shortcomings were initially attributed to the instability of such coatings in physiological solutions. Roosjen et al. observed hydrolysis of the bond connecting poly(ethylene oxide) to its substrate in saliva and urine. Kingshott et al. also demonstrated that stable, covalent attachment of PEG is critical for any success in resisting bacterial adhesion. By grafting PEG onto a covalently-immobilized branched poly(ethylenimine) macromolecule on stainless steel, the surfaces were able to reduce bacterial adhesion by 2—4 orders of magnitude over a 5-h period.[35]

The current state-of-the-art in PEG surfaces utilizes peptides to strengthen the bond between PEG and an underlying substrate. Using a process known as phage display, peptides with highly specific binding affinity for a biomedical titanium alloy were identified, isolated, and then modified with PEG.[36] The strength of attachment is further increased by utilizing multivalent peptides.[37] Tetravalent peptides (i.e., four linkages to the Ti substrate) were found to remain attached in serum for up to 14 d (the longest duration tested). In contrast, monovalent binding peptides lost over 90% of the PEG coating over the same time period.

The tetravalent PEG materials were able to resist *S. aureus* adhesion and subsequent biofilm formation.[36, 37]

Even if PEG is stably bound to a substrate, other issues arise with the PEG moiety itself. In oxygenated conditions, or those where transition metal ions are present, the PEG surface may degrade through oxidation.[38] PEG hydroxyl groups are also enzymatically converted to aldehydes in vivo.[38] As such, coatings less susceptible to degradation may be more appropriate for preventing bacterial adhesion.

1.2.2 Superhydrophobic materials

Superhydrophobic materials exhibit unique water contact properties. Such interfaces are characterized by large water contact angles ($\geq 150^{o}$) and low water-roll off angles. While the existence of such surfaces has been known since at least 1907, research in this area underwent a massive resurgence when Barthlott and Neinhuis discovered that superhydrophobicity led to the self-cleaning effects of the Lotus plant.[39] The authors determined that this self-cleaning property resulted from the combination of low surface energy (from its waxy epicuticular coating) and an innate surface roughness. The behavior of water droplets on rough surfaces had been previously described in two separate models by Cassie and Wenzel.[40, 41] In the Cassie model, a pocket of air is trapped within the recesses of the rough surface. Thus, the droplet sits on a pocket of air (known as a "Cassie state" droplet). Because of the extremely low contact area between the droplet and the surface, the droplet will roll off at negligibly small tilt angles, cleaning the surface in the process.[40] In the Wenzel model, the water droplet makes contact with all of the microscopic and sub-microscopic features of the surface (a "Wenzel state" droplet).[41] The contact angle is then dictated by the droplet minimizing its contact with the low surface energy material. Droplets

obeying the Wenzel model remain pinned to the interface even at high tilt angles (a "Wenzel state" droplet). In practice, Wenzel state droplets occur when water impregnates the valleys of the roughened surface, giving water droplets direct contact with the material itself rather than air (Figure 1.3). For a surface to be effective in self-cleaning and fouling prevention, the surface properties need to be tailored so that the droplets remain in the Cassie state. This condition is most effectively achieved through hierarchal roughness that exhibits both microscale and nanoscale dimensions.[42]

Water droplets on a surface become inadequate descriptors of the surface/water interaction when a superhydrophobic material is fully submerged in aqueous media (as would be the case for an implanted biomaterial). Instead, a pocket of entrapped air referred to as a *plastron* spans the divide between the solid-liquid interface when these materials are submerged.[43] Materials housing an air plastron are evident by a silvery-sheen present on the superhydrophobic surface, and are indicative of a Cassie-Baxter wetting state.[44] Contact with the surrounding water is limited, and thus opportunities for bacterial interactions are minimized. Supporting this hypothesis, Truong et al. found reduced *S. aureus* adhesion on superhydrophobic surfaces. Areas of the substrate with the most entrapped air contained the fewest number of bacteria.[45] Bacterial adhesion increased at extended immersion times, most likely a result of air dissolution into the surrounding aqueous layer. Indeed, superhydrophobic surfaces slowly lose their plastron through gas exchange with the surrounding aqueous media dependent on immersion depth, dissolved gas concentration, and other factors.[46] Even after complete plastron loss, evidence suggests that the nanoscale features present on many superhydrophobic surfaces reduce bacterial adhesion even in the absence of a plastron. Ma et al. forced complete wetting of a Taro leaf (a naturally occurring

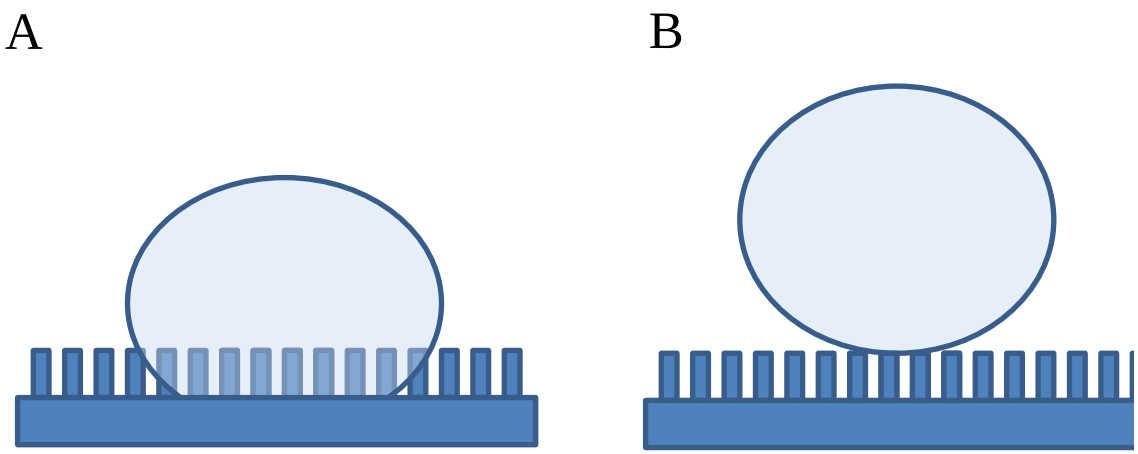

Figure 1.3 A water droplet atop a rough surface obeying the (A) Wenzel or (B) Cassie model.

superhydrophobic plant) such that no plastron remained, and still observed a resistance to *P. aeruginosa* adhesion. This anti-adhesive effect was attributed to surface architecture, as areas featuring dense nanostructures tended to have the fewest adhered bacteria. Those bacteria that did adhere were mostly located in the boundary regions between nanostructures.[44] Spatial variations in adhesive forces were further corroborated via atomic force microscopy, where those areas with high nanostructure densities had less adhesion than areas lacking nanostructures.

When bacteria require specific proteins to adhere to a surface, their adhesion to superhydrophobic substrates may be inhibited through reduced protein adsorption. Stallard and co-workers utilized spectroscopic ellipsometry to quantify fibrinogen adhesion to surfaces with water contact angles between <5 and >150^{o}. Adsorbed fibrinogen was lowest on the fluorinated superhydrophobic substrates. To determine if this reduction in protein binding led to decreased bacterial adhesion, the authors exposed the substrates to a suspension of SH1000, a strain of *S. aureus* that specifically binds to fibrinogen.[47] Compared to fibrinogen-bound controls, bacterial adhesion was reduced by ~99% for superhydrophobic substrates regardless of fibrinogen exposure. These findings indicate that superhydrophobicity reduces bacterial adhesion in the absence of proteins, but also reduces the adhesion of proteins that bind specifically to bacteria.[48]

Until recently, methods for producing superhydrophobic materials utilized processing conditions that were either complex, chemically harsh, or difficult to scale (e.g., lithography, acid etching, high temperatures). To remedy this, more facile techniques have been developed whereby a superhydrophobic material is applied as a thin coating.[49-51] Our group utilized sol-gel chemical techniques to fabricate superhydrophobic materials via mild

aqueous reaction conditions and low-temperature drying environments.[49] We first fabricated colloidal silica particles (to impart roughness), and then crosslinked those particles within a fluorinated sol-gel film (for low surface energy).[49] Utilized in chapters 2, 3, and 4 of this dissertation, the sol-gel method consists of the hydrolysis and condensation of silane precursors to yield a variety of materials depending on the reaction conditions (Figure 1.4). For example, low silane concentrations with basic ammonium hydroxide catalysts favor rapid silane condensation and tend to form particles. In contrast, sol-gel reactions in acidic conditions produce linear chains that further crosslink to form a 3-dimensional network (referred to as a "xerogel" when dried).

The antimicrobial adhesion potential of the superhydrophobic sol-gel materials fabricated by Privett et al. was assessed against *Pseudomonas aeruginosa* and *Staphylococcus aureus* at concentrations of 10^8 cfu mL^{-1}. A 1.8 and 2.1-log reduction in adhered bacteria was observed for the two strains, respectively.[49] Despite this reduction in bacterial adhesion, the materials were not capable of killing adhered bacteria. As such, bacteria proliferation and biofilm growth from adhered bacteria are still possible. Methods to kill bacteria through active release (or contact killing) are needed for truly anti-adhesive coatings to maximize their clinical potential.[52] Reports of antimicrobial superhydrophobic materials are limited. Shateri Khalil-Abad et al. developed superhydrophobic fibers coated with antimicrobial silver nanoparticles and evaluated their efficacy against *Escherichia coli* and *Staphylococcus aureus* using a zone of inhibition assay.[53] While common practice, these assays do not model the irreversible bacterial adhesion events that occur in fluid-submerged surfaces. To assess the potential of superhydrophobic materials for biomedical applications, implant-relevant antibacterial assays must be carried out in tandem with their development.

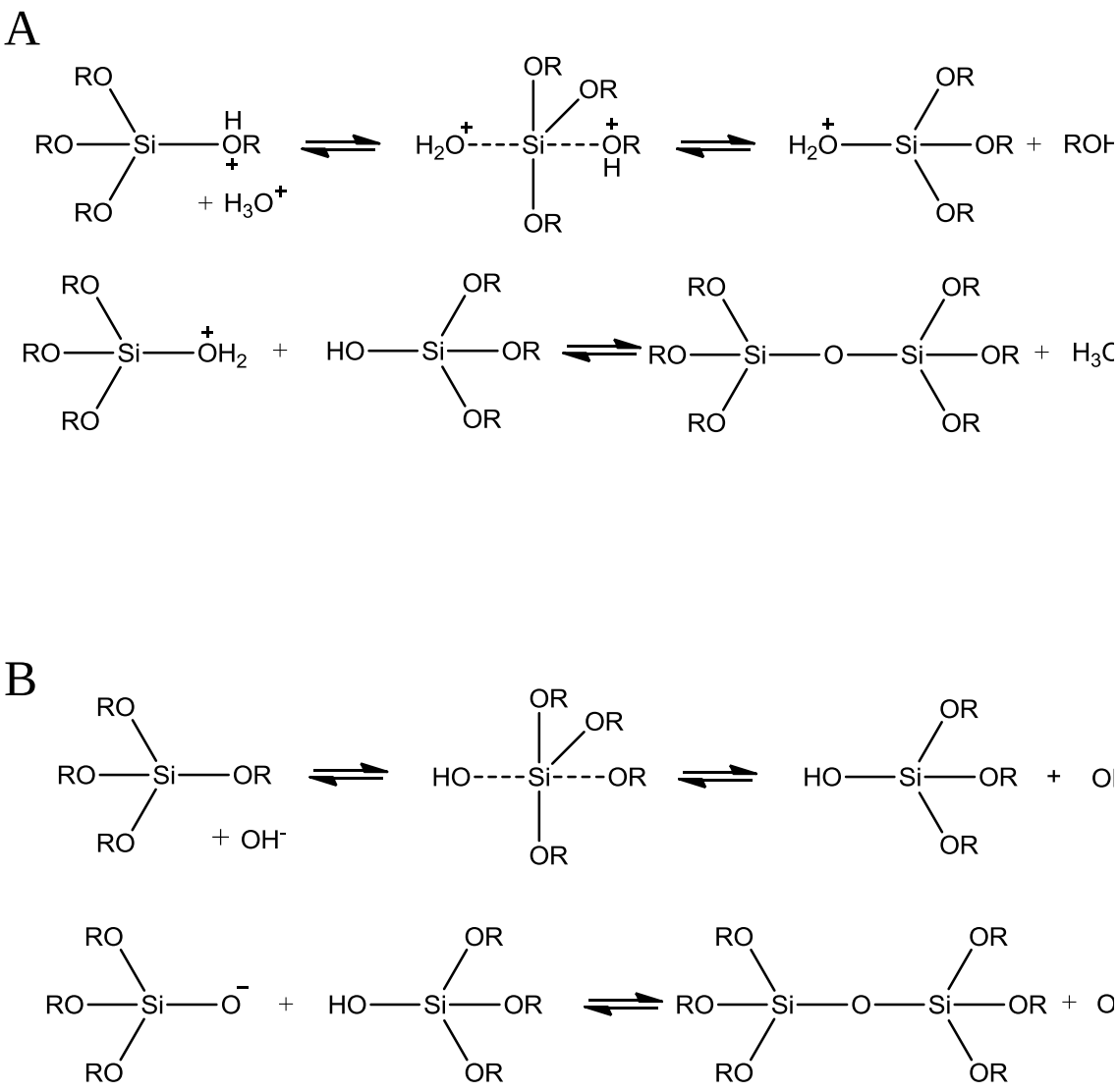

Figure 1.4 (A) Acid and (B) base-catalyzed sol-gel hydrolysis and condensation reactions.

1.2.3 Superhydrophobic materials for drug release

Controlled release of antimicrobials from superhydrophobic coatings remains relatively unexplored, but controlled release of cancer drugs from superhydrophobic materials has been the subject of recent study by Grinstaff and coworkers.[54-57] Superhydrophobic electrospun fiber meshes were doped with the cancer drug SN-38 for controlled drug release.[56] The polymeric meshes were synthesized using a mixture of poly(ε-caprolactone) and poly(glycerol monostearate-co-ε-caprolactone) (PGC-C18), a hydrophobic additive. By controlling the amount of PCG-C18 within the fiber mat, contact angles were tunable from roughly 120 (hydrophobic) to 153^{o} (superhydrophobic). The rate of drug release from the fibers was substantially slower from the superhydrophobic materials because of reduced water uptake. Superhydrophobic meshes doped with SN-38 could kill Lewis lung carcinoma (LLC) cells after >60 d incubation, whereas the non-superhydrophobic mats could only be incubated for 25 d before losing their cell-killing potential. This phenomenon was explained through reduced water uptake. As the mats are placed in aqueous media initially, the pocket of air within remains trapped, slowly displacing over time as water migrates into the material. The rate of release is controlled by the displacement of air in the material by water encompassing the sample. The rate at which water displaces entrapped air seems to be a property of the material itself (i.e., through varying the PGC-C18 dopant percentage in this particular case), but also can be accelerated by external means. For instance Yohe et al. synthesized fiber mats with a larger percentage (30 wt%) of the hydrophobic PGC-C18 dopant so that no measurable release of SN-38 occurred in aqueous buffer.[57] Release of the drug was then triggered by ultrasound, forcing water into the mat. Consistent with the lack of drug release from 30 wt% PGC-C18 fibers, these mats were not toxic towards LLC cells after

10 d. However, the cells could be killed (99%) after this period by releasing the entrapped drug with ultrasound. In summary, superhydrophobic fiber mats are an elegant approach for tuning drug release rates; however, doping drugs into fibers may not be feasible for all drug release chemistries. These superhydrophobic fiber mats serve as stand-alone implants (i.e., devices) rather than *coatings* on existing medical implants. A need still exists for a facile superhydrophobic coating that can be applied in bulk to a wide range of drug-releasing substrates for tuning release of the drug contained within.

1.2.4 Polycationic antimicrobial surfaces

Small molecule quaternary ammonium (QA) compounds have seen widespread use as antiseptics and disinfectants.[58] Mechanistically, the cationic charge on QAs promotes association of the molecules with the negatively charged surface of bacteria. Once QAs are surface-associated, the hydrophobic chains pendant from the ammonium cation cause bacterial membrane disruption, ultimately leading to cell death.[59] Additional antimicrobial action may be attributed to diffusion and uptake of the molecules into bacterial cells, but membrane-specific mechanisms have inspired the development of coatings with tethered-on antimicrobial QA moieties.[58, 60, 61]

Isquith and coworkers first developed QA-modified coatings by grafting the silane 3-(trimethoxysilyl) propyldimethyloctadecyl ammonium chloride onto glass and a variety of other surfaces.[58] These materials killed a broad array of organisms including Gram-negative and Gram-positive bacteria, fungi, and algae. When aerosolized onto the QA-functionalized glass slides, ~3-log (99.9%) reductions were observed against *Streptococcus faecalis*. To confirm that these antimicrobial effects were attributable to surface-bound QAs rather than

slow release of the compound, the surfaces were repeatedly washed in distilled water and their antimicrobial efficacy was reexamined. The authors found that the coatings largely retained their antimicrobial efficacy after washing, and thus attributed the mechanism of action to the surface-bound QAs.

Subsequent research of polycationic surfaces was largely stagnant until 2001 when the Klibanov laboratory used a graft copolymerization method to create *N*-hexylated poly(4-vinylpyridine) (PVP).[62] In agreement with the above study by Isquith and coworkers, *N*-hexylated PVP significantly reduced adhered viable bacteria introduced via aerosolization of bacteria suspensions. While such conditions are beneficial for decontaminating "everyday" surfaces (including those used in the clinical setting), assessing bacterial killing in this manner does not reflect the fluid conditions surrounding implanted devices. In follow-on work by Tiller et al., poly(vinyl-N-hexylpyridinium)-functionalized coatings were also found to kill waterborne *S. aureus* and *E.coli*.[63] The surfaces were submerged in suspensions of the bacteria (~1 x 10^6 cfu mL) for 2 h, then transferred to sterile phosphate buffered saline (PBS). A 1.7—2 log reduction was observed depending on the coated material and the bacteria strain. These results suggest that QA-modified coatings are effective for killing viable adhered bacteria. However, the low concentration of bacteria employed and the solution used (sterile PBS) were far different from the high concentrations of protein and cells present in biological milieu. Even in the absence of proteins and debris, bacteria killed by the QA coating remain adhered, thus masking the biocidal surface from newly adhered bacteria. Researchers in the Klibanov laboratory have studied this phenomenon by evaluating the antimicrobial efficacy of QA surfaces after multiple exposures to bacteria.[64] After spraying the surfaces four times with a suspension of *S. aureus*, the bactericidal activity

declined by 42%. While the antimicrobial activity could be restored by cleaning off the dead bacteria with surfactants, such a step would be impractical for implanted devices. Furthermore, these surfaces are much less effective at killing bacteria when challenged with high concentrations of bacteria (>1 x 10^7 cfu mL^{-1}).[65] The biocidal action of such coatings is only considered "permanent" insofar as the surface remains clean, or can be regenerated through cleaning. Since even dead bacteria are able to invoke an inflammatory response in vivo,[66] mechanisms that reduce bacterial adhesion in addition to killing bacteria are needed.

1.3 Active release strategies for antimicrobial surfaces

The other major branch of antimicrobial materials utilizes the active release of biocidal agents from an implant surface.[67] This approach offers several advantages. First, large systemic doses of the biocidal compound in question are avoided because antimicrobial concentrations of the agent are relegated to an area close to the device itself. Concentrations of a released agent in the stagnant layer immediately adjacent to the implant are several orders of magnitude larger than systemic concentrations due to dilution that occurs as the agent diffuses outward.[8] Second, active release mechanisms, unlike passive mechanisms, are not typically obstructed by surface fouling or the adhesion of dead cells.[67]

By their very nature, the antimicrobial duration of active-release surfaces are finite, and will depend on factors such as the size and release rate of the antimicrobial payload encapsulated within. While this disadvantage has been highlighted to justify passive approaches to antimicrobial materials,[68] such criticisms may be unnecessary. It has been suggested that bacterial killing within a post-operative window of 6 hours following implantation is critical for removing pathogens introduced during surgery.[6] This critical period emerges because truly sterile surgical sites are a near-impossibility, and because the

host immune response is severely compromised at the implant site due to localized inflammation. While longer durations may certainly be beneficial, a finite biocidal duration by no means renders the device unusable. A number of biocidal agents have been explored as active release materials, including those that release conventional antibiotics, silver, and nitric oxide. Each is discussed in detail below.

1.3.1 Release of antibiotics

To reduce the need for systemic antibiotic therapy, researchers have incorporated antibiotics into materials to facilitate localized release.[69] Since release of the drug is dictated by diffusion, the water uptake by the polymer significantly impacts release kinetics. Risbud et al. reported on amoxicillin-loaded chitosan/polyvinyl pyrrolidone (PVP) hydrogels that released a majority (73%) of their contents within 3 h. In a follow on-study, polyacrylamide-chitosan hydrogels with comparatively lower water uptake were able to slow the release, such that only ~75% of the total payload was released over 3 d.[70]

Choosing the appropriate drug release vehicle is critical for clinical success, as the scaffold itself may interact with surrounding tissue. For example, antibiotic-loaded sol-gel films have been utilized in the treatment of bone-related infections.[71-73] In these systems, the sol-gel coatings were selected due to their favorable interaction with bone matrices. The antibiotic release inhibited bacterial colonization. Adams et al. developed sol-gel coatings that released most of their vancomycin payload within 3 d, but the remaining drug released at slower rates over the next 2 weeks. The antibiotic-loaded sol-gels were coated on titanium alloy rods, implanted into the femoral canal of Wister rats, and challenged with an inoculum of *S. aureus.* The antibiotic-releasing sol-gels significantly decreased the number of

isolatable viable bacterial colonies in addition to improving bone integration and reducing osteomyelytis.[74] After 3 and 4 weeks, the films were no longer able to kill bacteria, suggesting that the vancomycin supply was exhausted.[74] Such findings support the benefit of long-term antibiotic release.[75] Unfortunately, extremely long-term sustained release of antibiotics may actually serve as a pitfall to successful treatment. Neut and colleagues analyzed a patient whom had been treated with gentamicin-loaded poly(methyl methacrylate) beads 5 years prior.[76] The beads still released residual levels of the antibiotic. This sustained, sub-inhibitory release fostered development of a gentamicin-resistant staphylococcal strain of bacteria. The authors concluded that antibiotic-loaded materials must be designed to prevent long-term sustained release, possibly through biodegradability mechanisms.[77,78] Similar concerns have been brought to light in other systems that release antibiotics. Antibiotic-loaded bone cements, for instance, were criticized by Hanssen for their ability to encourage drug-resistance.[79] Furthermore, multiple antibiotics are required from these materials to successfully inhibit a broad range of microorganisms.[79] Active release agents that operate via less specific pathways (i.e., broad-spectrum agents) and overcome bacterial resistance mechanisms may be more suitable candidates for localized antimicrobial release.

1.3.2 Nitric oxide-releasing surfaces

Nitric oxide is an endogenously produced molecule involved in a diverse array of physiological processes, including the immune response to pathogens.[80-83] Knockout mice lacking inducible nitric oxide synthase (iNOS; an enzyme used by macrophages to produce NO) were unable to combat replication of *Listeria monocytogenes*.[84] While NO exerts some of its antimicrobial efficacy directly, most of its action arises from secondary reactions of NO

that form peroxynitrite (by reaction with the superoxide anion), nitrogen dioxide, and dinitrogen trioxide (by reaction with oxygen).[85-87] These species place oxidative and nitrosative stress on bacteria, ultimately disrupting membrane, protein, enzyme, and DNA function.[88] Mammalian cells, like those located in the endothelium, are able to combat the effects of oxidative stress (especially via peroxynitrite) by lowering superoxide concentrations through the superoxide dismutase enzyme.[89] The wide array of mechanisms by which NO kills makes it difficult for bacteria to develop resistance to the molecule, as multiple simultaneous genetic mutations would be required for a survival advantage.[90] Taken together, NO's low toxicity, wide-spread distribution in the mammalian body, antimicrobial activity, and lack of demonstrated bacterial resistance make it an ideal candidate for active releasing antimicrobial surfaces.

Supplying exogenous NO to the body requires a means of delivery that is stable until the time of treatment and releases at controlled rates during treatment. A number of chemical NO donors exist for this purpose, including organic nitrates and nitrates,[91] metal nitrosyls,[92] *S*-nitrosothiols,[93] and *N*-diazeniumdiolates.[94, 95] While the clinical use of organic nitrates and metal nitrosyls is well-established (and in fact predates knowledge of NO's biological activity), the mechanisms by which these donor classes decompose into NO are highly dependent on host-specific factors such as enzyme activity.[96-99] At least some of the action of organic nitrates and metal nitrosyls involves the formation of *S*-nitrosothiol intermediates.[100] Thus, *N*-diazeniumdiolate (Figure 1.5) and *S*-nitrosothiol NO donors remain the most promising donors for their well-understood NO release triggers, rates, and mechanisms.

N-diazeniumdiolate NO donors were first synthesized by Drago and coworkers in the early 1960s,[101, 102] and then largely neglected until NO's physiological importance was

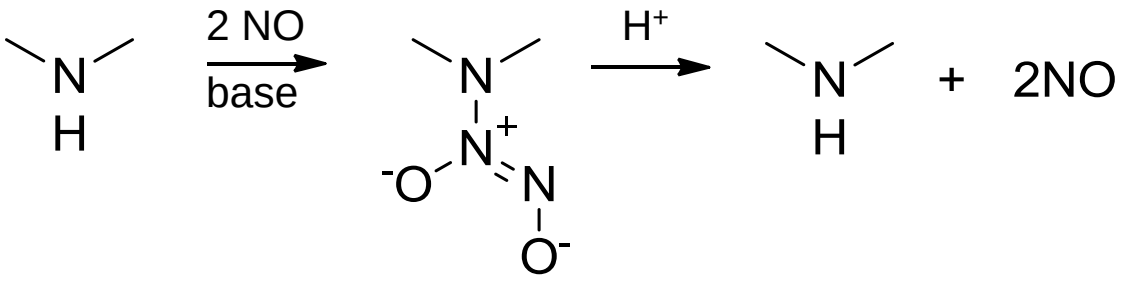

Figure 1.5 *N*-diazeniumdiolate formation on a secondary amine following exposure to NO and base. In the presence of a proton, the *N*-diazeniumdiolate decomposes to yield two equivalents of NO and the parent amine.

established in the late 1980s.[103] Formed via the reaction of secondary amines and NO under basic conditions, these compounds exhibit pH-dependent decomposition to two NO equivalents and the parent (i.e., precursor) amine. The decomposition rate (i.e., NO-release rate) is dependent on the structure, with certain chemical groups capable of stabilizing the *N*-diazeniumdiolate.[94] To control the release of NO and target bacteria directly, these functional groups have been incorporated within larger macromolecular scaffolds such as silica particles and dendrimers.[104-110] Like small molecules, the NO-release kinetics from such scaffolds are controllable by varying the environment surrounding the *N*-diazeniumdiolate (Figure 1.6).

The active release of NO from a surface can be achieved in a number of ways, but the first studies to demonstrate the antimicrobial effects of NO-releasing surfaces utilized amine-modified xerogels synthesized via the sol-gel process (Figure 1.7).[111-113] Researchers in the Schoenfisch laboratory covalently incorporated amine-functionalized silanes into a xerogel matrix. Upon exposure to high pressure NO (5 atm), the 2^{o} amines within were converted to *N*-diazeniumdiolates. Surrounding amines in the xerogel network served as the necessary base for *N*-diazeniumdiolate-formation. Nitric oxide-releasing xerogels were demonstrated to reduce the adhesion of biomedical pathogens such as *P. aeruginosa*, *S. aureus* (and its antibiotic-resistant counterpart, Methicillin Resistant *S. aureus*), *S. epidermidis*, *Eschericia coli*, and *Eschericia faecalis* by 80-95% depending on the bacterial exposure time and NO flux at the surface.[111, 114-117] Furthermore, bacteria that did adhere to the NO-releasing surfaces were effectively killed by NO after prolonged exposure.[115, 116] Recently, Cai et al. demonstrated significant reductions in biofilm formation on surfaces that slowly released NO for >7 d.[118] They hypothesized that the reduced biofilm formation was due to NO's ability to

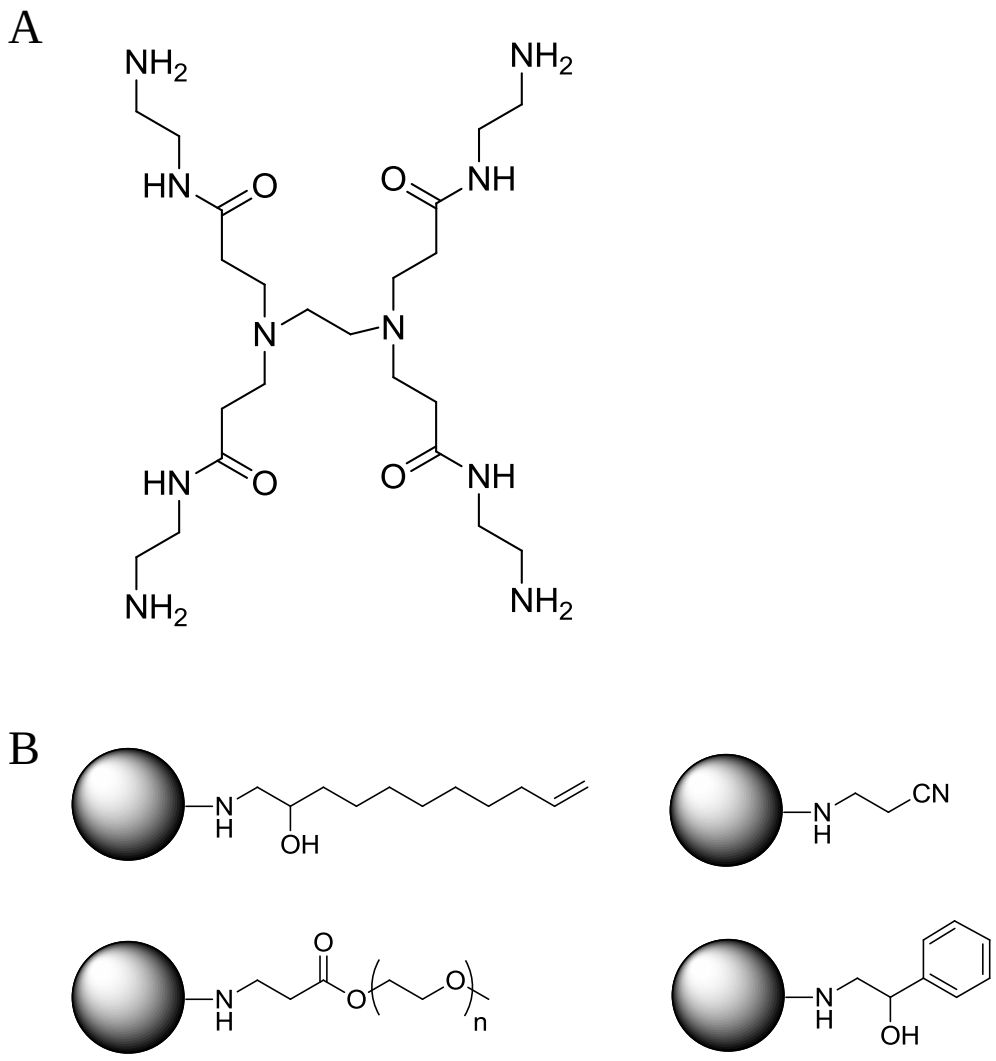

Figure 1.6 (A) Poly (amido amine) (PAMAM) dendrimers display 1^{o} amines, the number of which depends on the dendrimer generation (Generation 0 is shown). (B) Conversion of the 1^{o} to 2^{o} amines allows for *N*-diazeniumdiolate modification, with subsequent NO-release kinetics determined by the precursor used to form the 2^{o} amine.

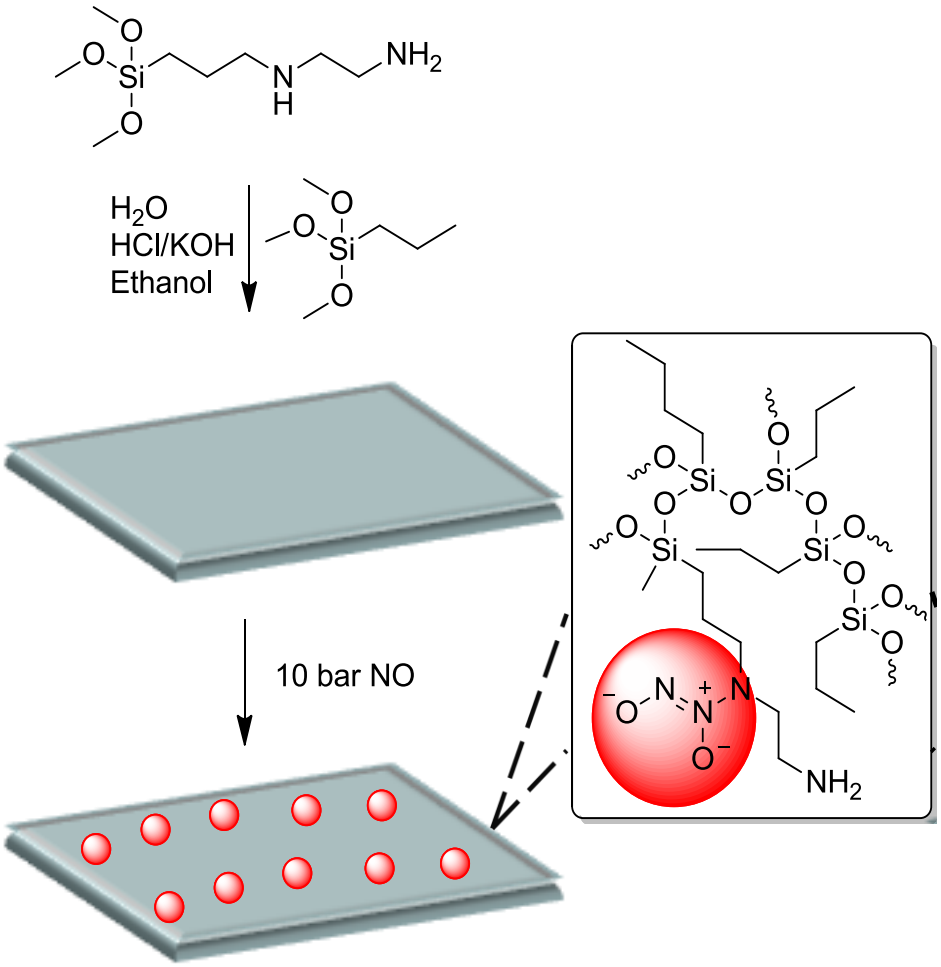

Figure 1.7 Nitric oxide-releasing xerogels synthesized via sol-gel chemical approaches. Amine-modified silanes are incorporated into a silica matrix and then exposed to high pressure NO to convert the 2^{o} amines to *N*-diazeniumdiolate NO donors.

initiate biofilm dispersal.[119] The ability for NO-releasing materials to both resist bacterial adhesion and kill adhered bacteria suggest that NO may be a suitable active release agent for reducing infection in medical implants.

Follow-on work demonstrated NO's ability to combat infection *in vivo*.[120, 121] Nablo et al. implanted NO-releasing xerogels into the subcutaneous tissue of male rats and inoculated the wound site with *S. aureus* (1×10^6 cfu). Compared to controls, an 82% reduction in infection incidences was observed in rats with NO-releasing implants.[120] Building upon this work, Holt et al. coated NO-releasing xerogels onto external fixation pins implanted into the tibia of rats. Because external fixators are percutaneous (i.e., exposed through skin), such devices are prone to infection as bacteria are able to migrate through the pin tract following implantation (Figure 1.8). Following 28 d implantation, significant reductions in bacterial colonies and clinical signs of infection were observed at the NO-releasing pins compared to controls.[121] Together, these studies illustrate NO's ability to reduce infection in implants.

While not the central aim of this research, it is important to note that NO-releasing materials also mitigate certain non-microbial fouling events such as platelet adhesion and the foreign body response (FBR).[122-126] The FBR is the cumulative host immune response that occurs when a device is implanted.[1, 126, 127] Frustrated cells that are unable to phagocytose an implant form a dense, avascular collagen capsule around the device, walling it off from surrounding tissue. This capsule often causes device failure through poor implant-tissue integration.[127] The deleterious consequences of the FBR have hindered the development of implantable sensors that monitor analytes such as glucose continuously in real-time.[126] Such devices would improve treatment outcomes for diabetics, but the events of the FBR (namely

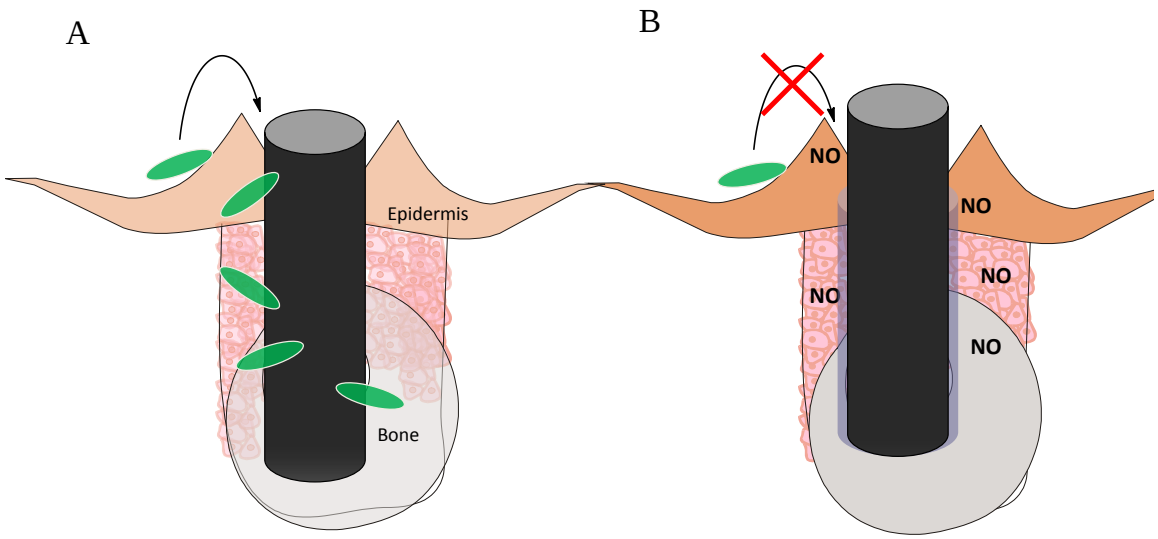

Figure 1.8 (A) Fixation pins coated with non-NO-releasing xerogels become infected as foreign microbes migrate into the pin tract and proliferate in tissue. (B) Fixation pins coated with NO-releasing xerogels are killed by NO, and infection incidences are reduced.

acute inflammation and inhibited analyte diffusion by collagen encapsulation) lead to erratic responses. Nitric oxide-release may alleviate some of these pitfalls. Unfortunately, sensor membranes made to release NO from xerogels are mostly impermeable to glucose. Thus while they reduce the FBR, they are not analytically useful. More permeable (to glucose) NO-releasing sensor membranes would enable the development of better performing continuous monitoring glucose sensors.

1.3.3 Antimicrobial silver-releasing materials

Silver's origins as a broad-spectrum antimicrobial agent date back to ancient times, where Persians, Greeks, Romans and Egyptians used it to preserve water and food.[128] Modern-day silver releasing biomaterials hold distinction as one of the few active release systems with demonstrated success in clinical trials.[129] Current Food and Drug Administration (FDA) approved devices include wound dressings for burn patients and coatings for urinary and intravascular catheters.[130-132] Most often, silver is impregnated into (or on) materials/devices in the form of ionic silver (e.g., silver nitrate,[133, 134] silver sulfadiazine,[135] etc.), silver metal,[136] or silver colloids and nanoparticles.[73, 137]

Mechanistically, the bactericidal action of Ag^+ occurs via three pathways: 1) direct membrane damage (i.e., detachment of the cytoplasm from the cell wall);[138] 2) inhibition of enzymatic activity following binding between Ag^+ and protein thiol residues; and 3) prevention of DNA replication.[139] The latter two mechanisms are contingent upon successful diffusion of Ag^+ into the cell. The thick peptidoglycan layer enveloping Gram-positive bacteria causes these strains to be less susceptible to silver than their Gram-negative counterparts.[139] The antimicrobial effects of silver metal and colloids in the Ag (0) oxidation

state are largely indirect, relying on oxidation of the metals to free Ag^+. Xiu et al. added convincing support to this theory by testing silver nanoparticles against bacteria in anaerobic conditions (i.e., conditions precluding the formation of Ag^+). They found that the toxicity of these materials against bacteria was drastically inhibited,[140] and ultimately concluded that differences in antimicrobial activity between different shapes and sizes of silver nanoparticles are intrinsically intertwined with differences in the rate of Ag^+ production.

These findings have since guided the development of silver releasing materials. For example, Marini et al. doped sol-gel films with both silver nitrate and silver nanoparticles, finding almost no antimicrobial efficacy from the nanoparticle-doped silica materials despite high antimicrobial activity from silica doped with silver nitrate.[133] The authors concluded that diffusion of Ag^+ from the tortuous silica network, combined with the slow release of Ag^+ from the nanoparticles resulted in a silver release rate too low for antimicrobial activity. Antimicrobial fluxes from silver nanoparticle-doped materials may be achieved if the materials are thin and/or the surrounding framework is open.[137, 141] However, direct addition of a silver salt is a simpler approach.

The potential cytotoxicity of silver compounds is well-known. Ionic silver compounds exhibit a dose-dependent toxicity towards fibroblasts.[142, 143] Other forms of silver, such as silver nanoparticles, are toxic to zebrafish embryos at antimicrobial concentrations.[144] However, reports of toxicity from silver-coated medical devices are conflicting. Bosetti and colleagues utilized a commercial vapor phase coating process to apply silver metal onto external fixation pins via ion beam deposition. No toxicity or genotoxicity towards fibroblasts (NIH3T3) was noted, but the study did not specify concentrations of silver released from the material nor its corresponding antimicrobial

relevance.[136] Hardes et al. examined the long-term toxicity of an implanted anti-infective silver megaprosthesis in humans over a mean period of 19 months. No damage to liver or kidneys (or any systemic side effects for that matter) was noted. Some bioaccumulation of silver occurred, with blood silver concentrations around 56.4 ppb (compared to basal levels of 2 ppb in untreated patients[145]) but these concentrations would not be expected to produce systemic toxic effects.[146] Trop et al. reported agyria-like symptoms, liver toxicity, and elevated levels of silver in plasma and urine for a burn patient treated with silver sulfadiazine (SSD)-coated polyethylene meshes.[147] These conflicting results likely emerge from the varied Ag^+ release rates of different materials. The Ag^+ release rate may also change for a specific material due to changes in localized pH,[128] ionic strength,[148] and dissolved oxygen content.[149] Nonetheless, clear evidence of dose-dependent toxicity for Ag^+ and its associated compounds exists. Given silver's ability to accumulate systemically, it is best to pursue strategies that minimize overall silver release while maximizing localized antimicrobial activity.

While intuition would suggest that silver's broad-spectrum nature makes bacterial resistance unlikely, silver-resistant bacteria have emerged from environments rich in the element (e.g., mining sites).[130] Resistant bacteria have also been isolated in clinical settings that make extensive use of silver in treatment.[150] Mechanisms for bacterial resistance primarily occur at the membrane, ultimately preventing Ag^+ entry into the cell. Both Ag^+-specific periplasmic binding proteins and cationic efflux pumps have been observed in silver-resistant bacteria.[150, 151] Despite these findings, current evidences suggests that widespread emergence of silver-resistant bacteria is unlikely.[152] Still, isolated incidents of resistance are undesirable and strategies to reduce such occurrences are needed.

Opportunities for resistance can be reduced through combination therapies (i.e., the use of multiple drugs to kill bacteria via multiple mechanisms).[153] Release of silver in conjunction with the antiseptic compound chlorhexidine has been used as an effective antimicrobial combination therapy, but its use is best avoided as it causes severe hypersensitivity reactions in some patients.[132] In addition to limiting opportunities for bacterial resistance, combination therapies may also reduce the overall concentrations of each agent necessary for an identical antimicrobial effect. This principle is especially pertinent to coatings that release silver, as even localized release can cause a systemic build up of silver concentrations throughout the body.[146, 147] Privett et al. demonstrated the synergy of silver (via silver sulfadiazine) and nitric oxide (via the small molecule NO donor PROLI/NO) against a number of Gram-positive and –negative bacteria. The membrane damage evoked by either silver (I) or NO facilitated entry of the other species into the cell. Oxidative stress resulting from silver likely caused an excess of superoxide anions in the vicinity of the bacterial cell. The NO then reacts with these superoxide anions to form peroxynitrite, an even more potent antimicrobial agent. As described in Section 1.4.2, NO's bactericidal effects in the absence of silver are largely attributed to an oxidative stress cascade that produces peroxynitrite from its reaction with superoxide. It is expected that increased superoxide concentrations would enhance NO's antimicrobial efficacy. Translating this work towards clinical applications requires the development of coatings that actively release both NO and silver. The multiple bactericidal mechanisms from such coatings would limit opportunities for bacterial resistance. Furthermore, synergy with NO would reduce the overall concentrations of silver necessary for bactericidal efficacy, and limit both toxicity and systemic accumulation of the metal.

1.4 Summary of dissertation research

The goal of my research was to design antimicrobial coatings that both resist bacterial adhesion and kill adhered bacteria. Rational approaches were employed to reduce toxicity to healthy cells. Specifically, my research aims included:

1. the development of NO-releasing coatings via facile sol-gel techniques that can easily be applied to functional glucose sensors;
2. the synthesis of superhydrophobic NO-releasing xerogels that combine passive and active antimicrobial strategies, exhibit superior resistance to bacterial adhesion and kill adhered bacteria;
3. the development of coatings that simultaneously release Ag^{+} and NO for the synergistic killing of adhered bacteria; and
4. utilization of NO-releasing dendrimers as dopants within polyurethane films and fibers to create materials that release low levels of NO over prolonged periods of time.

This introductory chapter has provided a survey of the most promising passive and active approaches towards antimicrobial surfaces for reducing bacterial adhesion and implant-associated infections. Passive surfaces that resist adhesion (e.g., PEGylated and superhydrophobic coatings) provide no means to kill bacteria. Contact-killing passive surfaces that feature QA groups kill bacteria, but are inactivated by fouling. Surfaces that actively release biocidal agents kill bacteria, but could be improved via combination with other strategies that reduce adhesion or kill bacteria more effectively. Nitric oxide-releasing coatings are particularly beneficial due to their ability to both resist adhesion and kill adhered bacteria, but the utility of current NO-releasing substrates could be

improved. In Chapter 2, *N*-diazeniumdiolate-modified silane precursors are used to create NO-releasing xerogel membranes that can be applied to orthopedic metals such as titanium, release bactericidal concentrations of NO for up to 4 d, and function as glucose sensors. In Chapter 3, superhydrophobic NO-releasing xerogels are introduced as a strategy for reducing and killing adhered bacteria via passive and active mechanisms. Chapter 4 details the preparation of surfaces that release both Ag^+ and NO for potential synergistic antimicrobial benefits. In Chapter 5, NO-releasing poly (amido amine) dendrimers are doped within polyurethane films and fibers to create low-flux materials to reduce the FBR and formation of biofilms. The ability for superhydrophobic coatings to control NO-release kinetics is also demonstrated. Lastly, Chapter 6 summarizes my dissertation work and suggests additional approaches for preparing antimicrobial surfaces in the future.

REFERENCES

1. Ratner, B.D.; Bryant, S.J., "Biomaterials: Where we have been and where we are going." *Annu. Rev. Biomed. Eng.* **2004**, *6*, 41-75.

2. Campoccia, D.; Montanaro, L.; Arciola, C.R., "The significance of infection related to orthopedic devices and issues of antibiotic resistance." *Biomaterials* **2006**, *27*, 2331-2339.

3. Katsikogianni, M.; Missirlis, Y.F., "Concise review of mechanisms of bacterial adhesion to biomaterials and of techniques used in estimating bacteria-material interactions." *Eur. Cells. Mater.* **2004**, *8*, 37-57.

4. Tiesenhausen, K.; Amann, W.; Koch, G.; Hausegger, K.; Thalhammer, M., "Endovascular stentgraft infection—a life-threatening complication." *Vasa* **2000**, *29*, 147-150.

5. Gristina, A.G., "Implant failure and the immuno-incompetent fibro-inflammatory zone." *Clin. Orthop. Relat.R.* **1994**, 106-18.

6. Poelstra, K.A.; Barekzi, N.A.; Rediske, A.M.; Felts, A.G.; Slunt, J.B.; Grainger, D.W., "Prophylactic treatment of gram-positive and gram-negative abdominal implant infections using locally delivered polyclonal antibodies." *J. Biomed. Mater. Res. A* **2001**, *60*, 206-215.

7. Berbari, E.F.; Hanssen, A.D.; Duffy, M.C.; Steckelberg, J.M.; Ilstrup, D.M.; Harmsen, W.S.; Osmon, D.R., "Risk factors for prosthetic joint infection: Case-control study." *Clin. Infect. Dis.* **1998**, *27*, 1247-1254.

8. Schierholz, J.M.; Beuth, J., "Implant infections: A haven for opportunistic bacteria." *J. Hosp. Infect.* **2001**, *49*, 87-93.

9. Kaplan, S.S.; Basford, R.E.; Kormos, R.L.; Hardesty, R.L.; Simmons, R.L.; Mora, E.M.; Cardona, M.; Griffith, B.L., "Biomaterial associated impairment of local neutrophil function." *ASAIO J.* **1990**, *36*, M172-174.

10. Sapatnekar, S.; Kao, W.J.; Anderson, J.M., "Leukocyte—biomaterial interactions in the presence of Staphylococcus epidermidis: Flow cytometric evaluation of leukocyte activation." *J. Biomed. Mater. Res.* **1997**, *35*, 409-420.

11. Marrie, T.J.; Nelligan, J.; Costerton, J., "A scanning and transmission electron microscopic study of an infected endocardial pacemaker lead." *Circulation* **1982**, *66*, 1339-1341.

12. Stewart, P.S.; Costerton, J.W., "Antibiotic resistance of bacteria in biofilms." *Lancet* **2001**, *358*, 135-8.

13. Mukherjee, P.K.; Zhou, G.; Munyon, R.; Ghannoum, M.A., "Candida biofilm: A well-designed protected environment." *Med. Mycol.* **2005**, *43*, 191-208.

14. Zhang, T.C.; Bishop, P.L., "Evaluation of substrate and pH effects in a nitrifying biofilm." *Water Environm. Res.* **1996**, 1107-1115.

15. Tack, K.J.; Sabath, L., "Increased minimum inhibitory concentrations with anaerobiasis for tobramycin, gentamicin, and amikacin, compared to latamoxef, piperacillin, chloramphenicol, and clindamycin." *Chemotherapy* **1985**, *31*, 204-210.

16. Tuomanen, E.; Cozens, R.; Tosch, W.; Zak, O.; Tomasz, A., "The rate of killing of Escherichia coli by β-lactam antibiotics is strictly proportional to the rate of bacterial growth." *J. Gen. Microbiol.* **1986**, *132*, 1297-1304.

17. Mah, T.F.; O'Toole, G.A., "Mechanisms of biofilm resistance to antimicrobial agents." *Trends Microbiol.* **2001**, *9*, 34-9.

18. Zimmerli, W., "Infection and musculoskeletal conditions: Prosthetic-joint-associated infections." *Best. Prac. Res. Cl. Rh.* **2006**, *20*, 1045-1063.

19. Parsek, M.R.; Greenberg, E., "Sociomicrobiology: The connections between quorum sensing and biofilms." *Trends Microbiol.* **2005**, *13*, 27-33.

20. Mermel, L.A.; Farr, B.M.; Sherertz, R.J.; Raad, I.I.; O'Grady, N.; Harris, J.S.; Craven, D.E., "Guidelines for the management of intravascular catheter-related infections." *Clin. Infect. Dis.* **2001**, *32*, 1249-1272.

21. Harriott, M.M.; Noverr, M.C., "Candida albicans and Staphylococcus aureus form polymicrobial biofilms: Effects on antimicrobial resistance." *Antimicrob. Agents Ch.* **2009**, *53*, 3914-22.

22. Peters, B.M.; Ward, R.M.; Rane, H.S.; Lee, S.A.; Noverr, M.C., "Efficacy of ethanol against Candida albicans and Staphylococcus aureus polymicrobial biofilms." *Antimicrob. Agents Ch.* **2013**, *57*, 74-82.

23. Cheng, G.; Zhang, Z.; Chen, S.; Bryers, J.D.; Jiang, S., "Inhibition of bacterial adhesion and biofilm formation on zwitterionic surfaces." *Biomaterials* **2007**, *28*, 4192-9.

24. Krishnan, S.; Weinman, C.J.; Ober, C.K., "Advances in polymers for anti-biofouling surfaces." *J. Mater. Chem.* **2008**, *18*, 3405-3405.

25. Andrade, J.; Hlady, V.; Jeon, S., "Poly(ethylene oxide) and protein resistance: Principles, problems, and possibilities." *Advances in Chemistry* **1996**, *248*, 51-60.

26. Park, K.D.; Kim, Y.S.; Han, D.K.; Kim, Y.H.; Lee, E.H.; Suh, H.; Choi, K.S., "Bacterial adhesion on PEG modified polyurethane surfaces." *Biomaterials* **1998**, *19*, 851-9.

27. Zhang, M.; Desai, T.; Ferrari, M., "Proteins and cells on PEG immobilized silicon surfaces." *Biomaterials* **1998**, *19*, 953-960.

28. Alcantar, N.A.; Aydil, E.S.; Israelachvili, J.N., "Polyethylene glycol-coated biocompatible surfaces." *J. Biomed. Mater. Res.* **2000**, *51*, 343-51.

29. Wei, J.; Ravn, D.B.; Gram, L.; Kingshott, P., "Stainless steel modified with poly(ethylene glycol) can prevent protein adsorption but not bacterial adhesion." *Colloid Surface B.* **2003**, *32*, 275-291.

30. Raeber, G. P.; Lutolf, M. P.; Hubbell, J. A., "Molecularly engineered PEG hydrogels: A novel model system for proteolytically mediated cell migration." *Biophys. J.* **2005**, *89*, 1374-88.31.

31. Jeon, S.; Andrade, J., "Protein—surface interactions in the presence of polyethylene oxide: II. Effect of protein siz." *J. Colloid. Interface Sci.* **1991**, *142*, 159-166.

32. Jeon, S.; Lee, J.; Andrade, J.; De Gennes, P., "Protein-surface interactions in the presence of polyethylene oxide: I. Simplified theory." *J Colloid. Interf. Sci.* **1991**, *142*, 149-158.

33. Sheth, S.R.; Leckband, D., "Measurements of attractive forces between proteins and end-grafted poly(ethylene glycol) chains." *Proc. Natl. Acad. Sci USA* **1997**, *94*, 8399-404.

34. Ostuni, E.; Chapman, R.G.; Liang, M.N.; Meluleni, G.; Pier, G.; Ingber, D.E.; Whitesides, G.M., "Self-assembled monolayers that resist the adsorption of cells." *Langmuir* **2001**, *17*, 6336-6343.

35. Kingshott, P.; Wei, J.; Bagge-ravn, D.; Gadegaard, N.; Gram, L., "Covalent attachment of poly(ethylene glycol) to surfaces, critical for reducing bacterial adhesion." *Langmuir* **2003**, *209*, 6912-6921.

36. Khoo, X.; Hamilton, P.; O'Toole, G.A.; Snyder, B.D.; Kenan, D.J.; Grinstaff, M.W., "Directed Assembly of PEGylated-Peptide Coatings for Infection-Resistant Titanium Metal." *J. Am. Chem. Soc.* **2009**, *131*, 10992-10997.

37. Khoo, X.; O'Toole, G.A.; Nair, S.A.; Snyder, B.D.; Kenan, D.J.; Grinstaff, M.W., "Staphylococcus aureus resistance on titanium coated with multivalent PEGylated-peptides." *Biomaterials* **2010**, *31*, 9285-92.

38. Ostuni, E.; Chapman, R.G.; Holmlin, R.E.; Takayama, S.; Whitesides, G.M., "A survey of structure-property relationships of surfaces that resist the adsorption of protein." *Langmuir* **2001**, *17*, 5605-5620.

39. Barthlott, W.; Neinhuis, C.; Verlot, H.; Schott, C.L., "Purity of the sacred lotus , or escape from contamination in biological surfaces." *Planta* **1997**, *202*, 1-8.

40. Cassie, A.; Baxter, S., "Wettability of porous surfaces." *T. Faraday Soc.* **1944**, *40*, 546-551.

41. Wenzel, R.N., "Resistance of solid surfaces to wetting by water." *Ind. Eng. Chem.* **1936**, *28*, 988-994.

42. Bhushan, B.; Koch, K.; Jung, Y.C., "Fabrication and characterization of the hierarchical structure for superhydrophobicity and self-cleaning." *Ultramicroscopy* **2009**, *109*, 1029-34.

43. Shirtcliffe, N.J.; McHale, G.; Newton, M.I.; Perry, C.C.; Pyatt, F.B., "Plastron properties of a superhydrophobic surface." *Appl. Phys. Lett.* **2006**, *104106*, 1-10.

44. Ma, J.; Sun, Y.; Gleichauf, K.; Lou, J.; Li, Q., "Nanostructure on taro leaves resists fouling by colloids and bacteria under submerged conditions." *Langmuir* **2011**, *27*, 10035-10040.

45. Fadeeva, E.; Truong, V. K.; Stiesch, M.; Chichkov, B. N.; Crawford, R. J.; Wang, J.; Ivanova, E. P., "Bacterial retention on superhydrophobic titanium surfaces fabricated by femtosecond laser ablation." *Langmuir* **2011**, 3012-3019.

46. Poetes, R.; Holtzmann, K.; Franze, K.; Steiner, U., "Metastable underwater superhydrophobicity." *Phys. Rev. Lett.* **2010**, *105*, 166104.

47. Corrigan, R.M.; Rigby, D.; Handley, P.; Foster, T.J., "The role of Staphylococcus aureus surface protein SasG in adherence and biofilm formation." *Microbiology* **2007**, *153*, 2435-2446.

48. Stallard, C. P.; McDonnell, K. A.; Onayemi, O. D.; O'Gara, J. P.; Dowling, D. P., "Evaluation of protein adsorption on atmospheric plasma deposited coatings exhibiting superhydrophilic to superhydrophobic properties." *Biointerphases* **2012**, *7*, 1-12.

49. Privett, B. J.; Youn, J.; Hong, S. a.; Lee, J.; Han, J.; Shin, J. H.; Schoenfisch, M. H., "Antibacterial fluorinated silica colloid superhydrophobic surfaces." *Langmuir* **2011**, *27*, 9597-601.

50. Yu, M.; Gu, G.; Meng, W.-D.; Qing, F.-L., "Superhydrophobic cotton fabric coating based on a complex layer of silica nanoparticles and perfluorooctylated quaternary ammonium silane coupling agent." *Appl. Surf. Sci.* **2007**, *253*, 3669-3673.

51. Ogihara, H.; Xie, J.; Okagaki, J.; Saji, T., "Simple method for preparing superhydrophobic paper: spray-deposited hydrophobic silica nanoparticle coatings exhibit high water-repellency and transparency." *Langmuir* **2012**, *28*, 4605-4608.

52. Banerjee, I.; Pangule, R.C.; Kane, R.S., "Antifouling coatings: Recent developments in the design of surfaces that prevent fouling by proteins, bacteria, and marine organisms." *Adv. Mater.* **2011**, *23*, 690-718.

53. Shateri Khalil-Abad, M.; Yazdanshenas, M. E., "Superhydrophobic antibacterial cotton textiles." *J. Colloid Interface Sci.* **2010**, *351*, 293-8

54. Wolinsky, J. B.; Yohe, S. T.; Colson, Y. L.; Grinstaff, M. W., "Functionalized hydrophobic poly(glycerol-co-ε-caprolactone) depots for controlled drug release." *Biomacromolecules* **2012**, *13*, 406-411.

55. Yohe, S. T.; Freedman, J. D.; Falde, E. J.; Colson, Y. L.; Grinstaff, M. W., "A Mechanistic Study of Wetting Superhydrophobic Porous 3D Meshes." *Adv. Funct. Mater.* **2013**, *23*, 3628-3637.

56. Yohe, S.T.; Colson, Y.L.; Grinstaff, M.W., "Superhydrophobic Materials for Tunable Drug Release: Using Displacement of Air To Control Delivery Rates." *J. Am. Chem. Soc.* **2012**, *134*, 2016-2019.

57. Yohe, S. T.; Kopechek, J. a.; Porter, T. M.; Colson, Y. L.; Grinstaff, M. W., "Triggered drug release from superhydrophobic meshes using high-intensity focused ultrasound." *Adv. Healthc. Mater.* **DOI: 10.1002/adhm.201200381**, [Available online April 17, 2013]

58. Isquith, A.J.; Abbott, E.A.; Walters, P.A., "Surface-bonded antimicrobial activity of an organosilicon quaternary ammonium chloride." *Appl. Microbiol.* **1972**, *24*, 859-63.

59. Denyer, S.P., "Mechanisms of action of antibacterial biocides." *Int. Biodeter. Biodegr.* **1995**, *36*, 227-245.

60. Gottenbos, B.; van der Mei, H.C.; Klatter, F.; Nieuwenhuis, P.; Busscher, H.J., "In vitro and in vivo antimicrobial activity of covalently coupled quaternary ammonium silane coatings on silicone rubber." *Biomaterials* **2002**, *23*, 1417-1423.

61. Oosterhof, J. J. H.; Buijssen, K. J. D. A.; Henk, J.; Laan, B. F. A. M. V. D.; Van, H. C.; Mei, D.; Busscher, H. J.; Mei, H. C. V. D., "Effects of quaternary ammonium silane coatings on mixed fungal and bacterial biofilms on tracheoesophageal shunt prostheses." *ACS Nano* **2006**, *12*, 7699-7707.

62. Tiller, J.C.; Liao, C.J.; Lewis, K.; Klibanov, a.M., "Designing surfaces that kill bacteria on contact." *Proc. Natl. Acad. Sci USA* **2001**, *98*, 5981-5.

63. Tiller, J.C.; Lee, S.B.; Lewis, K.; Klibanov, A.M., "Polymer surfaces derivatized with poly(vinyl-N-hexylpyridinium) kill airborne and waterborne bacteria." *Biotechnol. Bioeng.* **2002**, *79*, 465-71.

64. Mukherjee, K.; Rivera, J.J.; Klibanov, A.M., "Practical aspects of hydrophobic polycationic bactericidal "paints"." *Appl. Biochem. Biotech.* **2008**, *151*, 61-70.

65. Murata, H.; Koepsel, R.R.; Matyjaszewski, K.; Russell, A.J., "Permanent, non-leaching antibacterial surfaces--2: How high density cationic surfaces kill bacterial cells." *Biomaterials* **2007**, *28*, 4870-4879.

66. de Man, P.; van Kooten, C.; Aarden, L.; Engberg, I.; Linder, H.; Svanborg Edén, C., "Interleukin-6 induced at mucosal surfaces by gram-negative bacterial infection." *Infect. Immun.* **1989**, *57*, 3383-3388.

67. Hetrick, E.M.; Schoenfisch, M.H., "Reducing implant-related infections: Active release strategies." *Chem. Soc. Rev.* **2006**, *35*, 780-9.

68. Wong, S.Y.; Li, Q.; Veselinovic, J.; Kim, B.-S.; Klibanov, A.M.; Hammond, P.T., "Bactericidal and virucidal ultrathin films assembled layer by layer from polycationic N-alkylated polyethylenimines and polyanions." *Biomaterials* **2010**, *31*, 4079-4087.

69. Nelson, C.L.; Hickmon, S.G.; Skinner, R.A., "Treatment of experimental osteomyelitis by surgical debridement and the implantation of bioerodable, polyanhydride-gentamicin beads." *J. Orthopaed. Res.* **1997**, *15*, 249-255.

70. Risbud, M.V.; Bhonde, R.R., "Polyacrylamide-chitosan hydrogels: In vitro biocompatibility and sustained antibiotic release studies." *Drug. Deliv.* **2000**, *7*, 69-75.

71. Radin, S.; El-Bassyouni, G.; Vresilovic, E.J.; Schepers, E.; Ducheyne, P., "In vivo tissue response to resorbable silica xerogels as controlled-release materials." *Biomaterials* **2005**, *26*, 1043-1052.

72. Radin, S.; Ducheyne, P., "Controlled release of vancomycin from thin sol-gel films on titanium alloy fracture plate material." *Biomaterials* **2007**, *28*, 1721-1729.

73. Simchi, A.; Tamjid, E.; Pishbin, F.; Boccaccini, A.R., "Recent progress in inorganic and composite coatings with bactericidal capability for orthopaedic applications." *Nanomed-Nanotechnol.* **2011**, *7*, 22-39.

74. Adams, C.S.; Antoci, V.; Harrison, G.; Patal, P.; Freeman, T.A.; Shapiro, I.M.; Parvizi, J.; Hickok, N.J.; Radin, S.; Ducheyne, P., "Controlled release of vancomycin from thin sol-gel films on implant surfaces successfully controls osteomyelitis." *J. Orthopaed. Res.* **2009**, *27*, 701-709.

75. Gao, P.; Nie, X.; Zou, M.; Shi, Y.; Cheng, G., "Recent advances in materials for extended-release antibiotic delivery system." *J. Antibiot.* **2011**, *64*, 625-34.

76. Neut, D.; van de Belt, H.; van Horn, J.R.; van der Mei, H.C.; Busscher, H.J., "Residual gentamicin-release from antibiotic-loaded polymethylmethacrylate beads after 5 years of implantation." *Biomaterials* **2003**, *24*, 1829-1831.

77. Gürsel, I.; Korkusuz, F.; Türesin, F.; Alaeddinoglu, N.G.; Hasirci, V., "In vivo application of biodegradable controlled antibiotic release systems for the treatment of implant-related osteomyelitis." *Biomaterials* **2001**, *22*, 73-80.

78. Gerhart, T.N.; Roux, R.D.; Horowitz, G.; Miller, R.L.; Hanff, P.; Hayes, W.C., "Antibiotic release from an experimental biodegradable bone cement." *J. Orthopaed. Res.* **1988**, *6*, 585-92.

79. Hanssen, A., "Prophylactic use of antibiotic bone cement: an emerging standard--in opposition." *J. Arthroplasty* **2004**, *19*, 73.

80. Nathan, C.F.; Hibbs, J.B., "Role of nitric oxide synthesis in macrophage antimicrobial activity." *Curr. Opin. Immunol.* **1991**, *3*, 65-70.

81. MacMicking, J.; Xie, Q.-w.; Nathan, C., "Nitric oxide and macrophage function." *Annu. Rev. Immunol.* **1997**, *15*, 323-350.

82. Bogdan, C., "Nitric oxide and the immune response." *Nat. Immunol.* **2001**, *2*, 907-16.

83. Fang, F.C., "Perspectives series : Host / pathogen interactions." *J. Clin. Invest.* **1997**, *99*, 2818-2825.

84. MacMicking, J.D.; Nathan, C.; Hom, G.; Chartrain, N.; Fletcher, D.S.; Trumbauer, M.; Stevens, K.; Xie, Q.W.; Sokol, K.; Hutchinson, N., "Altered responses to bacterial infection and endotoxic shock in mice lacking inducible nitric oxide synthase." *Cell* **1995**, *81*, 641-50.

85. Brunelli, L.; Crow, J.P.; Beckman, J.S., "The comparative toxicity of nitric oxide and peroxynitrite to Escherichia coli." *Arch. Biochem. Biophys.* **1995**, *316*, 327-334.

86. Xia, Y.; Zweier, J.L., "Superoxide and peroxynitrite generation from inducible nitric oxide synthase in macrophages." *Proc. Natl. Acad. Sci USA* **1997**, *94*, 6954-8.

87. Carpenter, A.W.; Schoenfisch, M.H., "Nitric oxide release: part II. Therapeutic applications." *Chem. Soc. Rev.* **2013**, *41*, 3742-52.

88. Jones, M.L.; Ganopolsky, J.G.; Labbé, A.; Wahl, C.; Prakash, S., "Antimicrobial properties of nitric oxide and its application in antimicrobial formulations and medical devices." *Appl. Microbiol. Biot.* **2010**, *88*, 401-7.

89. Beckman, J.S.; Beckman, T.W.; Chen, J.; Marshall, P.A.; Freeman, B.A., "Apparent hydroxyl radical production by peroxynitrite: Implications for endothelial injury from nitric oxide and superoxide." *Proc. Natl. Acad. Sci USA* **1990**, *87*, 1620-1624.

90. Privett, B.J.; Broadnax, A.D.; Bauman, S.J.; Riccio, D.A.; Schoenfisch, M.H., "Examination of bacterial resistance to exogenous nitric oxide." *Nitric Oxide-Biol. Ch.* **2012**, *26*, 169-173.

91. Feelisch, M.; Kelm, M., "Biotransformation of organic nitrates to nitric oxide by vascular smooth muscle and endothelial cells." *Biochem. Bioph. Res. Co.* **1991**, *180*, 286-293.

92. Ford, P.C.; Bourassa, J.; Miranda, K.; Lee, B.; Lorkovic, I.; Boggs, S.; Kudo, S.; Laverman, L., "Photochemistry of metal nitrosyl complexes. Delivery of nitric oxide to biological targets." *Coordin. Chem. Rev.* **1998**, *171*, 185-202.

93. Arnelle, D.R.; Stamler, J.S., "NO^+, NO^-, and NO^- donation by S-nitrosothiols: Implications for regulation of physiological functions by S-nitrosylation and acceleration of disulfide formation." *Arch. Biochem. Biophys.* **1995**, *318*, 279-285.

94. Hrabie, J.A.; Klose, J.R.; Wink, D.A.; Keefer, L.K., "New nitric oxide-releasing zwitterions derived from polyamines." *J. Org. Chem.* **1993**, *58*, 1472-1476.

95. Keefer, L.K., "Fifty years of diazeniumdiolate research. From laboratory curiosity to broad-spectrum biomedical advances." *ACS Chem. Biol.* **2011**, *6*, 1147-1155.

96. Page, I.H.; Corcoran, A.C.; Dustan, H.P.; Koppanyi, T., "Cardiovascular actions of sodium nitroprusside in animals and hypertensive patients." *Circulation* **1955**, *11*, 188-198.

97. Chen, Z.; Zhang, J.; Stamler, J.S., "Identification of the enzymatic mechanism of nitroglycerin bioactivation." *Proc. Natl. Acad. Sci USA* **2002**, *99*, 8306-8311.

98. Chen, Z.; Foster, M.W.; Zhang, J.; Mao, L.; Rockman, H.A.; Kawamoto, T.; Kitagawa, K.; Nakayama, K.I.; Hess, D.T.; Stamler, J.S., "An essential role for mitochondrial aldehyde dehydrogenase in nitroglycerin bioactivation." *Proc. Natl. Acad. Sci USA* **2005**, *102*, 12159-12164.

99. Sydow, K.; Daiber, A.; Oelze, M.; Chen, Z.; August, M.; Wendt, M.; Ullrich, V.; Mülsch, A.; Schulz, E.; Keaney, J.F., "Central role of mitochondrial aldehyde dehydrogenase and reactive oxygen species in nitroglycerin tolerance and cross-tolerance." *J. Clin. Invest.* **2004**, *113*, 482-489.

100. Ignarro, L.J.; Lippton, H.; Edwards, J.C.; Baricos, W.H.; Hyman, A.L.; Kadowitz, P.J.; Gruetter, C.A., "Mechanism of vascular smooth muscle relaxation by organic nitrates, nitrites, nitroprusside and nitric oxide: Evidence for the involvement of S-nitrosothiols as active intermediates." *J. Pharmacol. Exp. Ther.* **1981**, *218*, 739-749.

101. Drago, R.S.; Paulik, F.E., "The reaction of nitrogen (I1) oxide with diethylamine." *J. Am. Chem. Soc.* **1960**, *82*, 96-98.

102. Drago, S.R.K., B.R., "The reaction of nitrogen (II) oxide with various primary and secondary amines." *J. Am. Chem. Soc.* **1961**, *83*, 1819-1822.

103. Ignarro, L.J.; Buga, G.M.; Wood, K.S.; Byrns, R.E., "Endothelium-derived relaxing factor produced and released from artery and vein is nitric oxide." *P. Natl. Acad. Sci. USA* **1987**, *84*, 9265-9269.

104. Carpenter, A.W.; Slomberg, D.L.; Rao, K.S.; Schoenfisch, M.H., "Influence of scaffold size on bactericidal activity of nitric oxide-releasing silica nanoparticles." *ACS Nano* **2011**, *5*, 7235-44.

105. Riccio, D.A.; Nugent, J.L.; Schoenfisch, M.H., "Stöber synthesis of nitric oxide-releasing S-nitrosothiol-modified silica particles." *Chem. Mater.* **2011**, *23*, 1727-1735.

106. Shin, J.H.; Metzger, S.K.; Schoenfisch, M.H., "Synthesis of nitric oxide-releasing silica nanoparticles." *J. Am. Chem. Soc.* **2007**, *129*, 4612-4619.

107. Shin, J.H.; Schoenfisch, M.H., "Inorganic/organic hybrid silica nanoparticles as a nitric oxide delivery scaffold." *Chem. Mater.* **2007**, *20*, 239-249.

108. Stasko, N.A.; Schoenfisch, M.H., "Dendrimers as a scaffold for nitric oxide release." *J. Am. Chem. Soc.* **2006**, *128*, 8265-8271.

109. Stasko, N.A.; Fischer, T.H.; Schoenfisch, M.H., "S-nitrosothiol-modified dendrimers as nitric oxide delivery vehicles." *Biomacromolecules* **2008**, *9*, 834-841.

110. Lu, Y.; Sun, B.; Li, C.; Schoenfisch, M.H., "Structurally diverse nitric oxide-releasing poly(propylene imine) dendrimers." *Chem. Mater.* **2012**, *23*, 4227-4233.

111. Nablo, B.J.; Chen, T.Y.; Schoenfisch, M.H., "Sol-gel derived nitric-oxide releasing materials that reduce bacterial adhesion." *J. Am. Chem. Soc.* **2001**, *123*, 9712-3.

112. Marxer, S.M.; Rothrock, A.R.; Nablo, B.J.; Robbins, M.E.; Schoenfisch, M.H., "Preparation of nitric oxide (NO)-releasing sol-gels for biomaterial applications." *Chem. Mater.* **2003**, *15*, 4193-4199.

113. Nablo, B.J.; Rothrock, A.R.; Schoenfisch, M.H., "Nitric oxide-releasing sol-gels as antibacterial coatings for orthopedic implants." **2005**, *26*, 917-924.

114. Nablo, B.J.; Schoenfisch, M.H., "Antibacterial properties of nitric oxide-releasing sol-gels." *J. Biomed. Mater. Res. A* **2003**, *67*, 1276-83.

115. Nichols, S. P.; Schoenfisch, M. H., "Nitric oxide flux-dependent bacterial adhesion and viability at fibrinogen-coated surfaces." *Biomater. Sci. 10.1039/C3BM60130G [Available online July 17, 2013]*.

116. Hetrick, E.M.; Schoenfisch, M.H., "Antibacterial nitric oxide-releasing xerogels: Cell viability and parallel plate flow cell adhesion studies." *Biomaterials* **2007**, *28*, 1948-1956.

117. Nablo, B. J.; Rothrock, A. R.; Schoenfisch, M. H., "Nitric oxide-releasing sol-gels as antibacterial coatings for orthopedic implants." *Biomaterials* **2005**, *26*, 917-924.

118. Cai, W.; Wu, J.; Xi, C.; Meyerhoff, M.E., "Diazeniumdiolate-doped poly(lactic-*co*-glycolic acid)-based nitric oxide releasing films as antibiofilm coatings." *Biomaterials* **2012**, *33*, 7933-7944.

119. Barraud, N.; Hassett, D.J.; Hwang, S.-H.; Rice, S.A.; Kjelleberg, S.; Webb, J.S., "Involvement of nitric oxide in biofilm dispersal of Pseudomonas aeruginosa." *J. Bacteriol.* **2006**, *188*, 7344-7353.

120. Nablo, B.J.; Prichard, H.L.; Butler, R.D.; Klitzman, B.; Schoenfisch, M.H., "Inhibition of implant-associated infections via nitric oxide release." *Biomaterials* **2005**, *26*, 6984-6990.

121. Holt, J.; Hertzberg, B.; Weinhold, P.; Storm, W., Schoenfisch, M.; Dahners, L. "Decreasing bacterial colonization of external fixation pins via nitric oxide release coatings." *J. Orthop. Trauma* **2011**, *25*, 432-437.

122. Mowery, K.A.; Schoenfisch, M.H.; Saavedra, J.E.; Keefer, L.K.; Meyerhoff, M.E., "Preparation and characterization of hydrophobic polymeric films that are thromboresistant via nitric oxide release." *Biomaterials* **2000**, *21*, 9-21.

123. Riccio, D.A.; Dobmeier, K.P.; Hetrick, E.M.; Privett, B.J.; Paul, H.S.; Schoenfisch, M.H., "Nitric oxide-releasing S-nitrosothiol-modified xerogels." *Biomaterials* **2009**, *30*, 4494-4502.

124. Hetrick, E.M.; Prichard, H.L.; Klitzman, B.; Schoenfisch, M.H., "Reduced foreign body response at nitric oxide-releasing subcutaneous implants." *Biomaterials* **2007**, *28*, 4571-80.

125. Nichols, S.P.; Le, N.N.; Klitzman, B.; Schoenfisch, M.H., "Increased in vivo glucose recovery via nitric oxide release." *Anal. Chem.* **2011**, *83*, 1180-4.

126. Nichols, S.P.; Koh, A.; Storm, W.L.; Shin, J.H.; Schoenfisch, M.H., "Biocompatible materials for continuous glucose monitoring devices." *Chem. Rev.* **2013**, *113*, 2528-49.

127. Ratner, B.D., "Reducing capsular thickness and enhancing angiogenesis around implant drug release systems." *J. Control. Release* **2002**, *78*, 211-8.

128. Chernousova, S.; Epple, M., "Silver as antibacterial agent: Ion, nanoparticle, and metal." *Angew. Chem. Int. Edit.* **2013**, *52*, 1636-53.

129. Stickler, D.J., "Biomaterials to prevent nosocomial infections: Is silver the gold standard?" *Curr. Opin Infect. Dis.* **2000**, *13*, 389-393.

130. Silver, S.; Phung, L.T.; Silver, G., "Silver as biocides in burn and wound dressings and bacterial resistance to silver compounds." *J. Ind. Microbiol. Biot.* **2006**, *33*, 627-34.

131. Bologna, R.A.; Tu, L.M.; Polansky, M.; Fraimow, H.D.; Gordon, D.A.; Whitmore, K.E., "Hydrogel/silver ion-coated urinary catheter reduces nosocomial urinary tract infection rates in intensive care unit patients: A multicenter study." *Urology* **1999**, *54*, 982-987.

132. Wu, P.; Grainger, D.W., "Drug/device combinations for local drug therapies and infection prophylaxis." *Biomaterials* **2006**, *27*, 2450-67.

133. Marini, M.; De Niederhausern, S.; Iseppi, R.; Bondi, M.; Sabia, C.; Toselli, M.; Pilati, F., "Antibacterial activity of plastics coated with silver-doped organic-inorganic hybrid coatings prepared by sol-gel processes." *Biomacromolecules* **2007**, *8*, 1246-1254.

134. Stobie, N.; Duffy, B.; McCormack, D.E.; Colreavy, J.; Hidalgo, M.; McHale, P.; Hinder, S.J., "Prevention of Staphylococcus epidermidis biofilm formation using a low-temperature processed silver-doped phenyltriethoxysilane sol-gel coating." *Biomaterials* **2008**, *29*, 963-969.

135. Brun-Buisson, C.; Doyon, F.; Sollet, J.-P.; Cochard, J.-F.; Cohen, Y.; Nitenberg, G., "Prevention of intravascular catheter-related infection with newer chlorhexidine-silver sulfadiazine-coated catheters: A randomized controlled trial." *Intens. Care. Med.* **2004**, *30*, 837-843.

136. Bosetti, M.; Massè, A.; Tobin, E.; Cannas, M., "Silver coated materials for external fixation devices: In vitro biocompatibility and genotoxicity." *Biomaterials* **2002**, *23*, 887-892.

137. Kumar, A.; Vemula, P.K.; Ajayan, P.M.; John, G., "Silver-nanoparticle-embedded antimicrobial paints based on vegetable oil." *Nat. Mater.* **2008**, *7*, 236-241.

138. Jung, W. K.; Koo, H. C.; Kim, K. W.; Shin, S.; Kim, S. H.; Park, Y. H., "Antibacterial activity and mechanism of action of the silver ion in Staphylococcus aureus and Escherichia coli." *Appl. Environ. Microb.* **2008**, *74*, 2171-2178.

139. Feng, Q. L.; Wu, J.; Chen, G. Q.; Cui, F. Z.; Kim, T. N.; Kim, J. O., "A mechanistic study of the antibacterial effect of silver ions on Escherichia coli and Staphylococcus aureus." *J. Biomed. Mater. Res.* **2000**, *52*, 662-668.

140. Xiu, Z.-m.; Zhang, Q.-b.; Puppala, H. L.; Colvin, V. L.; Alvarez, P. J. J., "Negligible particle-specific antibacterial activity of silver nanoparticles." *Nano Lett.* **2012**, *12*, 4271-4275.

141. Dubas, S.T.; Kumlangdudsana, P.; Potiyaraj, P., "Layer-by-layer deposition of antimicrobial silver nanoparticles on textile fibers." *Colloid Surface A.* **2006**, *289*, 105-109.

142. Cortese-Krott, M.M.; Münchow, M.; Pirev, E.; Heβner, F.; Bozkurt, A.; Uciechowski, P.; Pallua, N.; Kröncke, K.-D.; Suschek, C.V., "Silver ions induce

oxidative stress and intracellular zinc release in human skin fibroblasts." *Free Radical Bio. Med.* **2009**, *47*, 1570-1577.

143. Hidalgo, E.; Domínguez, C., "Study of cytotoxicity mechanisms of silver nitrate in human dermal fibroblasts." **1998**, *98*, 169-179.

144. Asharani, P.; Wu, Y.L.; Gong, Z.; Valiyaveettil, S., "Toxicity of silver nanoparticles in zebrafish models." *Nanotechnology* **2008**, *19*, 255102.

145. Wan, A.T.; Conyers, R.A.; Coombs, C.J.; Masterton, J.P., "Determination of silver in blood, urine, and tissues of volunteers and burn patients." *Clin. Chem.* **1991**, *37*, 1683-7.

146. Hardes, J.; Ahrens, H.; Gebert, C.; Streitbuerger, A.; Buerger, H.; Erren, M.; Gunsel, A.; Wedemeyer, C.; Saxler, G.; Winkelmann, W.; Gosheger, G., "Lack of toxicological side-effects in silver-coated megaprostheses in humans." *Biomaterials* **2007**, *28*, 2869-2875.

147. Trop, M.; Novak, M.; Rodl, S.; Hellbom, B.; Kroell, W.; Goessler, W., "Silver-coated dressing acticoat caused raised liver enzymes and argyria-like symptoms in burn patient." *J. Traum. Ac. Care. Surg.* **2006**, *60*, 648-652.

148. Liu, J.; Hurt, R.H., "Ion release kinetics and particle persistence in aqueous nano-silver colloids." *Environ. Sci. Technol.* **2010**, *44*, 2169-2175.

149. Xiu, Z.-m.; Zhang, Q.-b.; Puppala, H.L.; Colvin, V.L.; Alvarez, P.J.J., "Negligible particle-specific antibacterial activity of silver nanoparticles." *Nano Lett.* **2012**, *12*, 4271-4275.

150. Silver, S., "Bacterial silver resistance: Molecular biology and uses and misuses of silver compounds." *FEMS Microbiol. Rev.* **2003**, *27*, 341-353.

151. Gupta, A.; Matsui, K.; Lo, J.-F.; Silver, S., "Molecular basis for resistance to silver cations in Salmonella." *Nat. Med.* **1999**, *5*, 183-188.

152. Chopra, I., "The increasing use of silver-based products as antimicrobial agents: a useful development or a cause for concern?" *J Antimicrob. Chemoth.* **2007**, *59*, 587-590.

153. Schierholz, J.; Rump, A.; Pulverer, G.; Beuth, J., "Anti-infective catheters: Novel strategies to prevent nosocomial infections in oncology." *Anticancer Res.* **1998**, *18*, 3629-3638.

Chapter 2:

Nitric Oxide-Releasing Xerogels Synthesized from *N*-Diazeniumdiolate-Modified Silane Precursors

2.1 Introduction

For more than half of a century, researchers have developed materials capable of controllably releasing bioactive agents in vivo.[1] While timed pharmacological release of a drug or gene were initial goals,[2] much of the recent work has focused on the release of therapeutics from surfaces/coatings in an effort to enhance the function and biocompatibility of medical implants or devices.[3] For example, surfaces that release antibiotics and antimicrobial agents have been studied extensively as a strategy for reducing hospital-acquired infections associated with medical devices such as stents, catheters, and orthopedic implants.[4] By foregoing traditional means of administration (e.g., oral and intravenous) and relegating the drug or agent to the drug-releasing surface, therapeutic concentrations are maintained in the immediate vicinity of the implant while toxicity common to systemic delivery is avoided. Nitric oxide (NO) has garnered recent attention as an active release agent due to its broad activity, short half-life, and established presence in human physiology.[4-6]

Nitric oxide is a reactive radical that modulates a seemingly interminable number of physiological processes.[7, 8] Surface-generated NO has been shown to reduce bacterial adhesion and viability, platelet adhesion, and several deleterious consequences of the foreign body response (e.g., inflammation, avascularization and collagen capsule formation).[5, 6, 9-12] As NO is a gas at ambient pressures and temperatures, its controlled

release from a device or coating is best achieved chemically using donor species that decompose into NO. To this end, researchers have designed macromolecular scaffolds modified with *N*-diazeniumdiolate or *S*-nitrosothiol functional groups capable of generating NO at controlled rates (Scheme 2.1).[13-21]

Surfaces that slowly release NO are of particular importance for developing more biocompatible medical device coatings due to their ability to reduce biofouling and mitigate the foreign body response. The sol-gel synthesis of xerogel materials represents one method for facilitating NO release. Xerogels are attractive as biomaterials due to inherently mild synthetic conditions (e.g., aqueous solvents, low temperature), a high degree of material tailorability, and the capacity for enzyme immobilization with retained enzyme activity.[22, 23] Xerogels may be prepared using any number of precursor silanes, including those necessary for storing NO (e.g., amine- and thiol-bearing silanes that offer sites for *N*-diazeniumdiolate or *S*-nitrosothiol formation, respectively).[18, 21, 24] Careful selection of organically modified precursors provides a route to control surface area, pore structure, and hydrophobicity.[25] These attributes allow for the release of NO (and other therapeutic agents)[26,27,28] from the xerogel network while simultaneously allowing diffusion of external species into the xerogel. Coupling the beneficial attributes of NO release with glucose sensor membranes has thus been proposed as a means for developing more functional sensors.[29-31]

Previously, NO-releasing xerogels were prepared by forming an amine-functionalized matrix that was subsequently exposed to high pressures of NO (5 bar) to facilitate *N*-diazeniumdiolate formation.[5,10,13,22] While these films liberated NO under physiological conditions (37 ^{o}C, pH 7.4) at fluxes sufficient to reduce bacterial

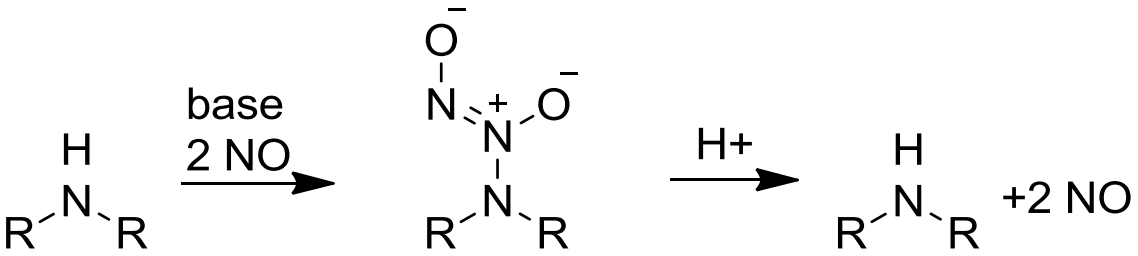

Scheme 2.1 Formation of *N*-diazeniumdiolates on secondary amines and pH-dependent decomposition to produce NO.

Adhesion (> ~1.5 pmol NO cm^{-2} s^{-1}),[12] lower the incidence of implant infections,[5, 32] and mitigate the FBR,[11] practical issues with their synthesis limited their potential utility. First, the conversion of amines to *N*-diazeniumdiolates after film synthesis required that the underlying substrate be exposed to high pressures of NO, an impractical step for many materials and medical devices. Secondly, the *N*-diazeniumdiolate conversion efficiencies from the secondary amines to NO donors for stable compositions were only 5-25%.[21] Finally, glucose oxidase-based sensors formed using these materials had low glucose sensitivities and limited hydrogen peroxide permeability due to network densification caused by the *N*-diazeniumdiolate formation process.[31, 33]

We hypothesize that the formation of *N*-diazeniumdiolates on aminosilane precursors prior to film formation may improve glucose sensor attributes while increasing NO loading (Scheme 2.2). The use of different *N*-diazeniumdiolate precursors may also enable improved tuning of both NO release totals and durations from these materials. In contrast to post-diazeniumdiolated materials that are generally impermeable to small polar analytes such as hydrogen peroxide, we expect that pre-diazeniumdiolated xerogels not requiring exposure to high pressures of NO will function more effectively as glucose sensor membranes

2.2 Materials and methods

N-2-(aminoethyl)-aminopropyltrimethoxysilane (AEAP), *N*-ethylaminoisobutyltrimethoxysilane (EAiB), *N*-methylaminopropyltrimethoxysilane (MAP), *N*-6-(aminohexyl)aminopropyltrimethoxysilane (AHAP), n-propyltrimethoxysilane (PTMOS), and isobutyltrimethoxysilane (BTMOS) were

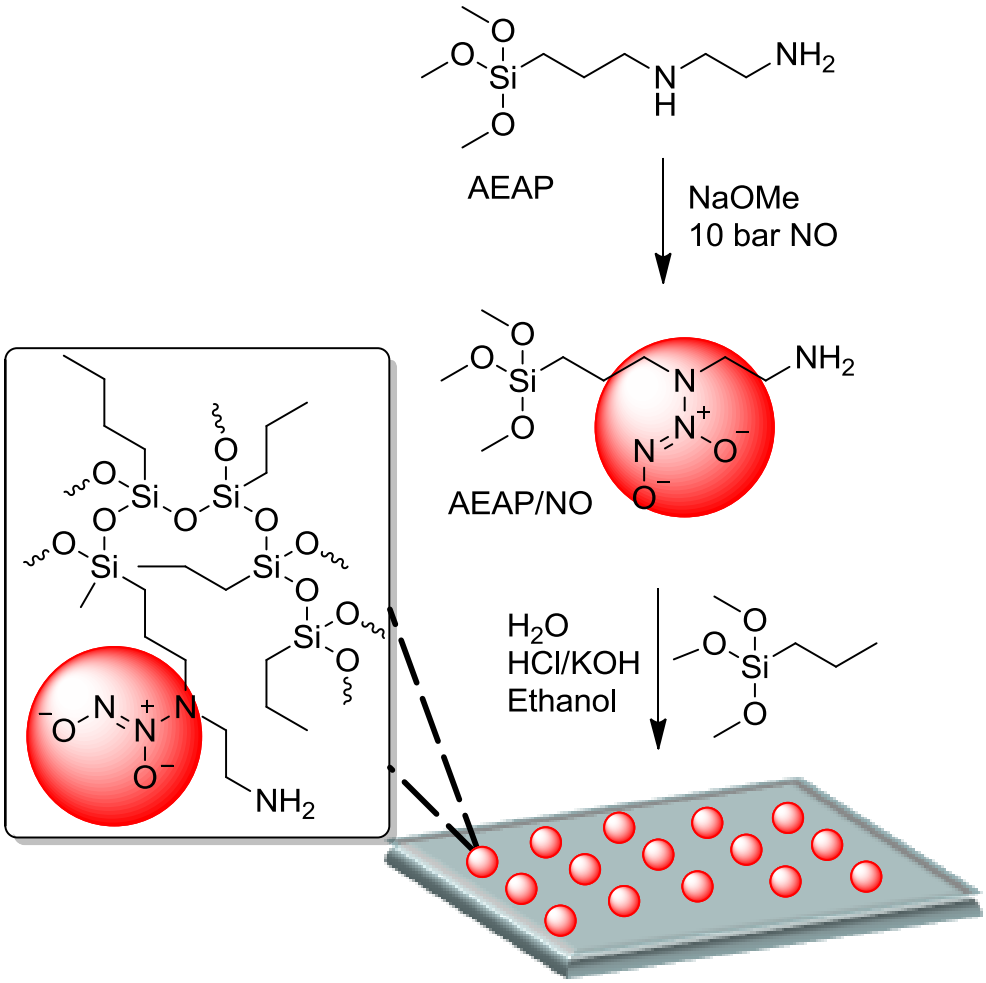

Scheme 2.2 Synthesis of the "pre-diazeniumdiolated" NO-releasing xerogels. After reacting AEAP with NO to yield AEAP/NO, the *N*-diazeniumdiolated precursor is reacted with PTMOS, and cast onto an appropriate substrate. Subsequent drying/curing results in the formation of an *N*-diazeniumdiolate-modified xerogel film.

purchased from Gelest (Tullytown, PA). Methyltrimethoxysilane (MTMOS), glucose oxidase, and D-glucose were purchased from Sigma Aldrich (St. Louis, MO). Nitric oxide gas was purchased from Praxair (Bethlehem, PA). Nitric oxide calibration (26.85 ppm, balance N_2) and argon gasses were purchased from Airgas National Welders (Durham, NC). Sodium methoxide (5.4 M in methanol) was purchased from Acros Organics (Fairlawn, NJ). Milli-Q water with a resistivity of <18.2 mΩ cm and a total organic content of <6 ppb was prepared by purifying distilled water using a Millipore Milli-Q UV Gradient A-10 system (Bedford, MA). Fibroblast L929 cells were acquired from the UNC tissue culture facility (Chapel Hill, NC). Dulbecco's modified essential media (DMEM), (3-(4,5-dimethylthiazol-2-yl)-5-(3-carboxymethoxyphenyl)-2-(4-sulfophenyl)-2H-tetrazolium) (MTS) and phenazine methosulfate (PMS) were acquired from Becton, Dickinson and Company (Sparks, MD). All other reagents were analytical grade and used as received.

2.2.1 Synthesis of N-diazeniumdiolate-modified silanes and xerogels

Silanes functionalized with *N*-diazeniumdiolates were prepared by dissolving 250 μL of the aminosilane (i.e., AEAP, EAiB, MAP) into 1750 μL of methanolic sodium methoxide (1 molar equivalent of sodium methoxide per secondary amine). The vials were placed in a 250 mL stainless steel Parr bomb, flushed with 100 psi argon for 6 cycles (three rapid, three for 10 min each), and then held at 10 bar NO for 3 d to yield the *N*-diazeniumdiolate silane form, or AEAP/NO, EAiB/NO and MAP/NO. After 3d, the vessel was purged with 100 psi argon for an additional 6 cycles (three rapid, three 10 min) prior to sample removal. Both prior to and following NO addition, great care was

taken to purge the vessel slowly (~50 psi min^{-1}) to avoid solvent evaporation. Indeed, no solvent loss was observed during the *N*-diazeniumdiolate-modification process. The solutions were transferred as-is into sealed vials, placed in vacuum-evacuated foil bags ("vacuum sealed") using a commercial MiniPack-Torre MV31 vacuum sealer (Orange, CA) and stored at -20 ^{o}C until further use.

Commercially pure, grade 3 titanium substrates (10 mm x 10 mm x 1 mm) were etched in 50% v/v sulfuric acid at 60 ^{o}C for 1 h with intermittent agitation. The substrates were then rinsed copiously with deionized water and their surfaces activated by exposing them to a solution of piranha (3 parts conc. sulfuric acid to 1 part 30% v/v hydrogen peroxide) for 10 min. Due to the highly reactive nature of this solution, care was taken to ensure that secondary containment and full personal protective equipment were used. Following additional rinsing, the substrates were ultrasonicated for 10 min in milli-Q water and stored in clean milli-Q until use.

Xerogel films containing covalently bound *N*-diazeniumdiolate precursors were synthesized via a two-step, one-pot reaction by combining either AEAP/NO, MAP/NO, or EAiB/NO with pre-hydrolyzed PTMOS. First, PTMOS (117, 111, or 105 μL for 5, 10, 15%, respectively) was prehydrolyzed by adding 100 μL ethanol and 0.1 M hydrochloric acid (10 μL) and mixing for 1 h. Following pre-hydrolysis of the backbone silane, water, ethanol, base catalyst (at an excess to the initial amount of acid added so that the solution was basic) and *N*-diazeniumdiolate-modified silanes were added as follows for each system: *15 mol% MAP/NO-PTMOS*: 196 μL ethanol, 79.6 μL water, 36 μL 0.5M KOH, and 164.8 μL MAP/NO; *15 mol% EAiB/NO-PTMOS*: 166 μL ethanol, 43.6 μL water, 72 μL 0.5 M KOH, 194.8 μL EAiB/NO; *15 mol% AEAP/NO-PTMOS:* 174 μL ethanol, 23

μL water, 36 μL 0.5 M KOH, 184.8 μL AEAP/NO. For 5 and 10 mol% xerogels, one- or two-thirds volumes of the silane/NO solutions were added instead of the amounts listed above, with total volumes kept constant via the addition of pure ethanol. Following reaction, 20 μL aliquots of the resulting sol was cast onto titanium substrates, pre-dried at 60 ^{o}C for 10 min, and then further cured under vacuum at 60 ^{o}C for 3 d.

2.2.2 Characterization of N-diazeniumdiolate-modified silanes and xerogels

Release of NO from *N*-diazeniumdiolate-modified precursor silanes and xerogels was measured using a Sievers 280 Nitric Oxide Analyzer (NOA; Boulder, CO). The NOA instrument was first calibrated using an NO zero tube (0 ppm NO) and an NO calibration tank (26.85 ppm, balance N_2). Approximately 30 mL of phosphate buffered saline (PBS; 10 mM, pH 7.4) was placed in a flask fitted with a porous frit and deoxygenated with nitrogen. During NO analysis, the instrument's flow uptake of 200 mL min^{-1} was matched by supplying nitrogen through the submerged frit at a flow rate of 80 mL min^{-1} with the remaining 120 mL min^{-1} supplied to the headspace of the vessel through a glass side arm, sweeping any liberated NO into the instrument's reaction cell. To calculate the conversion efficiency of the *N*-diazeniumdiolate NO donors, the following equation was used:

$$\%\ conversion = \frac{moles\ total\ NO\ released/2}{moles\ total\ silane} x\ 100\% \quad \text{(eq 2.1)}$$

Conversion of amines to *N*-diazeniumdiolate NO donors was confirmed using a Thermo Scientific Evolution Array UV-visible spectrophotometer. After reaction with NO, the aminosilane solutions were diluted to 50 μM total silane (i.e., by using the concentration of the parent aminosilane before charging) in 1.0 M sodium hydroxide. To calculate the molar absorptivity coefficient (ε), the total *N*-diazeniumdiolate content was

assumed to be equal to half of the total NO release (as determined via chemiluminescence).

ESI/MS was employed in positive ion mode to confirm formation of the *N*-diazeniumdiolate-modified aminosilanes. Sodiated product ions for MAP/NO, EAiB/NO and AEAP/NO were observed at m/z 298.03 (theor. 298.08), 326.11 (theor. 326.11) and 327.10 (theor. 327.11), respectively.

To assess the stability of the NO-releasing xerogels, substrates were submerged in 5 mL PBS and incubated at 37 ^{o}C. Films were transferred to new soak solutions after 4 and 7 d and ultimately removed after 14 d. To quantify material stability, the Si concentrations within the soak solutions were determined using inductively coupled plasma optical emission spectrometry (ICP-OES). A standard calibration curve was constructed using 0, 500, 1000, 5000, and 10000 ppb Si (via sodium silicate) in PBS. Each mole of silicon in solution was assumed to correlate directly with silanes that disassociated from the scaffold through rehydrolysis of siloxane bonds or unreacted silanes that leached out of the matrix. Total % leaching was determined by integrating the total Si leaching concentration over the 14 d period and dividing by the number of moles of Si in each film. To determine surfaces areas, nitrogen adsorption isotherms were acquired using a Micromeretics TriStar II 3020 (Norcross, GA) and analyzed via the Brunauer-Emmet-Teller (BET) method.[34] Elemental analysis was carried out using a PerkinElmer CHN/S O elemental analyzer Series 2400 (Waltham, MA). For both elemental and BET measurements, samples were prepared by casting an equivalent volume of sol per unit area substrate onto pre-cleaned (10 min sonication in water,

ethanol, and acetone) glass slides, drying accordingly, and mechanically removing the resulting films from the substrate via scraping.

2.2.3 Cytotoxicity

Leachate solutions (i.e., solutions that the xerogels were submerged in) from pre-diazeniumdiolated xerogels were evaluated for toxicity against L929 fibroblast cells. Leachate solutions were prepared by incubating the films for 1 week in 10 mL PBS at 37 ^{o}C. Cells were grown to confluence at 37 ^{o}C in a 5% CO_2/95% O_2 humidified environment in DMEM supplemented with 10% (v/v) fetal bovine serum (FBS) and 1 wt% penicillin/streptomycin. Following surface desorption of the cells by trypsinization, the suspension was diluted with additional DMEM, centrifuged for 10 min (1200 rpm, 4 ^{o}C), and resuspended in an equivalent volume of media. Cells were seeded in a 96-well plate, supplying additional media and an equal volume of leachate solutions so that the total cell concentration was 3 x 10^5 cells mL^{-1}. Following two days of incubation at 37 ^{o}C, cell viability was determined by removing excess media and replacing with MTS/PMS reagents in DMEM. After an additional 1 h of incubation at 37 ^{o}C, the absorbance of the MTS product was measured spectrophotometrically at 490 nm using a Thermo Scientific Multiskan EX plate reader. After accounting for the absorbance from blank wells (i.e., those containing no MTS), the results were normalized to PBS controls.

2.2.4 Fabrication and performance NO-releasing glucose sensors

Xerogel-coated enzymatic glucose sensors were prepared on insulated platinum disc macroelectrodes (total radius of 0.30 cm). Sol-gel immobilized glucose oxidase (GOx) was first deposited on the bare polished electrodes as described previously.[30, 31] After allowing the sensing layer to dry, 6.43 μL (20 μL cm^{-2}) 15 mol% AEAP/NO-

PTMOS sols were cast over the sensing layer, dried at 40 ^{o}C for 10 min and dried in vacuo at 40 ^{o}C for 3 d. Following curing, the sensors were stored at -20 ^{o}C under N_2 until further use.

The analytical performance of both post-diazeniumdiolated and pre-diazeniumdiolated AEAP/NO glucose membranes was assessed using a CH Instruments 1030A potentiostat configured with a 3-electrode platform; the glucose sensor, an Ag/AgCl electrode and a platinum wire served as the working, reference, and counter electrodes, respectively. Electrodes were submerged in 50 mL of 10 mM PBS at room temperature and pre-hydrated for one hour at a potential of +0.6 V vs. Ag/AgCl. The permeability ($P_{H_2O_2}$) of each xerogel-modified electrode was determined in 10 μM H_2O_2 solution from the oxidation current at both bare ($\Delta i_{(bare)}$) and AEAP/NO-PTMOS-coated ($\Delta i_{(coated)}$) electrodes using the following equation:

$$P_{H_2O_2} = \frac{\Delta i_{(coated)}}{\Delta i_{(bare)}} \times 100\% \quad \text{(eq 2.2)}$$

The glucose sensing properties of the membranes were determined by adding successive aliquots of 1.0 M D-Glucose in 3 μM increments until reaching a final concentration of 30 μM.

2.3 Results and discussion

2.3.1 N-diazeniumdiolate formation on aminosilanes

Prior to xerogel formation, it was first necessary to prepare and characterize the *N*-diazeniumdiolate-functionalized aminosilane precursors. We hypothesized that significant NO loading would occur on the aminosilane precursors when exposed to NO in the presence of exogenous base. Solvent type as well as aminosilane and sodium methoxide concentrations were varied to maximize amine to *N*-diazeniumdiolate NO

donor conversion efficiencies while minimizing the formation of byproducts. Initially, ethanol and methanol were tested; however, ethanol formed an NO-releasing byproduct under the conditions used herein.[35] Thus, only methanol was employed. Methanol proved superior as the solvent as it dissolved both the sodium methoxide base and each aminosilane (structures illustrated in Figure 2.1) successfully. In the absence of sodium methoxide, intramolecular amines in the AEAP precursor are able to serve as bases. Nevertheless, negligible diazeniumdiolate formation was observed as calculated from NO-release data (~5.3% conversion efficiency), indicating the need for a stronger base to optimize NO loading in methanol. Although reports have indicated the formation of sodium formate from methoxide and NO,[36] this byproduct does not decompose to release NO and is thus considered benign for our purposes. The alternative base suggested by DeRosa and coworkers (i.e., sodium trimethylsilanolate) is not compatible with silanes as it reacts to form polysiloxanes.[37] As such, all further *N*-diazeniumdiolate-modified silane preparation was carried out using 12.5% (v/v) aminosilane in methanol with 1.0 molar equivalent sodium methoxide per secondary amine.

Nitric oxide release totals and kinetics from *N*-diazeniumdiolate-modified silanes were characterized using chemiluminescence.[38] As provided in Table 2.1, *N*-diazeniumdiolate formation and subsequent NO release (theoretical release of two mol NO per mol of *N*-diazeniumdiolate NO donor) varied significantly with the structure of the precursor aminosilane. The conversion of secondary amines to *N*-diazeniumdiolate NO donors was greatest for the monoamines (MAP and EAiB at ~70%) and least for the diamine AEAP (~50%). The lower conversion for AEAP is attributed to stabilization of 2^o amines by neighboring 1^o amines. While changes in chemical structure may impact the

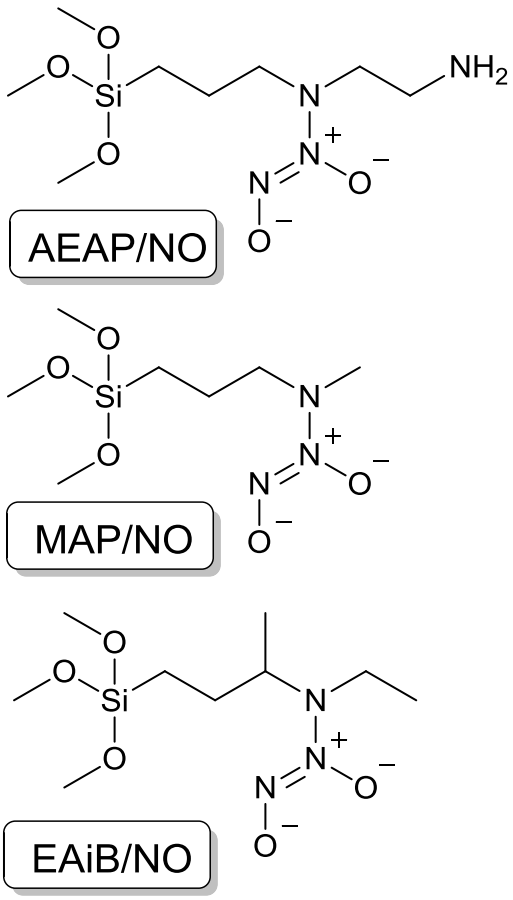

Figure 2.1 Chemical structures of the *N*-diazeniumdiolate-modified aminosilanes used to fabricate NO-releasing xerogels.

Table 2.1 Nitric oxide release, conversion efficiency, and spectroscopic parameters of *N*-diazeniumdiolate-modified silanes.

aminosilane	**$[NO]_t$ (μmol NO μmol^{-1} silane)**[a]	**half-life (min)**	**λ_{max}(nm)**	**ε (mM^{-1} cm^{-1})**
AEAP	0.98 ± 0.17[c]	130 ± 20	251	14.4 ± 2.5
MAP	1.47 ± 0.21	2.0 ± 0.3	249	10.0 ± 0.1
EAiB	1.38 ± 0.07	7.9 ± 1.7	249	9.5 ± 0.1

[a] Theoretical maximum of 2 mol NO per mol amine-functionalized silane

[b] Concentration of *N*-diazeniumdiolate-modified silane taken from chemiluminescent NO release totals

[c] Values are given as the mean ± standard deviation from at least n=3 independent syntheses

NO addition efficiency, they also control the resulting NO-release kinetics. For example, the NO release from EAiB/NO had a slightly longer $t_{1/2}$ than MAP/NO (7.9 and 2.0 min, respectively), due to increased organic character protecting the *N*-diazeniumdiolate from proton-initiated decomposition. The diamine-based aminosilane in this study, AEAP/NO, exhibited an NO release half-life of more than an order of magnitude longer (120 min) than either of the monoamine silanes as a result of hydrogen-bonding stabilization from the 1^{o} amine.[39]

The presence of a strong UV absorption band at a wavelength of ~250 nm confirmed successful *N*-diazeniumdiolate NO donor formation (Figure 2.2). Molar absorptivity coefficients (ε, Table 4.1**)** were calculated by using the absorbance at λ_{max} along with *N*-diazeniumdiolate concentrations inferred through chemiluminescent NO release totals. For all silanes, the molar absorptivity coefficients proved to be within the range of previously observed values (7 – 20 mM^{-1} cm^{-1}).[40, 41]

The long-term stability of the precursor solutions was evaluated by measuring their NO release after approximately 6 months of storage in a vacuum sealed container at -20 ^{o}C. The change in the resulting NO-release profiles was minimal for each system (Figure 2.3). As a result, long-term storage did not hamper NO-release capacity from the xerogels formed using these precursors.

2.3.2 Xerogel synthesis

Successful formation of stable *N*-diazeniumdiolate-modified xerogels required study of several reaction parameters in the initial sol including backbone silane identity, aminosilane concentration, acid and base catalyst concentration, water:silane ratio, and reaction time. Both the stability of the resulting xerogel framework and the *N*-

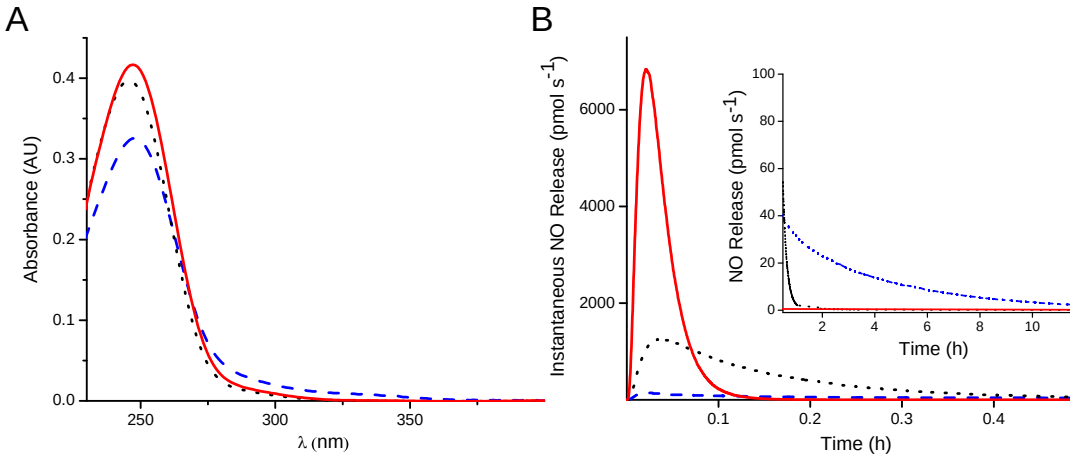

Figure 2.2 A) UV-vis spectra and B) NO-release curves of AEAP/NO (blue dashed line), MAP/NO (red solid line), and EAiB/NO (black dotted line) precursors. Absorption spectra were obtained at a concentration of 50 mM in 1 M NaOH. Nitric oxide release was measured in PBS (pH 7.4, 10 mM).

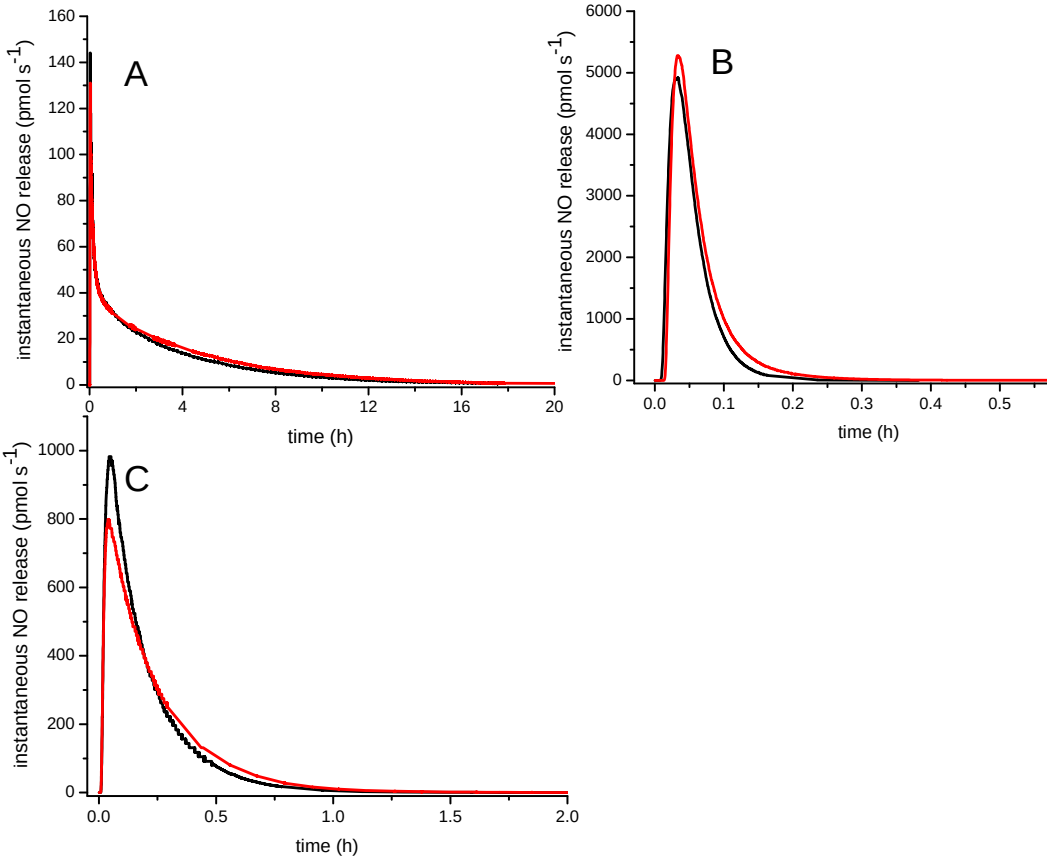

Figure 2.3 Nitric oxide release from (A) AEAP/NO, (B) MAP/NO and (C) EAiB/NO either immediately after synthesis (red line) or vacuum sealed at -20 ^{o}C for approximately 6 months (black line).

diazeniumdiolate groups contained within were evaluated upon all synthetic variations. Titanium was chosen as the substrate for the materials due to its common use in biomedical implants and ability to stably adhere the xerogel films.[42]

Although sol-gel synthesis of xerogels often employs only an acid catalyst, a base catalyst had to be incorporated during this synthesis to avoid proton-initiated decomposition of the *N*-diazeniumdiolate NO donors. Initially, a one-step hydrolysis and co-condensation of the backbone and *N*-diazeniumdiolate-modified silanes under basic conditions was attempted. While films synthesized in this manner appeared well-cured on the benchtop, xerogels made from this procedure were unstable when submerged in PBS (~20% total Si leached into solution). This instability is attributed to inadequate connectivity between the backbone silane (PTMOS) and the aminosilane. Indeed, previous reports have indicated the importance of well-matched reaction kinetics when co-condensing alkoxysilanes via the sol-gel method.[43] To remedy this instability, a two-step reaction was adapted to fabricate xerogels with *N*-diazeniumdiolated silane concentrations of up to 15 mol%. Of note, larger concentrations yielded physically unstable xerogels regardless of the synthetic strategy employed. As aminosilanes exhibit faster gelation times than n-alkylated silanes,[44] the PTMOS backbone was first pre-hydrolyzed in 4.9 mM HCl prior to the addition of the *N*-diazeniumdiolated aminosilane. Further increasing acid concentrations to 24.5 mM and 49.0 mM HCl destabilized the xerogel (as determined via leaching), suggesting that hydrolysis and condensation rates are well-matched at the optimal acid concentration of 4.9 mM. Experiments conducted with other backbone silanes also illustrated the need for similar hydrolysis and condensation rates. For example, the xerogels displayed a significant amount of cracking,

even at relatively low water:silane ratios (3.2) and reaction times (1 h), when 15 mol% AEAP/NO, MAP/NO, and EAiB/NO films were synthesized using an MTMOS backbone. Conversely, films synthesized using bulkier BTMOS did not adequately cure and remained highly viscous and tacky even after catalyst-assisted reaction and drying. When using PTMOS as the backbone, stable, non-tacky films were synthesized by adjusting water:silane ratios. For AEAP/NO-PTMOS, 3.2 H_2O:Si was ideal, while 10:1 ratios of H_2O:Si were necessary to form stable MAP/NO-PTMOS and EAiB/NO-PTMOS xerogels. Reactions involving EAiB/NO were particularly torpid, requiring an additional increase in base catalyst concentration for adequate cocondensation. The bulky, hydrophobic nature of EAiB/NO-PTMOS, and to a lesser extent MAP/NO-PTMOS, xerogels was further evidenced by xerogel opacity that developed after extended soaking in PBS. As these films were translucent in dry, ambient conditions, this is strong evidence of microsyneresis—a phenomenon that occurs in organic gels when a polymer exhibits greater affinity for itself than its surrounding solvent (i.e., a hydrophobic polymer surrounded by water).[45]

2.3.3 Xerogel NO-release characterization

We hypothesized that xerogels synthesized from *N*-diazeniumdiolate-modified silanes would provide enhanced NO loading per amine relative to post-diazeniumdiolated xerogels. Post-diazeniumdiolated xerogels rely on deprotonation of 2^o amines by neighboring amines within the scaffold to facilitate xerogel formation. Thus, NO release is limited by base (i.e., internal amine) availability. Addition of exogenous bases is not feasible, as silica constructs are often unstable in high pH conditions.[25] Since the xerogels in this work were synthesized from silanes converted to *N*-diazeniumdiolates prior to

network formation, conversion of secondary amines to *N*-diazeniumdiolates was enhanced without compromising network stability. To confirm this hypothesis, the NO release from pre-diazeniumdiolated xerogels was measured in physiologically relevant conditions (PBS at 37 ^{o}C and pH 7.4) using chemiluminescence (NOA) and compared to that of post-diazeniumdiolated xerogels.

As expected, 15 mol% pre-diazeniumdiolated xerogels released orders of magnitude more NO than post-diazeniumdiolated xerogels at equivalent aminosilane mol percentages (Table 2.2). This increase was greatest for MAP/NO-PTMOS and EAiB/NO-PTMOS xerogels due to their low NO donor conversion efficiencies when post-diazeniumdiolated—a finding consistent with the hypothesis that amines within the xerogels are responsible for deprotonation necessary for *N*-diazeniumdiolate formation. When diamine-containing xerogels are post-diazeniumdiolated, the overall amine content is larger and the close proximity of intramolecular amines makes deprotonation more likely. In turn, post-diazeniumdiolated AEAP/NO-PTMOS xerogels release more NO than post-diazeniumdiolated MAP/NO-PTMOS and EAiB/NO-PTMOS. Nonetheless, each pre-diazeniumdiolated xerogel system studied released greater levels of NO than post-diazeniumdiolated systems (at equivalent mol%).

With respect to NO totals, the pre-diazeniumdiolated AEAP/NO-PTMOS, MAP/NO-PTMOS, and EAiB/NO-PTMOS xerogels released 2.6, 2.4, and 3.2 μmol NO cm^{-2}, respectively. When synthesized with 15 mol% *N*-diazeniumdiolated silane precursors, the NO storage capacity (i.e., the percentage of secondary amines that are *N*-diazeniumdiolate-modified) of these xerogels was 52.8% for EAiB/NO-PTMOS and approximately ~40% for both AEAP/NO-PTMOS and MAP/NO-PTMOS xerogels.

Table 2.2 Nitric oxide release characteristics from *N*-diazeniumdiolate modified xerogels measured using chemiluminescence

Silane	mol% silane	total NO ($\mu mol\ cm^{-2}$)	max flux ($pmol\ cm^{-2}\ s^{-1}$)	half-life (h)	duration[a] (h)
AEAP	5	0.55 ± 0.05[b]	73.8 ± 5.0	5.7 ± 0.2	29.2 ± 7.6
AEAP	10	1.75 ± 0.53	193 ± 83	6.4 ± 2.1	52.4 ± 13.4
AEAP	15	2.60 ± 0.60	307 ± 101	4.0 ± 0.5	41.7 ± 4.0
MAP	5	0.39 ± 0.04	162 ± 71	1.7 ± 1.3	11.1 ± 0.95
MAP	10	1.41 ± 0.35	262 ± 93	3.1 ± 1.3	27.7 ± 7.4
MAP	15	2.40 ± 0.51	590 ± 174	1.9 ± 0.7	35.7 ± 6.4
EAiB	5	0.45 ± 0.04	126 ± 8	3.8 ± 1.2	20.4 ± 1.9
EAiB	10	1.48 ± 0.09	439 ± 9	2.6 ± 0.5	48.8 ± 10.5
EAiB	15	3.13 ± 0.40	312 ± 142	4.2 ± 1.7	90.8 ± 22.6

[a] Time until flux drops below a threshold of 1.5 pmol $cm^{-2}\ s^{-1}$, i.e., the flux required to inhibit bacterial adhesion.

[b] Values are given as the mean ± standard deviation from at least n=3 independent syntheses

These losses are a result of both incomplete conversion of the precursors and *N*-diazeniumdiolate degradation during synthesis (Tables 2.1 and 2.3). Of note, AEAP/NO-PTMOS and MAP/NO-PTMOS released equivalent levels of NO (2.40 and 2.60 μmol cm^{-2}, respectively) despite the much greater 74% conversion efficiency of secondary amines to *N*-diazeniumdiolates in the MAP/NO precursor (compared to 49% for AEAP/NO). This disparity is best explained by the fast release kinetics of the MAP/NO small molecule. While NO donor degradation during reaction of the sol was negligible (Figure 2.4), a significant loss of NO occured during the initial 10 min of drying. Such NO loss ceases once the materials/coatings are placed under vacuum. Thus, NO loss during synthesis will be most drastic for those systems with rapid *N*-diazeniumdiolate decomposition kinetics. As such, NO retention (i.e., the percentage of *N*-diazeniumdiolates remaining after xerogel synthesis) is greatest for AEAP/NO-PTMOS and EAiB/NO-PTMOS xerogels at 80.7 and 74.9%, respectively, and least (56.8%) for MAP/NO-PTMOS xerogels (Table 2.3).

Elemental analysis of the xerogel films (Table 2.4) confirmed that the mass percentage of nitrogen (%N) in the xerogels increased with increasing mol% of *N*-diazeniumdiolated precursors. As expected from its diamine structure, 15 mol% AEAP/NO-PTMOS xerogels were found to have the largest %N. In using the %N in each xerogel to calculate a theoretical NO release, it was found that CHN overestimated NO totals by 16-35%. We attribute this difference to residual nitrite in the matrix that is present from NO loss during synthesis. Supporting this hypothesis, the magnitude by which this overestimation occurs for each system trends remarkably well with the amount

Table 2.3 Nitric oxide release totals and conversion efficiency from both pre- and post-diazeniumdiolated xerogels.

xerogel (15 mol%) balance PTMOS	storage capacity[a] (%)		NO retention[b] (%)
	post-diazeniumdiolated	pre-diazeniudiolated	pre-diazeniumdiolated
AEAP	0.40 ± 0.12[c]	39.6 ± 9.1	80.7 ± 18.6
MAP	0.034 ± 0.01	41.7 ± 8.9	56.8 ± 12.1
EAiB	0.078 ± 0.03	51.6 ± 6.6	74.9 ± 9.6

[a] Percentage of *N*-diazeniumdiolates in the film compared to the total amount of secondary amines contained within

[b] Percentage of *N*-diazeniumdiolates in the film compared to the total amount of *N*-diazeniumdiolate-modified precursors added

[c] Values are given as the mean ± standard deviation from at least n=3 independent syntheses

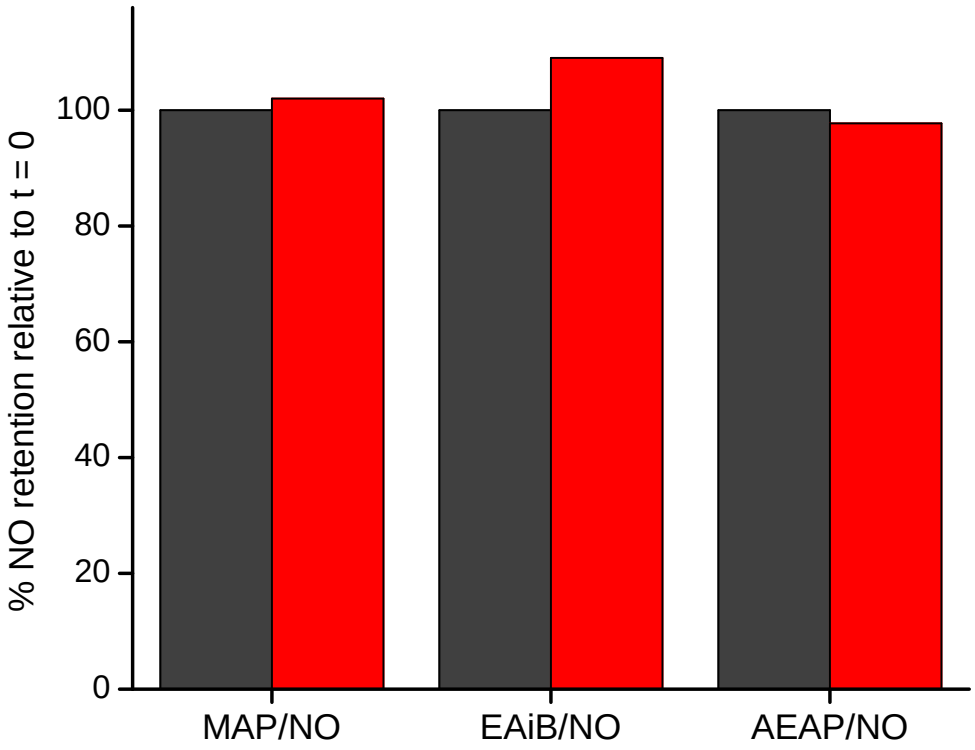

Figure 2.4 Total NO release from MAP/NO, EAiB/NO, and AEAP/NO sols before (black bar; left) and after (red bar; right) the sol-gel reaction. Data is normalized to the "0" reaction time, which was acquired immediately after addition of the *N*-diazeniumdiolate NO donor (n=1).

Table 2.4 Carbon, hydrogen, and nitrogen content of pre-diazeniumdiolated xerogels as determined via elemental combustion analysis.

Xerogel	%C	%H	%N
5% MAP/PTMOS	36.11 ± 1.01[a]	7.42 ± 0.03	1.19 ± 0.24
10% MAP/PTMOS	35.24 ± 0.18	7.02 ± 0.14	2.80 ± 0.17
15% MAP/PTMOS	33.84 ± 0.32	6.85 ± 0.08	4.26 ± 0.58
15% AEAP/PTMOS	32.63 ± 0.27	6.67 ± 0.09	5.91 ± 0.33
15% EAiB/PTMOS	33.96 ± 3.73	6.55 ± 0.13	4.06 ± 0.09

[a] Values are given as the mean ± standard deviation from at least n=3 independent syntheses

of NO lost during synthesis for the respective systems (MAP/NO-PTMOS > EAiB/NO-PTMOS > AEAP/NO-PTMOS) (Table 2.5).

The NO release from the *N*-diazeniumdiolate-modified xerogels synthesized in this work was tunable by varying the aminosilane identity. As shown in Table 2.2, MAP/NO-PTMOS xerogels have the shortest NO release half-lives (1.9 h) and durations (35.7 h), consistent with the rapid decomposition of the MAP/NO precursor. While MAP/NO has an NO-release half-life nearly 60 times lower than AEAP/NO (2.0 and 130 min, respectively), this difference is much less pronounced from the xerogels themselves. The NO-release half-life of the AEAP/NO-PTMOS xerogels was only twice as long as MAP/NO-PTMOS xerogels, demonstrating that the hydrophobicity of the xerogel matrix has a significant influence on the NO release rates versus any intramolecular *N*-diazeniumdiolate stabilization by 1^{o} amines. The non-polar EAiB/NO precursor clearly increased matrix hydrophobicity (evidenced by the microsyneresis phenomenon described above), slowing NO release kinetics. Others have reported the accumulation of hydroxide ions within hydrophobic NO-donor matrices as the *N*-diazeniumdiolates decompose.[6] This phenomenon would further contribute to prolonged NO release due to enhanced *N*-diazeniumdiolate donor stability at elevated pH. The longer NO-release duration (90.8 h) for 15 mol% EAiB/NO-PTMOS xerogels would thus be expected relative to the other systems.

The largest maximum NO flux obtainable using these materials (590 pmol cm^{-2} s^{-1}) exceeds the flux required for a ~90% reduction in bacterial adhesion in vitro (25–30 pmol cm^{-2} s^{-1} for *E. coli, S. aureus, and P. aeruginosa*).[4, 46] The maximum NO fluxes from each film (Table 2.2 and Figure 2.5) potentially raise concerns, as large NO

Table 2.5 Comparison of NO release totals measured directly using chemiluminescence with NO release totals predicted by elemental analysis.

Xerogel (15 mol%)	predicted μmol NO mg^{-1}	experimental μmol NO mg^{-1}	% error
MAP/PTMOS	1.35[a]	1.03	35.0
AEAP/PTMOS	1.21	1.00	17.5
EAiB/PTMOS	1.45	1.22	18.9

[a] Values are given as the mean from at least n=3 independent syntheses

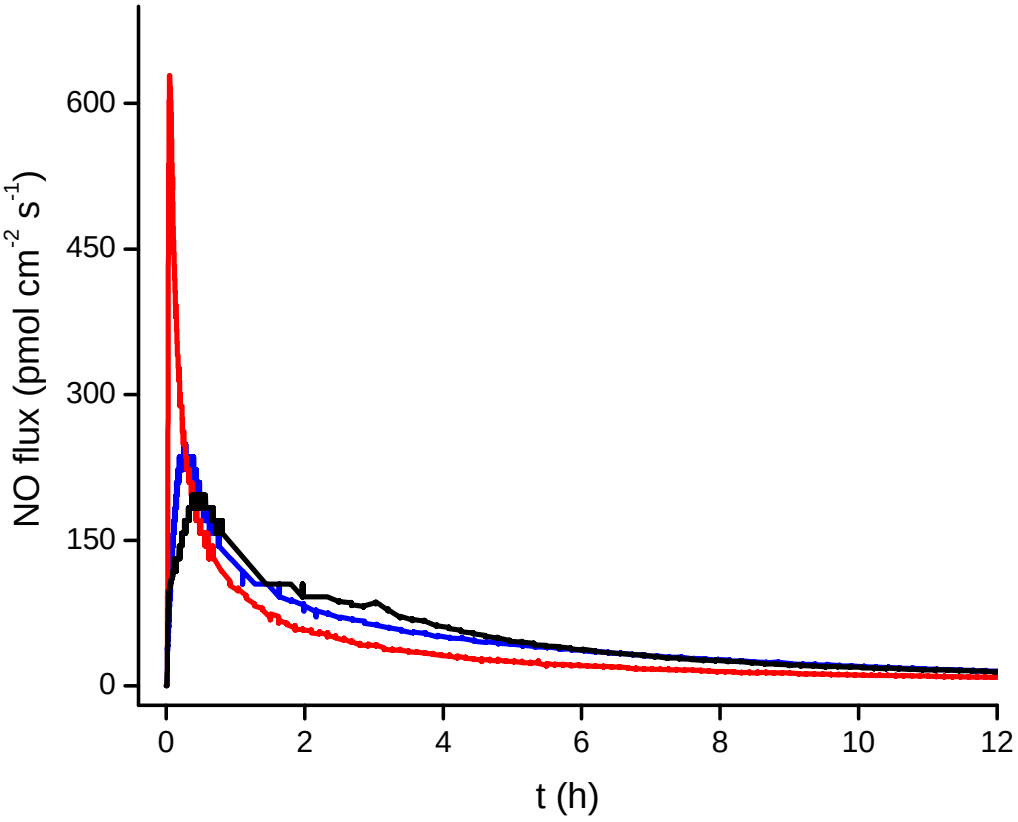

Figure 2.5 The initial 12 h of NO release from 15 mol% MAP/NO-PTMOS (red), EAiB/NO-PTMOS (black) and AEAP/NO-PTMOS (blue). During measurement, films submerged in 30 mL PBS (pH 7.4) at 37 ^{o}C.

concentrations may promote undesirable inflammation.[47] However, previous studies have assesed the FBR as a function of NO-release kinetics, and demonstrated no ill effect on localized inflammation for materials with far greater maximum NO fluxes (~1440 pmol cm^{-2} s^{-1} vs. 700 pmol cm^{-2} s^{-1} for the xerogels herein).[10] Of note, the 15 mol% xerogel systems presented above have NO-release properties and kinetics comparable to NO-releasing polyurethane membranes reported to reduce in vivo inflammation and collagen capsule thickness (total NO = 3.0 μmol cm^{-2} and NO flux at 48 h = 1.13 pmol cm^{-2} s^{-1}).[10]

As detailed earlier, xerogels synthesized using *N*-diazeniumdiolate-modified silanes exhibited physical instability (i.e., fragmentation in aqueous solution) when formed with concentrations exceeding of 15 mol%. In contrast, stable post-diazeniumdiolated xerogels have been reported up to concentrations of approximately 30 mol%.[21] As such, the NO release of pre-diazeniumdiolated xerogels at their highest mole percentage were compared to materials containing even greater mole percentages of post-diazeniumdiolated xerogels. Using a similar two-step reaction, post-diazeniumdiolated xerogels prepared using AHAP (40 vol%, 31 mol%) and BTMOS demonstrated efficacy in combatting bacterial and fungal adhesion in vitro, preventing infection, and alleviating the foreign body response in vivo.[5, 11, 12, 48] This system released a total of 3.3 ± 0.6 μmol NO cm^{-2}, nearly equivalent to the 15 mol% EAiB/NO xerogels synthesized herein. The similar NO release totals between these two systems illustrates the larger conversion efficiency of pre-diazeniumdiolated xerogel systems, despite the difference in total aminosilane incorporation.

2.3.4 Xerogel stability

To assess the physical stability of the *N*-diazeniumdiolate-modified xerogels, films were immersed in PBS (pH 7.4, 37 ^{o}C) for 4, 7, and 14 d. Subsequent analysis of the soak solutions was carried out using ICP-OES. The amount of silicon in the solutions was assumed to correlate to silane leaching from the silica network, and would represent poor physical integrity of the xerogels upon solution immersion. As shown in Figure 2.6 and Table 2.6, the xerogels leached <5 mol% of their total silicon content, indicating excellent stability under these solution conditions. Marxer and coworkers characterized leaching in a similar manner from post-diazeniumdiolated xerogels.[21] While one composition (40% AEMP/BTMOS) only exhibited <0.5 mol% Si loss after two weeks, 40% AHAP/BTMOS films lost 8.3 mol% Si content after two weeks in 37 ^{o}C PBS.[21] To evaluate the potential cytotoxicity of these systems, we tested leaching solutions from the largest mol% xerogel of each aminosilane (corresponding to the films with the greatest degree of instability) against L929 murine fibroblast cells. After 24 hours of exposure to an equal volume of leachate solution and media, no significant toxicity was observed relative to PBS controls (Figure 2.7) indicating negligible leaching.

In addition to the physical stability of the silica network, the chemical stability of the *N*-diazeniumdiolate functionalities within the xerogel was also considered. Release of NO from pre-diazeniumdiolated 15 mol% AEAP/NO-PTMOS xerogels was measured immediately following xerogel synthesis and again following 10 d of vacuum-sealed storage at -20 ^{o}C, vacuum sealed storage at room temperature, and storage under ambient conditions. No significant reduction in NO storage was observed when the xerogels were vacuum sealed, regardless of temperature. Xerogels stored on the benchtop (and thus exposed to ambient humidity) lost ~60% NO over the same period (Table 2.7). While

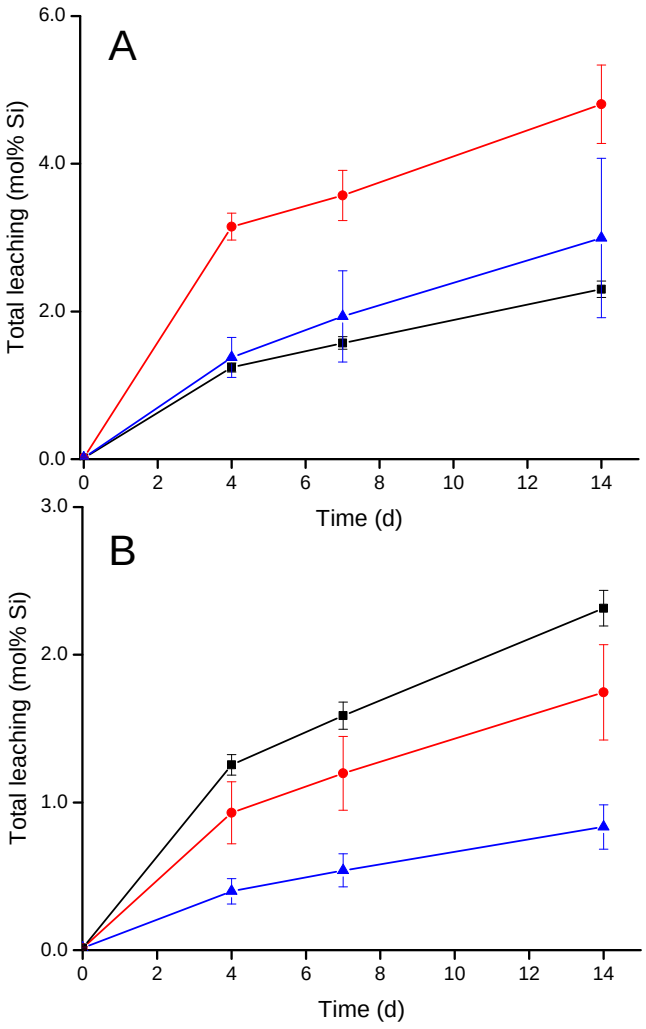

Figure 2.6 Silicon leaching from pre-diazeniumdiolated xerogels as a function of NO donor A) identity and B) concentration. Silicon content was measured at 4, 7, and 14 d from A) 15 mol% AEAP/NO-PTMOS (black square), MAP/NO-PTMOS (red diamond), and EAiB/NO-PTMOS (blue triangle) and B) 5 (blue triangle), 10 (red diamond) and 15 mol% (black square) AEAP. Error bars represent the standard deviation of the mean from n=3 independent syntheses.

Table 2.6 Total amount of silicon liberated from each xerogel system after 14 d. Xerogels were stored in 10 mM PBS (pH 7.4, 37 oC) and transferred to new solutions at 4 or 7 d. Cumulative Si concentrations are the integrated totals from each time point as determined via ICP-OES.

Aminosilane	mol %	Cumulative Si concentration (ppm)	% Fragmentation
AEAP	5	1.08 ± 0.19[a]	0.82 ± 0.14
AEAP	10	2.28 ± 0.41	1.73 ± 0.31
AEAP	15	3.03 ± 0.15	2.30 ± 0.11
MAP	5	1.70 ± 0.33	1.50 ± 0.29
MAP	10	4.09 ± 0.34	3.60 ± 0.30
MAP	15	5.46 ± 0.60	4.81 ± 0.53
EAiB	5	1.57 ± 0.87	1.39 ± 0.76
EAiB	10	3.69 ± 1.87	3.25 ± 1.65
EAiB	15	3.40 ± 1.22	3.00 ± 1.08

[a] Values are given as the mean ± standard deviation from at least n=3 independent syntheses

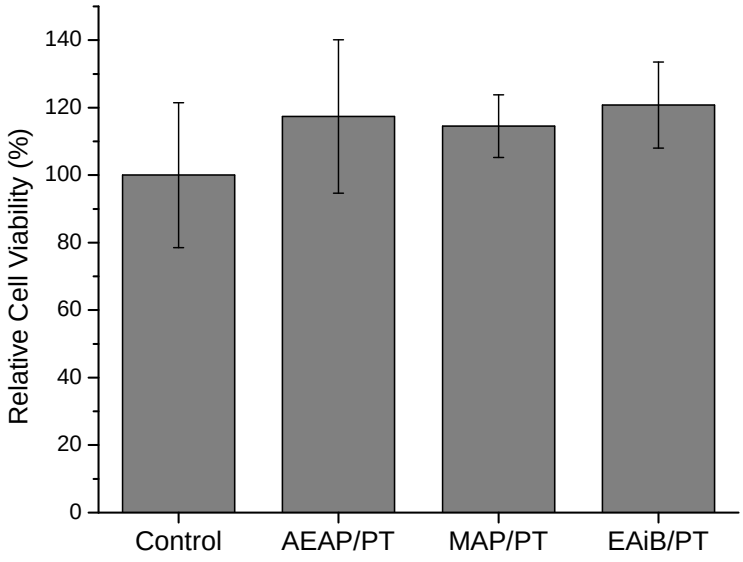

Figure 2.7 Cytotoxicity of AEAP/PT, MAP/PT, and EAiB/PT leachate solutions against L929 fibroblast cells. Error bars represent the standard deviation of the mean from n=3 independently prepared samples.

Table 2.7 Nitric oxide release totals from 15 mol% AEAP/PT xerogels when stored in different atmospheric conditions and temperatures for 10 d. The control xerogel was analyzed immediately after drying. Each film was analyzed in 30 mL PBS (pH 7.4, 37 ^{o}C) (n=1).

Storage conditions	**Temperature**	**NO Total (μmol cm^{-2})**
Control	Control	2.1
Vacuum sealed	-20 ^{o}C	2.0
Vacuum sealed	23 ^{o}C	2.2
Ambient	23 ^{o}C	0.8

decomposition of the *N*-diazeniumdiolate NO donors in solution is strongly dependent on temperature, elevated temperatures alone were not observed to initiate NO release until a certain threshold (typically much larger temperature) is reached. For example, Batchelor and coworkers observed the decomposition of lipophilic *N*-diazeniumdiolate compounds at temperatures above 104 ^{o}C.[49] Thus, storage in a vacuum-sealed container, free from water, is sufficient for maintaining NO storage for the materials described herein.

2.3.5 Electrochemical glucose sensor membranes

Nitric oxide has a number of properties that make it favorable for release from the surface of an implanted electrochemical sensor. For example, several problems that disrupt these devices such as excessive collagen encapsulation, avascularization, and infection are mitigated through the release of NO.[50] In prior work, we reported that glucose biosensors coated with post-diazeniumdiolated xerogels exhibited poor sensitivity to glucose.[31, 33] This result was attributed to decreased analyte permeability through the sensor membrane after NO charging. Shin and colleagues hypothesized that NO catalyzed xerogel condensation, thus reducing the overall porosity of the material and greatly limiting analyte (e.g., glucose permeability.[31] We hypothesized that these pre-diazeniumdiolated xerogels might have greater porosity than post-diazeniumdiolated xerogels due to slower hydrolysis and condensation reactions. In this respect, the coatings would prove useful as outer glucose sensor membranes.[51] Electrochemical glucose biosensors were fabricated with xerogel membranes synthesized from *N*-diazeniumdiolate-modified xerogels; specifically, 15 mol% AEAP/NO-PTMOS was used as it represented a highly stable system. A two-layer sensor membrane was cast onto a platinum disc working electrode with an Ag/AgCl reference. The bottom layer contained

glucose oxidase immobilized within an MTMOS sol-gel, while either a pre-diazeniumdiolated or post-diazeniumdiolated 15 mol% AEAP/NO-PTMOS xerogel comprised the outer-most layer. This two-layer approach mirrors previous work carried out by our laboratory previously.[30, 31, 33]

The hydrogen peroxide (H_2O_2) permeability of the NO-releasing sensor membranes was determined by measuring the oxidation current for the xerogel-modified electrodes relative to bare electrodes at +0.6 V (vs. Ag/AgCl). Consistent with previous work, post-diazeniumdiolated sensor membranes exhibited responses below our limit of detection ($P_{H_2O_2} < 0.01\%$). As expected, the $P_{H_2O_2}$ for pre-diazeniumdiolated xerogels was more than an order of magnitude larger. To determine if a larger overall surface area explained the enhanced permeability, the specific surface area of pre-diazeniumdiolated xerogels was measured and compared to post-diazeniumdiolated xerogels. Indeed, the specific surface area of post-diazeniumdiolated 15 mol% AEAP/NO-PTMOS was <0.1 $m^2\ g^{-1}$ while the specific surface area of its pre-diazeniumdiolated equivalent was 2.1 $m^2\ g^{-1}$.

Next, we determined if the increased permeability led to an improved sensor response. Using the same electrode configuration, D-glucose was added to PBS to achieve final glucose concentrations from 3 to 30 mM (Figure 2.8) Of note, +0.6 V was employed as the working electrode potential to limit interference by oxidation of NO.[29, 30] Perhaps not surprising given the increased analyte permeability, sensors fitted with pre-diazeniumdiolated xerogel membranes featured larger glucose sensitivities than post-diazeniumdiolated xerogels (3.4 nA mM^{-1} and < 0.1 nA mM^{-1}, respectively). Consistent with this observation, previously reported post-diazeniumdiolated xerogels (20 mol%

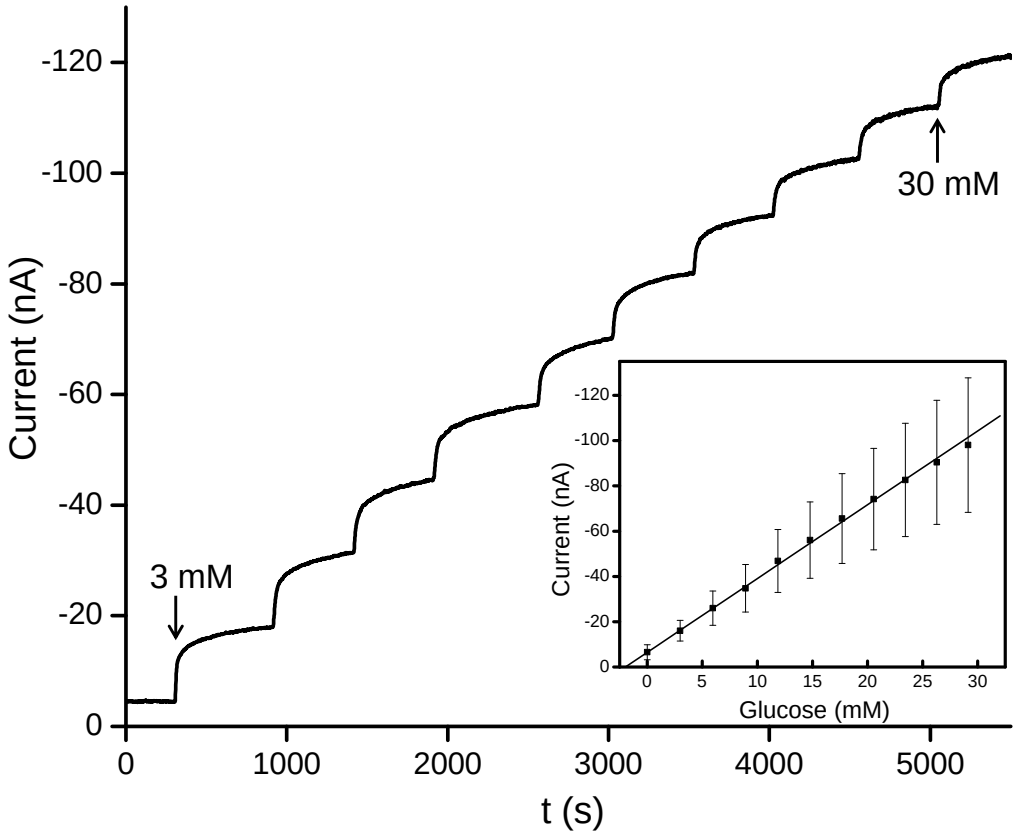

Figure 2.8 Representative calibration curve for glucose biosensors coated with 15 mol% AEAP/NO-PTMOS xerogels, both real-time (main graph) and as a function of glucose concentration (inset). Error bars represent the standard deviation of the mean from n=3 independently synthesized sensor membranes.

AEAP, balance BTMOS) constructed by Schoenfisch and coworkers suffered from a similarly low glucose sensitivity (0.14 nA mM^{-1}) that was addressed via inclusion of a hydrophilic polymer within the xerogel membrane.[33] When compared to other sensors that do not generate NO, the sensitivity observed using 15% AEAP/NO-PTMOS membranes was similar in magnitude.[52, 53]

To verify the viability of these membranes for continuous glucose monitoring, glucose measurements were repeated after soaking the electrodes in PBS for 4 and 7 d. As illustrated in Table 2.8, the change in glucose sensitivity was only 3.6% after one week of soaking in physiological buffer. With increasing soak time the dynamic range increased and the glucose response time decreased, likely a result of greater hydration of the enzymatic membrane over time. Nonetheless, the membranes proved functional over clinically relevant diabetic patient glucose concentrations without pre-soaking beyond the 3 h pre-hydration period. The in vitro sensitivity reported here is similar to NO-releasing sensors evaluated by Gifford and coworkers (4.88 – 6.77 nA mM^{-1}) that functioned reliably when implanted percutaneously in rats.[29] Although the response times of the sensors herein are slower (274 – 530 s compared to 75 s), the NO release durations of these sensors are nearly 2.5 times longer. These response times are not prohibitive to glucose sensor development; others have reported success (as determined via Clarke error grid analysis) using subcutaneously implanted glucose sensors with in vitro response time of ~10 min in humans.[54]

Of note, functional NO-releasing glucose sensors have been fabricated using other synthetic strategies. Silica xerogels doped with poly(vinylpyrrolidone) were shown to overcome the permeability limitations resulting from post-diazeniumdiolation.[31] While

Table 2.8 Properties of enzyme-based glucose biosensors coated with pre-diazeniumdiolated 15 mol% AEAP/NO-PTMOS xerogels after 0, 4 or 7 d immersion in PBS.

immersion time (d)	sensitivity (nA mM^{-1})	response time (s)	dynamic range (mM)	R^2
0	3.4 ± 0.8[a]	530 ± 5	1–24	0.9787
4	3.3 ± 1.1	375 ± 26	1–30	0.9980
7	3.5 ± 1.3	274 ± 19	1–30	0.9992

[a] Values are given as the mean ± standard deviation from at least n=3 independently synthesized sensor membranes.

this strategy improved sensor response (sensitivity) from ~0.14 to 4.6 nA mM^{-1}, the NO storage was much less than that from the pre-diazeniumdiolated xerogels. As an alternative to silica-based xerogels, glucose sensors have also been fabricated using NO-releasing silica-modified polyurethanes.[30, 31] Polyurethanes modified with NO-releasing nanoparticles demonstrate similar NO-release totals (~2 μmol cm^{-2} s^{-1}) and glucose sensitivities (7.3–14.5 nA mM^{-1}) for sensors covering equivalent dynamic ranges.[30] While both strategies are promising, the direct synthetic route of *N*-diazeniumdiolate-modified xerogels offers a more facile approach to preparing the NO-releasing sensor membrane.

2.4 Conclusions

Sol-gel chemistry allows for the design of surfaces that release bioactive agents using facile synthetic methods with mild reaction conditions and easily obtainable precursors. Herein, xerogels fabricated from *N*-diazeniumdiolate-modified silanes were demonstrated useful for storing and releasing NO in a concentration-dependent manner, with NO-release kinetics dependent on the identity of the donor. At equivalent mole percentages, pre-diazeniumdiolated xerogels release significantly more NO (>10x) than their post-diazeniumdiolated counterparts and pre-diazeniumdiolated xerogels containing 15 mol% of the NO donor released similar amounts of NO as ~30 mol % NO donor films that are post-diazeniumdiolated. Unlike post-diazeniumdiolated films, the sensors herein function as glucose sensor membranes, operating over a clinically relevant glucose range with adequate glucose sensitivity and response for up to 1 week. To achieve larger NO-storage capacity without compromising matrix stability, future work should focus on

methods for isolating the *N*-diazeniumdiolate-modified silanes before using the precursors to form xerogels. If longer NO-release durations are desired, the purification of more stable intramolecular *N*-dizeniumdiolate-modified silanes may be an important strategy. Overall, the one-pot reaction used herein provides a simple and effective strategy for fabricating NO-releasing glucose sensors. To further demonstrate the utility of these coatings for other applications, future work should make use of alternative coating methods (i.e., spraycoating and dipcoating) with a variety of substrate types and geometries.

REFERENCES

1. Hoffman, A. S., "The origins and evolution of "controlled" drug delivery systems." *J. Control. Release.* **2008**, *132*, 153-163.

2. Rosen, H.; Abribat, T., "The rise and rise of drug delivery." *Nat. Rev. Drug. Discov.* **2005**, *4*, 381-385.

3. Wu, P.; Grainger, D. W., "Drug/device combinations for local drug therapies and infection prophylaxis." *Biomaterials* **2006**, *27*, 2450-2467.

4. Hetrick, E. M.; Schoenfisch, M. H., "Reducing implant-related infections: active release strategies." *Chem. Soc. Rev.* **2006**, *35*, 780-789.

5. Nablo, B. J.; Prichard, H. L.; Butler, R. D.; Klitzman, B.; Schoenfisch, M. H., "Inhibition of implant-associated infections via nitric oxide release." *Biomaterials* **2005**, *26*, 6984-6990.

6. Mowery, K. A.; H. Schoenfisch, M.; Saavedra, J. E.; Keefer, L. K.; Meyerhoff, M. E., "Preparation and characterization of hydrophobic polymeric films that are thromboresistant via nitric oxide release." *Biomaterials* **2000**, *21*, 9-21.

7. Nichols, S. P.; Storm, W. L.; Koh, A.; Schoenfisch, M. H., "Local delivery of nitric oxide: Targeted delivery of therapeutics to bone and connective tissues." *Adv. Drug. Deliver. Rev.* **2012**, *64*, 1177-1188.

8. Carpenter, A. W.; Schoenfisch, M. H., "Nitric oxide release: Part II. Therapeutic applications." *Chem. Soc. Rev.* **2012**, *41*, 3742-3752.

9. Nablo, B. J.; Chen, T. Y.; Schoenfisch, M. H., "Sol-gel derived nitric-oxide releasing materials that reduce bacterial adhesion." *J. Am. Chem. Soc.* **2001**, *123*, 9712-9713.

10. Nichols, S. P.; Koh, A.; Brown, N. L.; Rose, M. B.; Sun, B.; Slomberg, D. L.; Riccio, D. A.; Klitzman, B.; Schoenfisch, M. H., "The effect of nitric oxide surface flux on the foreign body response to subcutaneous implants." *Biomaterials* **2012**, *33*, 6305-6312.

11. Hetrick, E. M.; Prichard, H. L.; Klitzman, B.; Schoenfisch, M. H., "Reduced foreign body response at nitric oxide-releasing subcutaneous implants." *Biomaterials* **2007**, *28*, 4571-4580.

12. Hetrick, E. M.; Schoenfisch, M. H., "Antibacterial nitric oxide-releasing xerogels: Cell viability and parallel plate flow cell adhesion studies." *Biomaterials* **2007**, *28*, 1948-1956.

13. Stasko, N. A.; Schoenfisch, M. H., "Dendrimers as a scaffold for nitric oxide release." *J. Am. Chem. Soc.* **2006**, *128*, 8265-8271.

14. Shin, J. H.; Metzger, S. K.; Schoenfisch, M. H., "Synthesis of nitric oxide-releasing silica nanoparticles." *J. Am. Chem. Soc.* **2007**, *129*, 4612-4619.

15. Coneski, P. N.; Nash, J. A.; Schoenfisch, M. H., "Nitric oxide-releasing electrospun polymer microfibers." *ACS Appl. Mater. Interfaces* **2012**, *3*, 426-432.

16. Lu, Y.; Sun, B.; Li, C.; Schoenfisch, M. H., "Structurally diverse nitric oxide-releasing poly(propylene imine) dendrimers." *Chem. Mater.* **2011**, *23*, 4227-4233.

17. Riccio, D. A.; Schoenfisch, M. H., "Nitric oxide release: Part I. Macromolecular scaffolds." *Chem. Soc. Rev.* **2012**, *41*, 3731-3741.

18. Riccio, D. A.; Coneski, P. N.; Nichols, S. P.; Broadnax, A. D.; Schoenfisch, M. H., "Photoinitiated nitric oxide-releasing tertiary S-nitrosothiol-modified xerogels." *ACS Appl. Mater. Interfaces* **2012**, *4*, 796-804.

19. Wold, K. A.; Damodaran, V. B.; Suazo, L. A.; Bowen, R. A.; Reynolds, M. M., "Fabrication of biodegradable polymeric nanofibers with covalently attached NO donors." *ACS Appl. Mater. Interfaces* **2012**, *4*, 3022-3030.

20. Harding, J. L.; Reynolds, M. M., "Metal organic frameworks as nitric oxide catalysts." *J. Am. Chem. Soc.* **2012**, *134*, 3330-3333.

21. Marxer, S. M.; Rothrock, A. R.; Nablo, B. J.; Robbins, M. E.; Schoenfisch, M. H., "Preparation of nitric oxide (NO)-releasing sol-gels for biomaterial applications." *Chem. Mater.* **2003**, *15*, 4193-4199.

22. Dave, B. C.; Dunn, B.; Valentine, J. S.; Zink, J. I., "Sol-gel encapsulation methods for biosensors." *Anal. Chem.* **1994**, *66*, 1120A-1127A.

23. Braun, S.; Rappoport, S.; Zusman, R.; Avnir, D.; Ottolenghi, M., "Biochemically active sol-gel glasses: the trapping of enzymes." *Mater. Lett.* **1990**, *10*, 1-5.

24. Riccio, D. A.; Dobmeier, K. P.; Hetrick, E. M.; Privett, B. J.; Paul, H. S.; Schoenfisch, M. H., "Nitric oxide-releasing S-nitrosothiol-modified xerogels." *Biomaterials* **2009**, *30*, 4494-4502.

25. Lev, O.; Tsionsky, M.; Rabinovich, L.; Glezer, V.; Sampath, S.; Pankratov, I.; Gun, J., "Organically modified sol-gel sensors." *Anal. Chem.* **1995**, *67*, 22A-30A.

26. Stobie, N.; Duffy, B.; McCormack, D. E.; Colreavy, J.; Hidalgo, M.; McHale, P.; Hinder, S. J., "Prevention of Staphylococcus epidermidis biofilm formation using a low-temperature processed silver-doped phenyltriethoxysilane solâ€“gel coating." *Biomaterials* **2008**, *29*, 963-969.

27. Quintanar-Guerrero, D.; Ganem-Quintanar, A.; Nava-Arzaluz, M. G.; Piñón-Segundo, E., "Silica xerogels as pharmaceutical drug carriers." *Expert Opin. Drug. Del.* **2009**, *6*, 485-498.

28. Iafisco, M.; Margiotta, N., "Silica xerogels and hydroxyapatite nanocrystals for the local delivery of platinum bisphosphonate complexes in the treatment of bone tumors: A mini-review." *J. Inorg. Biochem.* **2012**, *117*, 237-247.

29. Gifford, R.; Batchelor, M. M.; Lee, Y.; Gokulrangan, G.; Meyerhoff, M. E.; Wilson, G. S., "Mediation ofin vivo glucose sensor inflammatory response via nitric oxide release." *J. Biomed. Mater. Res.* **2005**, *75A*, 755-766.

30. Koh, A.; Riccio, D. A.; Sun, B.; Carpenter, A. W.; Nichols, S. P.; Schoenfisch, M. H., "Fabrication of nitric oxide-releasing polyurethane glucose sensor membranes." *Biosens. Bioelectron.* **2011**, *28*, 17-24.

31. Shin, J. H.; Marxer, S. M.; Schoenfisch, M. H., "Nitric oxide-releasing sol-gel particle/polyurethane glucose biosensors." *Anal. Chem.* **2004**, *76*, 4543-4549.

32. Holt, J.; Hertzberg, B.; Weinhold, P.; Storm, W.; Schoenfisch, M.; Dahners, L., "Decreasing bacterial colonization of external fixation pins through nitric oxide release coatings." *J. Orthop. Trauma.* **2011**, *25*, 432-437.

33. Schoenfisch, M. H.; Rothrock, A. R.; Shin, J. H.; Polizzi, M. A.; Brinkley, M. F.; Dobmeier, K. P., "Poly(vinylpyrrolidone)-doped nitric oxide-releasing xerogels as glucose biosensor membranes." *Biosens. Bioelectron.* **2006**, *22*, 306-312.

34. Brunauer, S., "Adsorption of gases in multimolecular layers." *J. Am. Chem. Soc.* **1938**, *60*, 309-319.

35. Traube, W., "Ueber synthesen stickstoffhaltiger verbindungen mit hülfe des stickoxyds." *Justus Liebigs Ann. Chem.* **1898**, *300*, 81-128.

36. DeRosa, F.; Keefer, L. K.; Hrabie, J. A., "Nitric oxide reacts with methoxide." *J. Org. Chem.* **2008**, *73*, 1139-1142.

37. Sommer, L. H.; Pietrusza, E. W.; Whitmore, F. C., "Properties of the silicon-hydroxyl bond in trialkylsilanols." *J. Am. Chem. Soc.* **1946**, *68*, 2282-2284.

38. Coneski, P. N.; Schoenfisch, M. H., "Nitric oxide release: Part III. Measurement and reporting." *Chem. Soc. Rev.* **2012**, *41*, 3753-3758.

39. Hrabie, J. A.; Klose, J. R.; Wink, D. A.; Keefer, L. K., "New nitric oxide-releasing zwitterions derived from polyamines." *J. Org. Chem.* **1993**, *58*, 1472-1476.

40. Reynolds, M. M.; Zhou, Z.; Oh, B. K.; Meyerhoff, M. E., "Bis-diazeniumdiolates of dialkyldiamines: Enhanced nitric oxide loading of parent diamines." *Org. Lett.* **2005**, *7*, 2813-2816.

41. Keefer, L. K.; Flippen-Anderson, J. L.; George, C.; Shanklin, A. P.; Dunams, T. M.; Christodoulou, D.; Saavedra, J. E.; Sagan, E. S.; Bohle, D. S., "Chemistry of

the diazeniumdiolates I. Structural and spectral characteristics of the [N(O)NO]ate functional group." *Nitric Oxide-Biol. Chem.* **2001**, *5*, 377-394.

42. Niinomi, M., "Mechanical properties of biomedical titanium alloys." *Mat. Sci. Eng. A-Struct.* **1998**, *243*, 231-236.

43. Schubert, U.; Huesing, N.; Lorenz, A., "Hybrid inorganic-organic materials by sol-gel processing of organofunctional metal alkoxides." *Chem. Mater.* **1995**, *7*, 2010-2027.

44. Osterholtz, F. D.; Pohl, E. R., "Kinetics of the hydrolysis and condensation of organofunctional alkoxysilanes: a review." *J. Adhes. Sci. Technol.* **1992**, *6*, 127-149.

45. Brinker, C. J.; Scherer, G. W., *Sol-gel science : the physics and chemistry of sol-gel processing*. Academic Press: Boston, 1990.

46. Charville, G. W.; Hetrick, E. M.; Geer, C. B.; Schoenfisch, M. H., "Reduced bacterial adhesion to fibrinogen-coated substrates via nitric oxide release." *Biomaterials* **2008**, *29*, 4039-4044.

47. Grisham, M. B.; Jourd'Heuil, D.; Wink, D. A., "I. Physiological chemistry of nitric oxide and its metabolites: implications in inflammation." *Am. J. Physiol. Gastrointest. Liver Physiol.* **1999**, *276*, G315-G321.

48. Privett, B. J.; Nutz, S. T.; Schoenfisch, M. H., "Efficacy of surface-generated nitric oxide against Candida albicans adhesion and biofilm formation." *Biofouling* **2010**, *26*, 973-983.

49. Batchelor, M. M.; Reoma, S. L.; Fleser, P. S.; Nuthakki, V. K.; Callahan, R. E.; Shanley, C. J.; Politis, J. K.; Elmore, J.; Merz, S. I.; Meyerhoff, M. E., "More lipophilic dialkyldiamine-based diazeniumdiolates: Synthesis, characterization, and application in preparing thromboresistant nitric oxide release polymeric coatings." *J. Med. Chem.* **2003**, *46*, 5153-5161.

50. Nichols, S. P.; Koh, A.; Storm, W. L.; Shin, J. H.; Schoenfisch, M. H., "Biocompatible materials for continuous glucose monitoring devices." *Chem. Rev.* **2013**, *113*, 2528-2549.

51. Shin, J. H.; Schoenfisch, M. H., "Improving the biocompatibility of in vivo sensors via nitric oxide release." *Analyst* **2006**, *131*, 609-615.

52. Dempsey, E.; Diamond, D.; Smyth, M. R.; Urban, G.; Jobst, G.; Moser, I.; Verpoorte, E. M. J.; Manz, A.; Michael Widmer, H.; Rabenstein, K.; Freaney, R., "Design and development of a miniaturised total chemical analysis system for on-line lactate and glucose monitoring in biological samples." *Anal. Chim. Acta* **1997**, *346*, 341-349.

53. Bindra, D. S.; Zhang, Y.; Wilson, G. S.; Sternberg, R.; Thevenot, D. R.; Moatti, D.; Reach, G., "Design and in vitro studies of a needle-type glucose sensor for subcutaneous monitoring." *Anal. Chem.* **1991**, *63*, 1692-1696.

54. Gilligan, B. C.; Shults, M.; Rhodes, R. K.; Jacobs, P. G.; Brauker, J. H.; Pintar, T. J.; Updike, S. J., "Feasibility of continuous long-term glucose monitoring from a subcutaneous glucose sensor in humans." *Diabetes. Technol. The.* **2004**, *6*, 378-386.

Chapter 3:

Superhydrophobic Nitric Oxide-Releasing Xerogels for Tunable Release Kinetics and Reduced Bacterial Adhesion

3.1 Introduction

A combination of surface roughness and low surface energy yields "superhydrophobic" materials characterized by high water contact angles ($\geq 150^{o}$).[1] Due to their non-wetting properties, such surfaces have found use in a wide-array of applications, including droplet-direction in microfluidics,[2] anti-fouling coatings,[3] and drug release.[4, 5] The characteristics that govern a water droplet's behavior on superhydrophobic surfaces are described by the Cassie-Baxter model.[6] Water droplets on superhydrophobic interfaces rest over a pocket of air trapped within the micro- and/or nanoscopic valleys of its surface. This property tends to make these surfaces resistant to fouling from debris, cells, and biomolecules.[7-9]

The ability for superhydrophobic materials to resist adhesion, specifically of bacteria, holds great promise for biomedical applications.[10] Microbial proliferation on medical implants is an undesirable event with indwelling medical devices responsible for many of the two million hospital acquired infections that occur annually.[11] Researchers have sought to address this problem by designing surfaces that reduce the incidence of adhered bacteria through altered surface composition or through release of antimicrobial agents.[12] While superhydrophobic interfaces have been shown to reduce the adhesion of viable bacteria via passive mechanisms, they provide no means to kill bacteria that do adhere. In contrast, actively released antimicrobial agents from a surface are able to kill

bacteria, but only over finite periods (e.g., duration of drug release). By combining passive and active approaches simultaneously, we hypothesize that the resulting interface will exhibit improved antimicrobial efficacy by both preventing adhesion and killing bacteria.

Nitric oxide (NO) is a broad-spectrum antimicrobial agent with a proven ability to reduce infections.[13] Due to NO's high reactivity and short biological half life,[14] we and others have developed NO-releasing macromolecules and coatings to facilitate controlled NO-release.[13] For example, silica xerogels formed from aminosilane precursors represent a template for generating NO. When exposed to high pressures of NO, the secondary amine sites within are converted to *N*-diazeniumdiolate NO donors.[15] In water, the NO donors decompose to yield the parent amine along with two equivalents of NO. In this work, this synthesis was modified to develop NO-releasing superhydrophobic interfaces using a dual-layer approach (Scheme 3.1). Herein, we evaluate the antimicrobial capabilities of superhydrophobic surfaces that actively release nitric oxide (NO), assessing the potential of each independent of one another. Moreover, we examine how a superhydrophobic coating on top of an NO-storage reservoir controls and extends NO-release kinetics.

3.2 Materials and methods

Isobutyltrimethoxysilane (BTMOS), methyltrimethoxysilane (MTMOS) and low molecular weight poly(vinyl chloride) (PVC) were purchased from Sigma Aldrich (St. Louis, MO). *N*-(6-aminohexyl)aminopropyltrimethoxysilane (AHAP), tetraethylorthosilicate (TEOS), and (heptadecafluoro-1,1,2,2-tetrahydrodecyl) trimethoxysilane (17-FTMS) were acquired from Gelest (Tullytown, PA). Milli-Q water

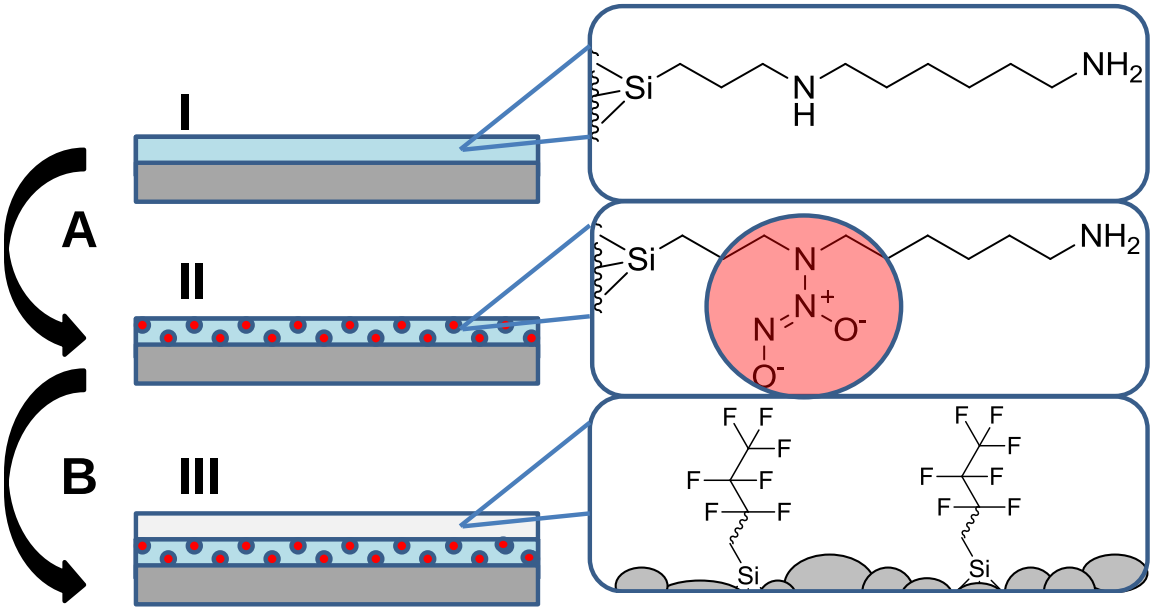

Scheme 3.1 (**I**) Amine-modified xerogels on glass subtrates are (**A**) exposed to 10 atm NO to yield (**II**) N-diazeniumdiolate-modified xerogels. (**B**) A fluorinated silica composite is then spraycoated onto the xerogels to yield (**III**) superhydrophobic NO-releasing xerogels.

was purified from distilled water to a resistivity of 18.2 MΩ cm and a total organic content of <5 ppb using a Millipore Milli-Q UV Gradient A-10 system (Bedford, MA). Nitric oxide gas (NO) was purchased from Praxair (Bethlehem, PA). Standardized NO (26.85 ppm, balance N_2), argon (Ar), and nitrogen (N_2) gasses were acquired from Airgas National Welders (Durham, NC). Dulbecco's modified essential media (DMEM), (3-(4,5-dimethylthiazol-2-yl)-5-(3-carboxymethoxyphenyl)-2-(4-sulfophenyl)-2H-tetrazolium) (MTS), phenazine methosulfate (PMS), tryptic soy broth and tryptic soy agar were obtained from Becton, Dickinson and Company (Sparks, MD). All other reagents were analytical grade and used as received.

3.2.1 Synthesis of NO-releasing xerogels

Glass slides served as the underlying substrate for all coatings. Slides were cut to dimensions of 9 x 25 mm^2 and cleaned via successive sonication in water, ethanol, and acetone. The substrates were then dried with N_2 and UV/O_3 cleaned for 20 min using a Bioforce TipCleaner (Ames, IA).

Secondary amine-modified xerogels were prepared via a two-step, one-pot reaction. First, 378 μL of BTMOS was prehydrolyzed in 633 μL ethanol, 190 μL water and 31.7 μL 0.5 M hydrochloric acid for 1h. Following prehydrolysis of the backbone silane, 255 μL of AHAP was added and mixed for an additional 1 h. Afterwards, 40 μL of the resulting sol was cast onto a glass substrate, cured on the bench for 1 h, and further dried and cured in an oven at 70 ^oC for 3 d. After drying, films were modified with *N*-diazeniumdiolate NO donors via reaction with high pressure NO gas. Amine-modified xerogels were placed in a Parr hydrogenation bomb and purged copiously with argon. Xerogels were then exposed to 10 atm NO for 3 d to convert 2^o amines to *N*-

diazeniumdiolate NO donors. The *N*-diazeniumdiolate NO donor-modified xerogels were purged again with argon to remove unreacted NO. For bacteria experiments, non-superhydrophobic control and NO-releasing xerogels were coated with low molecular weight PVC to ensure identical surface attributes between the two groups.[16, 17] Briefly, 400 mg of PVC was dissolved in 4 mL tetrahydrofuran, then 300 μL of the resulting solution was spin coated on the xerogels at 3000 rpm for 10 s, and then dried *in vacuo* for 24 h. Xerogels were stored under nitrogen at -20 ^{o}C until further use.

3.2.2 Preparation of superhydrophobic composite layers

Fluorinated silica particles were synthesized via the Stöber method by co-condensing tetraethylorthosilicate (TEOS) and (heptadecafluoro-1,1,2,2-tetrahydrodecyl) trimethoxysilane (17-FTMS). In a 50 mL round-bottom flask, ethanol (30 mL) was combined with 12 mL ammonium hydroxide (28 wt% in water). To this solution, a mixture of 17-FTMS (690 μL) and TEOS (973 μL) was added via syringe pump (0.056 mL min^{-1} over 30 min). Following dropwise addition of the silane, the reaction was allowed to proceed for an additional 1.5 h to yield 30 mol% 17-FTMS (balance TEOS) particles. Particles were collected via centrifugation at 4500 rpm for 5 min, washed three times in ethanol via the same centrifugation regimen, and dried under vacuum overnight (representative SEM image shown in Figure 3.1)

Control and NO-releasing xerogels were made superhydrophobic by spraycoating the substrates with a mixture of fluorinated silica particles and silane precursors. First, 800 mg 30 mol% 17-FTMS (balance TEOS) particles were suspended in ethanol (9.4 mL) via 30 min of ultrasonication. To the suspension, 17-FTMS (221.4 μL), methyltrimethoxysilane (MTMOS; 199.7 μL), water (2.00 mL), and 0.1 M hydrochloric

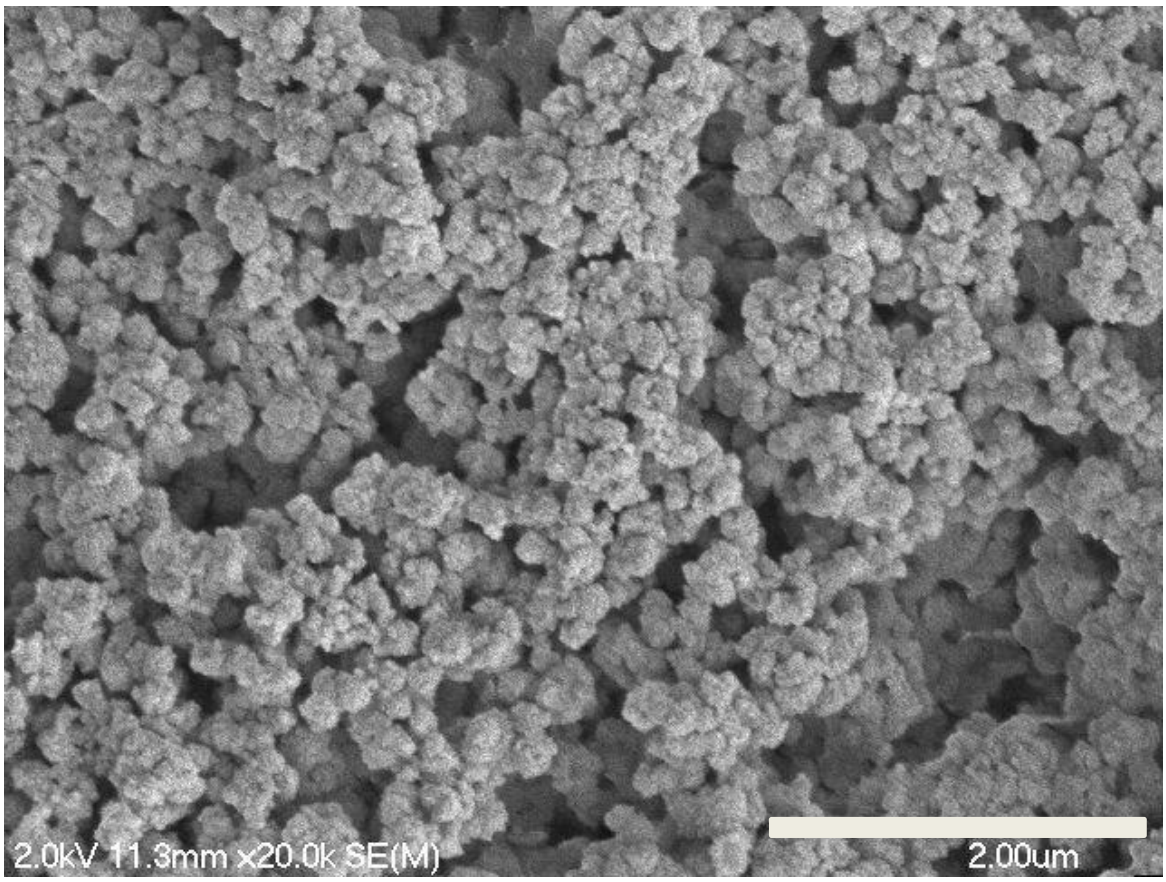

Figure 3.1 Scanning electron micrograph of 30 mol% 17-FTMS (balance TEOS) colloids.

acid (200 μL) were added and allowed to react for 1.5 h. After reaction, the suspension was spraycoated using an Iwata HP-BC PLUS airgun with a nitrogen feed pressure of 6 bar at a distance of 30 cm. The nozzle pass rate over each substrate was approximately 2.5 cm s^{-1} (i.e., the entire vertical distance of the xerogels was covered in 1 s). Either 6, 12, 18, or 24 passes were made with the spraygun over each xerogel. Following coating, the resulting superhydrophobic xerogels were dried on the bench for 5 min and placed *in vacuo* for 48 h. In addition to the characterization described below, films were imaged using a Hitachi S-4700 Cold Cathode Field Emission Scanning Electron Microscope with an accelerating voltage of 2 kV.

3.2.3 Xerogel characterization

Static water contact angles were determined from images obtained with a KSV Instruments Cam 200 Optical Contact Angle Meter (Helsinki, Finland). For each film, measurements were taken in at least n = 3 locations. To assess long-term contact angle stability, superhydrophobic NO-releasing xerogels were immersed in 37 ^{o}C PBS for 7, 14, 21, or 28 d. For each timepoint, the xerogels were removed from the soak solutions and static water contact angles were remeasured.

A silicon leaching assay was used to assess the chemical stability of the xerogels.[18, 19] Glass substrates, NO-releasing xerogels, and superhydrophobic NO-releasing xerogels were submerged in 10 mL PBS for 7, 14, 21, or 28 d at 37 ^{o}C. At set periods, the Si content in each soak solution was analyzed using an inductively coupled plasma optical emission spectrometer (Teledyne Leeman Prodigy ICP-OES; Hudson, NH) with calibration standards ranging from 0 – 10 ppm Si (present as sodium silicate) at a wavelength of 251.611 nm.

Release of NO from the non-superhydrophobic and superhydrophobic xerogels was measured using a chemiluminescent nitric oxide analyzer (NOA). Approximately 30 mL of PBS (pH 7.4, 37 ^{o}C) was placed in a round-bottom flask, and deoxygenated by supplying nitrogen through a porous glass frit at a rate of 80 mL min^{-1}. Following addition of the xerogels to the buffer, released NO was carried to a pre-calibrated NOA by an additional stream of nitrogen gas (120 mL min^{-1}) supplied through a glass side arm on the round bottom flask.

3.2.4 Adhered viable bacteria assays

To assess the antibacterial properties of superhydrophobic and NO-releasing xerogels, *Pseudomonas aeruginosa* (ATCC #19143) was grown from an overnight culture to 10^{8} cfu mL^{-1} (i.e., mid-log growth), centrifuged at 4500 rpm for 10 min, and resuspended in an equivalent volume of PBS. Each xerogel was submerged in 4 mL of the bacteria suspension and gently agitated using an orbital shaker for 6 h at 37 ^{o}C. After 6 h, the xerogel substrates were removed, and then dipped into distilled water to remove loosely adhered bacteria. Bare portions of the substrate were swabbed with ethanol for 30 s to kill bacteria not associated with the xerogel. To determine the number of viable adhered bacteria, each xerogel was then submerged in 4 mL sterile PBS and sonicated for 15 min. The resulting supernatant was serially diluted and enumerated on tryptic soy agar plates (IUL Flash & Go colony counter; Farmingdale, NY). To assess the ability of NO to kill bacteria over extended periods, the xerogels were rinsed and transferred to sterile PBS immediately following the 6 h bacteria suspension exposure. After 12 h gentle agitation, the xerogels were removed and their uncoated area was swabbed with ethanol. The xerogels were ultrasonicated and plated on tryptic soy agar as described above.

3.2.5 Xerogel cytotoxicity

The cytotoxicity of superhydrophobic and non-superhydrophobic control and NO-releasing xerogels was assessed against L929 mouse fibroblasts. First, the cells were cultured in DMEM supplemented with 10% (v/v) FBS and 1 wt% penicillin/streptomycin in a humidified 5% CO_2 environment. After reaching confluency (80% coverage), the cells were trypsinized and seeded onto tissue-culture treated 24-well plates. Following an additional 72 h of incubation, the supernatant was removed via aspiration and replaced with 1 mL fresh DMEM. The xerogels were placed face down on the fibroblast cells and incubated for 24 h at 37 ^{o}C (humidified; 5% CO_2). Following removal of the xerogels, the supernatant was aspirated and each well was rinsed three times with PBS and replaced by a mixture of DMEM/MTS/PMS (1 mL total at a volume ratio of 105/20/1). The cells were incubated for 90 min, and 120 μL aliquots of the supernatant were transferred to a microtiter plate. The absorbance of the solutions was measured using a Thermoscientific Multiskan EX plate reader at a wavelength of 490 nm and compared against blanks (i.e., the DMEM/MTS/PMS mixture) and control wells (seeded cells with no xerogel substrate).

3.3 Results and Discussion

3.3.1 Xerogel synthesis and characterization

Superhydrophobic NO-releasing xerogels were synthesized via a two-layer approach (Scheme 3.1). The bottom consists of an amine-modified xerogel that is exposed to high pressure NO (10 bar) to convert the secondary amines within to *N*-diazeniumdiolate NO donors. Following, the top layer (fluorinated silica particles

encased within a low-surface energy fluorocarbon sol-gel matrix; Figure 3.2) is applied. Addition of this top layer increased the contact angle of the *N*-diazeniumdiolated xerogels from $92.1^{o} \pm 1.2$ (slightly hydrophobic) to $158.7^{o} \pm 2.3$ (superhydrophobic). Upon immersion in aqueous media, a silver-hued sheen was observed on the films, indicating the formation of an entrapped pocket of air (or plastron) and thus a metastable underwater Cassie wetting state.[20, 21] The thickness of the superhydrophobic topcoat, which had no effect on the measured surface contact angle, was altered by increasing the number of spray passes made with the spraycoating apparatus. In turn, altering the thickness of the superhydrophobic membrane was explored as a method for controlling the NO-release kinetics.

The release of NO from the non-superhydrophobic and superhydrophobic films in physiologically relevant buffer (phosphate buffered saline; PBS, pH 7.4; 37 ^{o}C) was measured using a chemiluminescent nitric oxide analyzer.[22, 23] The maximum NO flux ($[NO]_m$) decreased from 102 to 53 pmol cm^{-2} s^{-1} as the number of superhydrophobic passes increased (Table 3.1). Mechanistically, the ensuing plastron (i.e., a thin metastable pocket of air entrapped between the superhydrophobic surface and the surrounding water[20]) for the superhydrophobic materials acted as a barrier to water uptake, slowing the rate of proton-initiated *N*-diazeniumdiolate NO donor decomposition. The total NO ($[NO]_t$) decreased when increasing the thickness of the superhydrophobic layers. This behavior was most apparent for films with 18 and 24 layers (Figure 3.3 and Table 3.1). This NO loss is most likely a result of *N*-diazeniumdiolate decomposition during the spraycoating process; though mild, a low concentration of HCl (1.67 mM) is required to catalyze the reaction of the superhydrophobic composite mixture, prompting NO donor

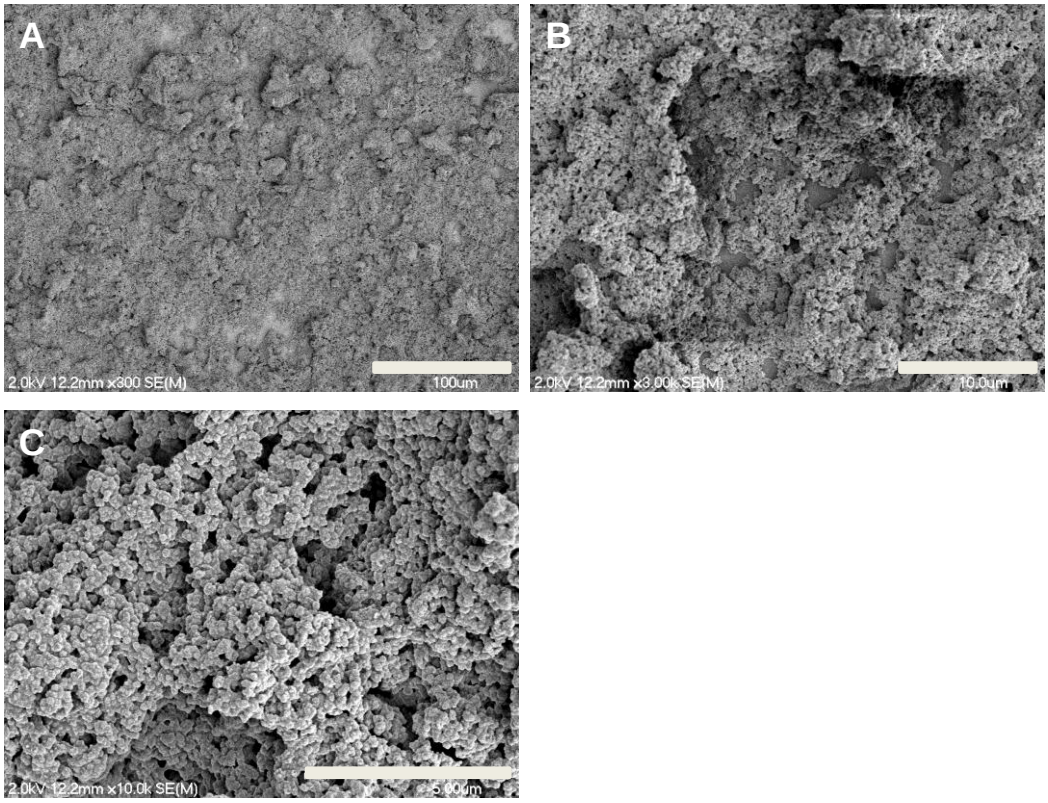

Figure 3.2 Scanning electron micrographs of superhydrophobic xerogels at A) 300x (scale bar = 100 μm), B) 3,000x (scale bar = 100 μm), and C) 10,000x (scale bar = 5 μm) magnification.

Table 3.1 Variation in NO-release kinetics as a function of superhydrophobic coating thickness.

# layers	$[NO]_t$ μmol cm^{-2}	$[NO]_m$ pmol cm^{-2} s^{-1}	half-life h	t_d h
0	3.3 ± 0.4[a]	102 ± 9	11.4 ± 0.7	59 ± 1.4
6	2.5 ± 0.6	60 ± 23	13.6 ± 1.4	85[b]
12	2.6 ± 0.3	56 ± 14	17.8 ± 4.3	105 ± 10
18	1.9 ± 0.3	53 ± 16	13.2 ± 0.6	83 ± 4
24	2.3 ± 0.3	53 ± 11	16.3 ± 2.4	91 ± 8

[a] Values are given as the mean ± standard deviation from at least 3 independent syntheses

[b] n=1

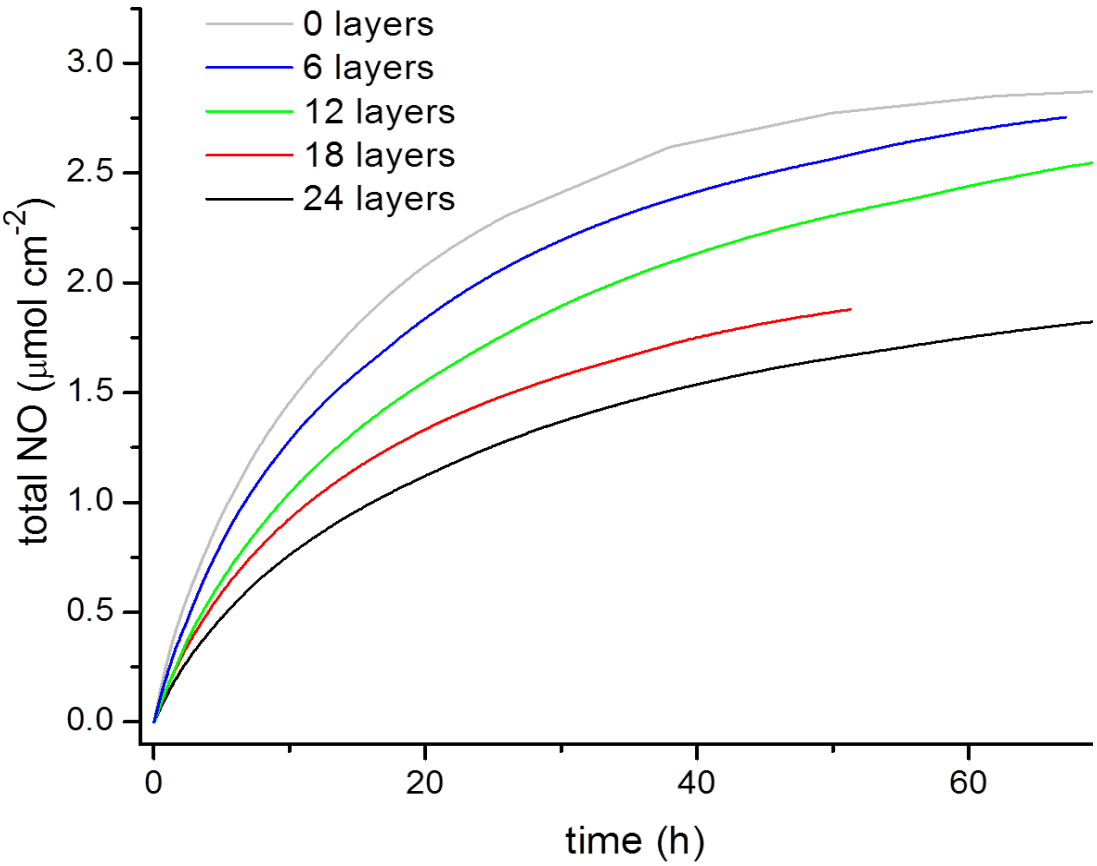

Figure 3.3 Representative integrated NO-release totals from uncoated and superhydrophobic-coated xerogels as a function of superhydrophobic layer thickness (# layers) and immersion time.

degradation. The duration of NO release was tunable by varying the thickness of the superhydrophobic membrane. As shown in Table 3.1, increasing the number of spraycoated superhydrophobic layers from 0 to 6 extended the NO-release duration (t_d) from 59 to 83 h. Xerogels with 12 coatings showed even longer NO-release durations, up to 105 h—nearly a 1.8-fold increase from non-superhydrophobic NO-releasing xerogels. Above 12 layers, the duration for 18 or 24 pass films decreased slightly, a phenomenon that may be attributed again to a diminished reservoir of total NO. Utilizing superhydrophobic topcoats may be a useful strategy to extend the release kinetics of any macromolecule or drug. Yohe et al. have demonstrated extended drug-release kinetics by including a dopant *within* a superhydrophobic fiber mesh.[4] However, the two-layer approach utilized herein is more straightforward (e.g., ease of application) and may prove useful when utilizing more complex drug-release chemistries.

The stability of the coatings is of obvious importance to most applications for these materials. As such, the durability of the substrates was evaluated by soaking the substrates in 37 ^{o}C PBS for up to one month. For all superhydrophobic-modified xerogels evaluated, water contact angles were maintained up to the longest duration tested (28 d; Figure 3.4). Minor instability in the superhydrophobic layer, specifically leaching of fluorinated silanes or particles, may go unnoticed with contact angle measurements alone. A leaching assay was thus employed to measure the presence of silicon (Si; indicative of leached silicate species) in soak solutions using inductively coupled plasma optical emission spectrometry (ICP-OES).[24] As demonstrated in Figure 3.5, both the NO-releasing xerogels (with and without a superhydrophobic coating) leached far less Si than the glass slide on which they were coated, suggesting that the membranes act as a barrier

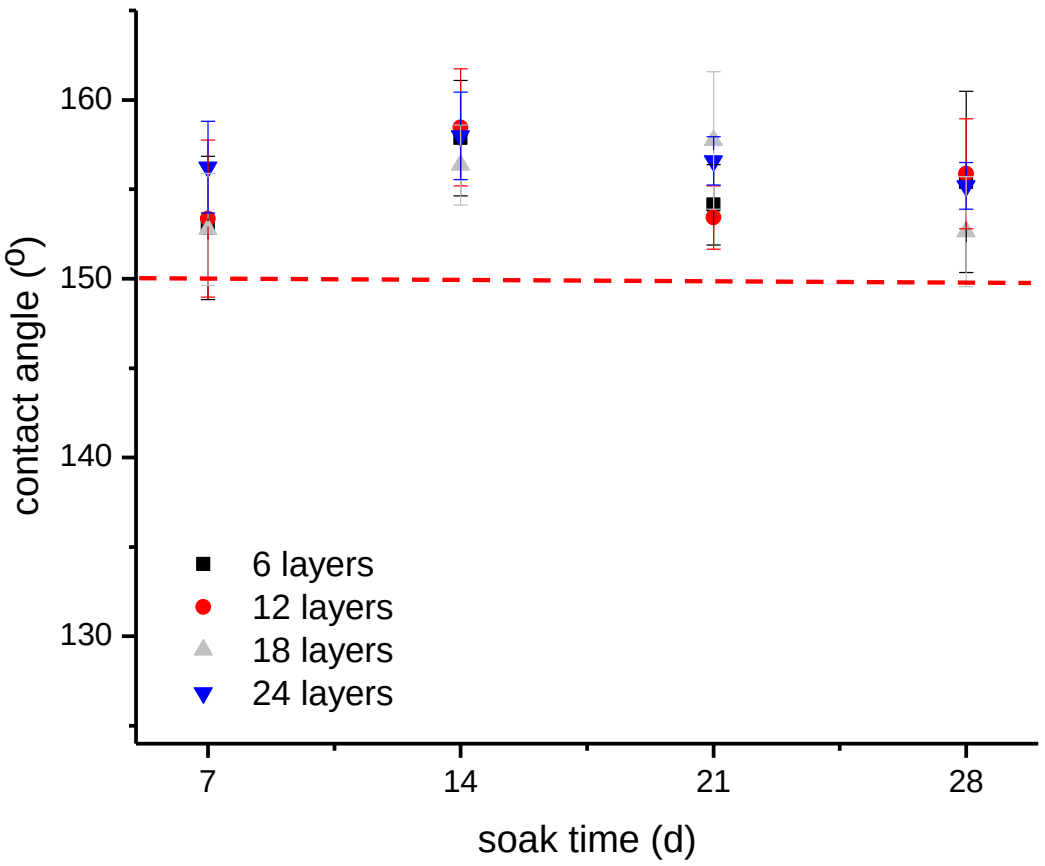

Figure 3.4 Contact angle stability of superhydrophobic-modified NO-releasing xerogels after soaking in 37 °C PBS up to 28 d. Error bars represent the standard deviation of the mean from at least n=7 measurements on n=3 xerogels.

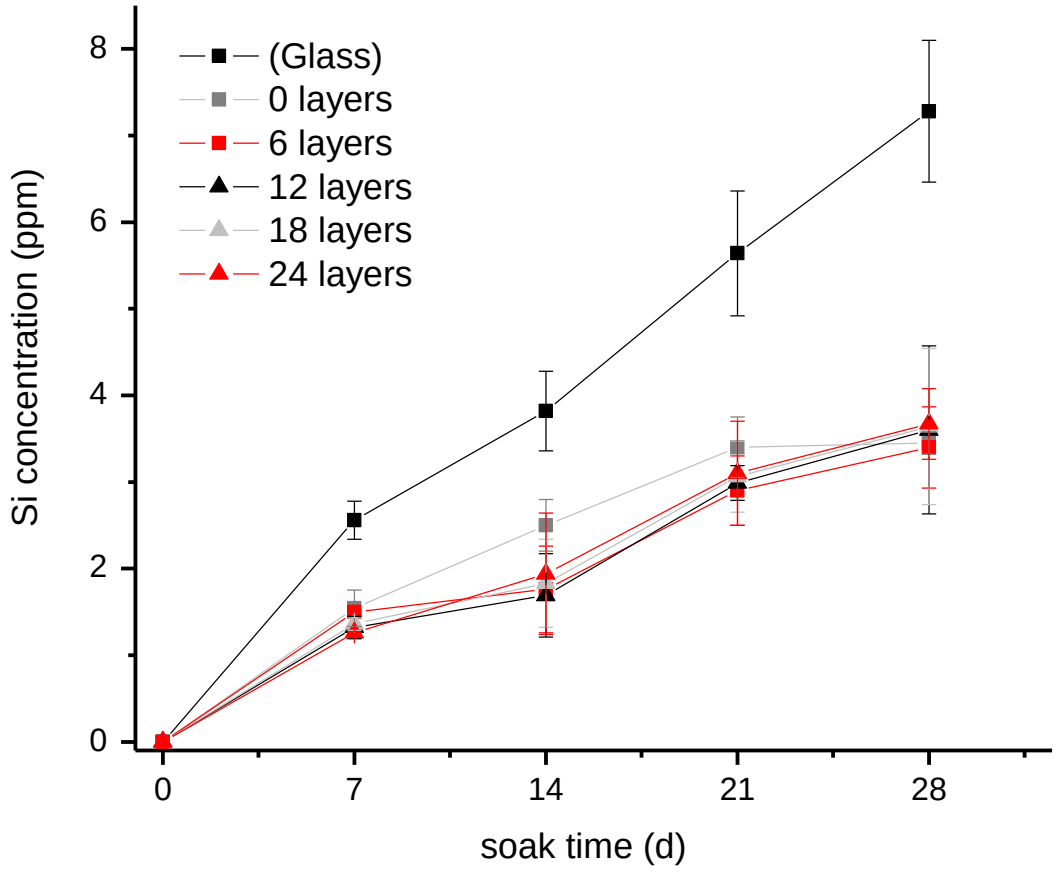

Figure 3.5 Cumulative silicon concentrations from superhydrophobic-modified NO-releasing xerogels after soaking in 37 °C PBS for up to 28 d measured by ICP-OES. Error bars represent the standard deviation of the mean from n=3 independent samples.

to silica leaching from glass substrates—as reported previously for highly stable xerogels.[19] Combined with contact angle measurements, these results indicate excellent material stability in physiological buffer solutions.

3.3.2 Antibacterial efficacy

In terms of antibacterial potential, our hypothesis was that the combination of superhydrophobicity and NO release would result in even greater antibacterial adhesion action compared to either alone. Although superhydrophobic textiles coated with silver nanoparticles have been reported previously, only the killing effect of silver was examined.[25] Moreover, the assay conditions utilized by Shateri Khalil-Abad et al. (placement of substrates directly onto a bacterial-laden agar plate) did not account for the adhesion events that occur in fluid.[26] To assess both bacterial adhesion and killing, control and NO-releasing xerogels were coated with 24 layers of the superhydrophobic composite. Non-superhydrophobic xerogels were coated with a thin layer of poly(vinyl chloride) (PVC) to ensure that any differences in the surface chemistries between control and NO-releasing xerogels were not responsible for observed anti-adhesive effects.[17, 27] Previous studies from our laboratory have shown this PVC layer (static water contact angle of 91.9 ± 0.9^{o}) to have only a minor effect on NO-release kinetics (<20% change in maximum NO flux).[27] The xerogels were submerged in a 10^{8} cfu mL^{-1} suspension of *Pseudomonas aeruginosa* (*P. aeruginosa*) for 6 h. Following exposure to the bacterial suspension, adhered colonies were removed via sonication and enumerated on agar.[28] As shown in Figure 3.6, the number of viable adhered colonies was reduced for all superhydrophobic and NO-releasing systems versus controls. Reduction in adhesion for the superhydrophobic surface alone (0.80 ± 0.02 log) was lower than that reported

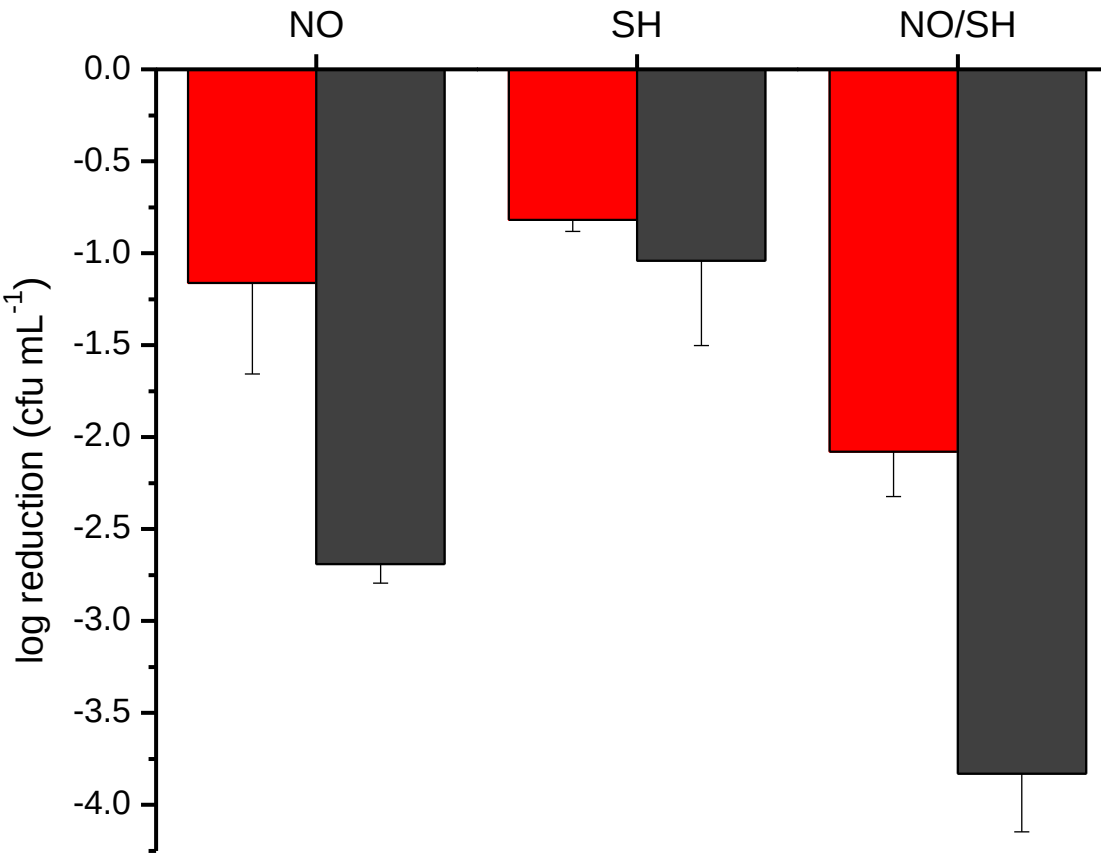

Figure 3.6 Reduction in viable P. aeruginosa adhesion vs. controls for (NO) NO-releasing xerogels, (SH) superhydrophobic xerogel controls and (NO/SH) NO-releasing superhydrophobic-modified xerogels after (red) 6 h exposure in 10^8 cfu mL-1 PA and (grey) an additional 12 h in PBS. Error bars represent the standard deviation of the mean from at least n=3 independent experiments.

previously.[10] This discrepancy may be attributed to the bacterial adhesion assay. The experiments described herein were performed under static conditions (to more accurately model the environment surrounding prosthetic implants)[29] whereas the prior report utilized a flow cell configuration to assess bacterial adhesion.[30] In a related study, Koc et al. also observed increased detachment of adhered biomolecules on superhydrophobic surfaces under flow conditions.[9] Nevertheless, the combination of passive and active approaches proved more effective at reducing viable *P. aeruginosa* adhesion than either individually, with the greatest reduction in bacterial adhesion (number of viable colonies) observed for the NO-releasing superhydrophobic membranes (2.1 ± 0.3 log).

In the experimental conditions used in the assay in this work, the reduction in adhered viable bacteria caused by NO release is likely a result of reduced bacterial *adhesion* rather than bacterial *killing*.[17, 31] Hetrick et al. exposed NO-releasing xerogels with similar NO-release fluxes to *P. aeruginosa* for 2 h.[17] After allowing bacteria to adhere, killing was monitored in real-time using propidium iodide (i.e., a fluorescent dye indicating membrane damage) while keeping the bacteria in PBS. No bacterial membrane damage was observed until ≥7 h, a longer period than the 6 h assay used for the assays in this work. Thus, to more directly examine the role that NO had on bacterial killing, the xerogels herein were transferred to sterile PBS for an additional 12 h following exposure to bacteria. Nitric oxide-release decreased the number of viable adhered bacteria by an additional ~1.5 log for both superhydrophobic and non-superhydrophobic xerogels (no such reduction was observed on superhydrophobic membranes without NO). Over this period, the two approaches reduced viable adhered PA by 3.8 ± 0.3 log, a 1-log improvement over the NO-releasing substrate alone. Reducing the overall population of

viable surface-adhered bacteria in this manner may prove useful for combating infections and biofilm growth.

3.3.3 Cytotoxicity

Unfortunately, NO-releasing xerogels have demonstrated mild cytotoxicity towards L929 fibroblasts, attributed both to NO (at fluxes > 50 pmol cm^{-2} s^{-1}) and the amine-modified xerogel scaffold itself.[16] In this work, it was hypothesized that the reduced NO fluxes from the superhydrophobic-coated materials would reduce dose-related toxicity of NO. The superhydrophobic layer may also act as a barrier to reduce toxicity from the amine-modified xerogel itself. Consistent with reports by Nablo et al. mild toxicity against L929 fibroblasts was observed for both the NO-releasing (~68 ± 4.5% viable) and non-NO-releasing (78 ± 1.5% viable) xerogels (Figure 3.7). Addition of the superhydrophobic layer reduced associated toxicity for both sets of films. After applying 24 layers of the superhydrophobic composite, a 13.3 and 11.1% increase in cell viability was observed for non-NO-releasing and NO-releasing xerogels, respectively. We attribute this to the slight decrease in leached matrix components from the xerogel scaffold upon application of the superhydrophobic layer (Figure 3.5). Reductions in the maximum NO flux of superhydrophobic NO-releasing materials (Table 3.1) likely decreases dose-dependent toxicity resulting from NO. Indeed, Nablo et al. observed that maximum NO fluxes of ~50 pmol cm^{-2} s^{-1} (i.e., similar to the 24 layer superhydrophobic xerogels herein) resulted in little cytotoxicity towards L929 fibroblasts. In contrast, maximum NO fluxes of ~95 pmol cm^{-2} s^{-1} (i.e., identical to the 0-layer superhydrophobic xerogels herein) resulted in toxicity. In whole, these results indicate that the application of a superhydrophobic coating to NO-releasing xerogels may reduce toxicity by both

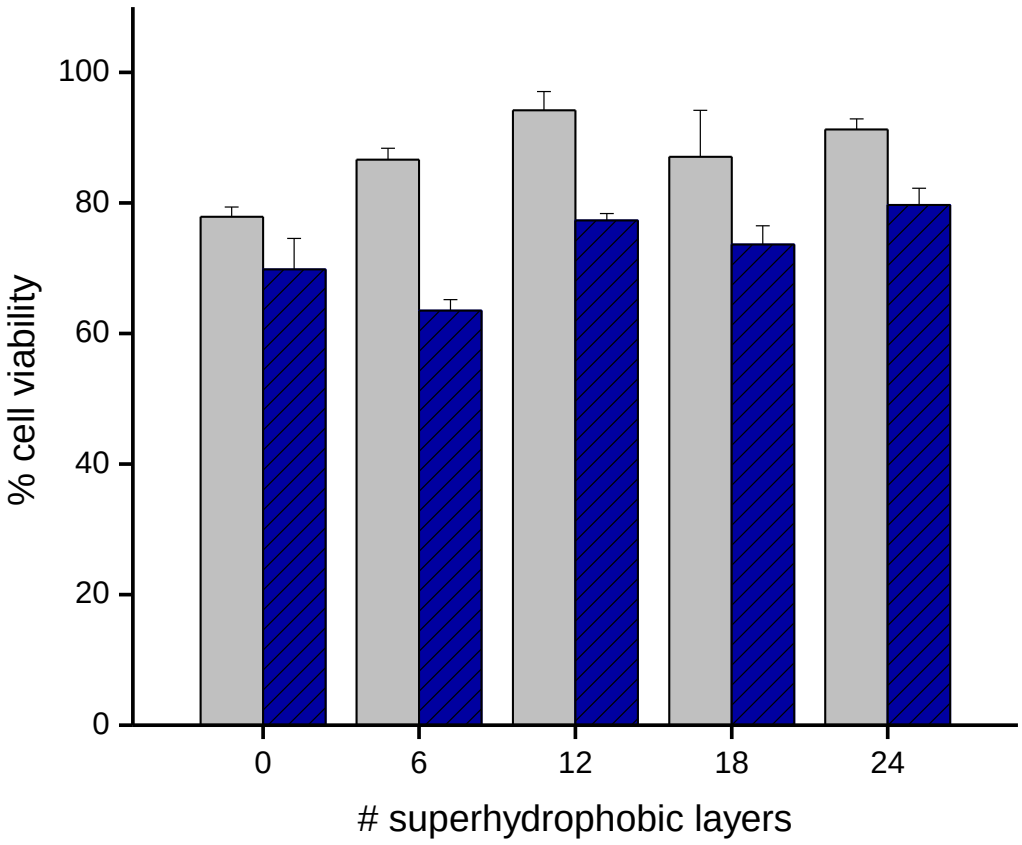

Figure 3.7 Relative viability of L929 fibroblasts exposed to (grey) non-NO-releasing and (blue) NO-releasing superhydrophobic xerogels as a function of superhydrophobic layer thickness. Viability was determined using the MTS assay. Error bars represent the standard deviation of the mean from n=3 measurements of n=1 samples.

preventing leaching of amine-based xerogel matrix components and reducing the NO dose delivered from these materials over a given period.

3.4 Conclusions

Herein, NO-releasing superhydrophobic coatings were prepared to examine how the combination of passive and active antimicrobial strategies function in tandem may be used to reduce adhesion and kill adhered bacteria. Superhydrophobic topcoats synthesized under aqueous, low-temperature conditions prolonged NO-release from *N*-diazeniumdiolate NO donor-modified xerogels. Such an approach may be beneficial for controlling the release rates of other drugs from anti-fouling biomedical coatings. In terms of antibacterial performance, the passive antifouling approach of superhydrophobicity and the active release of NO enhanced antibacterial activity while reducing cytotoxicity towards L929 fibroblasts. Future studies should examine the anti-bacterial adhesion and killing characteristics of these interfaces using a library of infection-causing bacteria. Other architectures that incorporate the NO donors within the superhydrophobic matrix itself should also be investigated to examine the versatility of this approach. Yohe and coworkers were able to trigger the release of a cancer drug from superhydrophobic meshes using ultrasound.[32] Such a strategy may prove useful for NO donors and eradicating slower proliferating, less virulent bacteria or biofilms that develop at extended periods after implantation.

REFERENCES

1. Lafuma, A.; Quéré, D., "Superhydrophobic states." *Nat. Mater.* **2003**, *2*, 457-460.

2. Mumm, F.; van Helvoort, A. T. J.; Sikorski, P., "Easy route to superhydrophobic copper-based wire-guided droplet microfluidic systems." *ACS Nano* **2009**, *3*, 2647-2652.

3. Zhang, H.; Lamb, R.; Lewis, J., "Engineering nanoscale roughness on hydrophobic surfaces: Preliminary assessment of fouling behaviour." *Sci. Technol. Adv. Mat.* **2005**, *6*, 236-239.

4. Yohe, S. T.; Colson, Y. L.; Grinstaff, M. W., "Superhydrophobic materials for tunable drug release: Using displacement of air to control delivery rates." *J. Am. Chem. Soc.* **2012**, *134*, 2016-2019.

5. Yohe, S. T.; Herrera, V. L. M.; Colson, Y. L.; Grinstaff, M. W., "3D superhydrophobic electrospun meshes as reinforcement materials for sustained local drug delivery against colorectal cancer cells." *J. Control. Release* **2012**, *162*, 92-101.

6. Cassie, A. B. D.; Baxter, S., "Wettability of porous surfaces." *T. Faraday. Soc.* **1944**, *40*, 546-551.

7. Zhang, X.; Wang, L.; Levanen, E., "Superhydrophobic surfaces for the reduction of bacterial adhesion." *RSC. Adv.* **2013**, *3*, 12003-12020.

8. Genzer, J.; Efimenko, K., "Recent developments in superhydrophobic surfaces and their relevance to marine fouling: a review." *Biofouling* **2006**, *22*, 339-360.

9. Koc, Y.; de Mello, A. J.; McHale, G.; Newton, M. I.; Roach, P.; Shirtcliffe, N. J., "Nano-scale superhydrophobicity: suppression of protein adsorption and promotion of flow-induced detachment." *Lab Chip* **2008**, *8*, 582-586.

10. Privett, B. J.; Youn, J.; Hong, S. A.; Lee, J.; Han, J.; Shin, J. H.; Schoenfisch, M. H., "Antibacterial fluorinated silica colloid superhydrophobic surfaces." *Langmuir* **2011**, *27*, 9597-9601.

11. Schierholz, J. M.; Beuth, J., "Implant infections: a haven for opportunistic bacteria." *J. Hosp. Infect.* **2001**, *49*, 87-93.

12. Hetrick, E. M.; Schoenfisch, M. H., "Reducing implant-related infections: active release strategies." *Chem. Soc. Rev.* **2006**, *35*, 780-789.

13. Riccio, D. A.; Schoenfisch, M. H., "Nitric oxide release: part I. Macromolecular scaffolds." *Chem. Soc. Rev.* **2012**, *41*, 3731-3741.

14. Carpenter, A. W.; Schoenfisch, M. H., "Nitric oxide release: Part II. Therapeutic applications." *Chem. Soc. Rev.* **2012**, *41*, 3742-3752.

15. Marxer, S. M.; Rothrock, A. R.; Nablo, B. J.; Robbins, M. E.; Schoenfisch, M. H., "Preparation of nitric oxide (NO)-releasing sol-gels for biomaterial applications." *Chem. Mater.* **2003**, *15*, 4193-4199.

16. Nablo, B. J.; Schoenfisch, M. H., "In vitro cytotoxicity of nitric oxide-releasing sol-gel derived materials." *Biomaterials* **2005**, *26*, 4405-4415.

17. Hetrick, E. M.; Schoenfisch, M. H., "Antibacterial nitric oxide-releasing xerogels: Cell viability and parallel plate flow cell adhesion studies." *Biomaterials* **2007**, *28*, 1948-1956.

18. Marxer, S. M.; Rothrock, A. R.; Nablo, B. J.; Robbins, M. E.; Schoenfisch, M. H., "Preparation of nitric oxide (NO)-releasing sol-gels for biomaterial applications." *Chem. Mater.* **2003**, *15*, 4193-4199.

19. Riccio, D. A.; Dobmeier, K. P.; Hetrick, E. M.; Privett, B. J.; Paul, H. S.; Schoenfisch, M. H., "Nitric oxide-releasing S-nitrosothiol-modified xerogels." *Biomaterials* **2009**, *30*, 4494-4502.

20. Poetes, R.; Holtzmann, K.; Franze, K.; Steiner, U., "Metastable underwater superhydrophobicity." *Phys. Rev. Lett.* **2010**, *105*, 166104.

21. McHale, G.; Newton, M. I.; Shirtcliffe, N. J., "Immersed superhydrophobic surfaces: Gas exchange, slip and drag reduction properties." *Soft Matter* **2010**, *6*, 714-719.

22. Hetrick, E. M.; Schoenfisch, M. H., "Analytical chemistry of nitric oxide." *Annu. Rev. Anal. Chem.* **2009**, *2*, 409-433.

23. Coneski, P. N.; Schoenfisch, M. H., "Nitric oxide release: Part III. Measurement and reporting." *Chem. Soc. Rev.* **2012**, *41*, 3753-3758.

24. Riccio, D. A.; Coneski, P. N.; Nichols, S. P.; Broadnax, A. D.; Schoenfisch, M. H., "Photoinitiated nitric oxide-releasing tertiary S-nitrosothiol-modified xerogels." *ACS Appl. Mater. Interfaces* **2012**, *4*, 796-804.

25. Shateri Khalil-Abad, M.; Yazdanshenas, M. E., "Superhydrophobic antibacterial cotton textiles." *J. Colloid. Interf. Sci.* **2010**, *351*, 293-298.

26. Katsikogianni, M.; Missirlis, Y. F., "Concise review of mechanisms of bacterial adhesion to biomaterials and of techniques used in estimating bacteria-material interactions." *Eur. Cells. Mater.* **2004**, *8*, 37-57.

27. Nablo, B. J.; Schoenfisch, M. H., "Poly(vinyl chloride)-coated sol-gels for studying the effects of nitric oxide release on bacterial adhesion." *Biomacromolecules* **2004**, *5*, 2034-2041.

28. Rojas, I. A.; Slunt, J. B.; Grainger, D. W., "Polyurethane coatings release bioactive antibodies to reduce bacterial adhesion." *J. Control. Release* **2000**, *63*, 175-189.

29. Mandell, B. F.; Schmitt, S., Diagnosis and management of prosthetic joint infection. In *Perioperative management of patients with rheumatic disease*, Springer New York: 2012; pp 261-269.

30. Privett, B. J.; Youn, J.; Hong, S. a.; Lee, J.; Han, J.; Shin, J. H.; Schoenfisch, M. H., "Antibacterial fluorinated silica colloid superhydrophobic surfaces." *Langmuir* **2011**, *27*, 9597-601.

31. Nichols, S. P.; Schoenfisch, M. H., "Nitric oxide flux-dependent bacterial adhesion and viability at fibrinogen-coated surfaces." *Biomater. Sci. 10.1039/C3BM60130G [Available online July 17, 2013]*.

32. Yohe, S. T.; Kopechek, J. A.; Porter, T. M.; Colson, Y. L.; Grinstaff, M. W., "Triggered drug release from superhydrophobic meshes using high-intensity focused ultrasound." *Adv. Healthcare Mater. DOI: 10.1002/adhm.201200381 [Available online April 17, 2013]*

Chapter 4:

Dual-Action Antimicrobial Surfaces: Silver and Nitric Oxide-Releasing Xerogels

4.1 Introduction

Despite modern advances in surgical care, many medical device infections occur each year due to several confounding factors: 1) native bacteria residing on the skin of medical personnel and patients make a truly sterile wound site impossible in practice;[1] 2) the introduction of a foreign device into host tissue causes a localized inflammatory response that inhibits the pathogen-killing efficacy of immune cells;[2] and 3) bacteria readily colonize surfaces and form a protective exopolysaccharide matrix known as a biofilm.[3-5] As a result, the tissue surrounding indwelling medical devices such as catheters and orthopedic implants succumbs to infection more readily than normal tissue.[1,6] The bacterial biofilms that result are resistant to conventional antibiotic treatments and cause recurrent infections through the release of planktonic bacteria.[7] To address this issue, researchers have developed antimicrobial coatings that resist bacterial adhesion or kill adhered bacteria before biofilm formation ever occurs.[8]

Silver-releasing materials have been used successfully to kill bacteria and prevent biofilm formation.[9, 10] However, growing concern has emerged regarding the potential toxicity of silver-releasing compounds and the emergence of silver-resistant pathogens.[9, 11-15] Systemic concentrations of the metal may become elevated even when silver is released locally from a material.[16, 17] One case report describes argyria-like symptoms in a burn patient treated with silver-releasing wound dressings.[11] Even in light of these concerns, the clinical efficacy of silver-releasing materials against a broad range of

nosocomial pathogens necessitates their use. Thus, new strategies are needed that circumvent silver-associated toxicity and limit opportunities for antimicrobial resistance to these compounds.

Delivering two or more biocidal agents in tandem may limit opportunities for resistance and lower dose-associated toxicity.[16,18, 19] Certain biocidal combinations may also lead to synergy, where two agents acting in tandem are more effective than the sum of their individual biocidal activities.[20] Combination therapies have emerged that utilize silver compounds in tandem with traditional antibiotics or broad-spectrum antimicrobials.[21-23] Privett et al. reported synergistic killing of bacteria co-treated with silver sulfadiazine (SSD) and a small molecule nitric oxide (NO)-donor ("PROLI/NO"). Nitric oxide (NO) is a potent broad-spectrum agent itself, utilized by macrophages and other immune cells to kill foreign microbes.[24] Controlled release of NO reduces bacterial adhesion,[25, 26] kills bacteria,[27, 28] prevents biofilm formation,[29] and reduces the likelihood of infection in vivo.[30, 31] The previously studied combination of SSD and PROLI/NO exhibited synergytic bactericidal efficacy against multiple standard and drug-resistant pathogens, resulting in lower overall concentrations needed for each biocidal agent.[22]

Combined release of NO and silver from a surface may enable the fabrication of interfaces with superior anti-adhesive and biocidal efficacy. Combining two broad-spectrum antimicrobials would limit opportunities for bacterial resistance by promoting additional mechanisms for cell death. Likewise, the potential for synergistic killing between NO and silver could lead to enhanced bacterial killing without causing unnecessary mammalian cell toxicity. Herein, dual-action silver/NO-releasing xerogels are prepared utilizing sol-gel chemistry. We hypothesize that this combination of agents

would lead to a more effective biocidal surface while minimizing unneeded mammalian cell toxicity. Herein, amine-modified xerogels are coated with a silver nitrate-loaded sol. Following conversion of these internal amines to *N*-diazeniumdiolate NO donors, the materials simultaneously release antimicrobial concentrations of Ag^+ and NO. The antifouling/antimicrobial efficacy of the films is assessed against two biomedically relevant bacteria.

4.2 Materials and methods

Ethyltrimethoxysilane (ETMOS), propyltrimethoxysilane (PTMOS), and *N*-(6-aminohexyl)aminopropyltrimethoxysilane (AHAP) were purchased from Gelest, Inc. (Morrisville, PA). Glass micro slides were acquired from Gold Seal (Portsmouth, NH). Methyltrimethoxysilane (MTMOS), isobutyltrimethoxysilane (BTMOS), and silver nitrate ($AgNO_3$; analysis grade) were purchased from Sigma Aldrich (St. Louis, MO). Milli-Q water was purified from distilled water using a Millipore Milli-Q UV Gradient A-10 system (Bedford, MA) to a resistivity of 18.2 MΩ cm and a total organic content of <5 ppb. Nitric oxide gas (NO) was purchased from Praxair (Bethlehem, PA). Standardized NO (26.85 ppm, balance N_2) and nitrogen gasses were acquired from Airgas National Welders (Durham, NC). Silver nitrate (analysis grade) was purchased from Acros Organics (Geel, Belgium). *Pseudomonas aeruginosa* (*P. aeruginosa;* ATCC #19413) and *Staphylococcus aureus* (*S. aureus*; ATCC #29213) were acquired from American Type Tissue Culture Collection (Mannasas, VA). Tryptic soy broth (TSB) and agar were obtained from Becton, Dickinson and Company (Sparks, MD). L929 fibroblast cells were acquired from the UNC tissue culture facility (Chapel Hill, NC). Dulbecco's

modified essential media (DMEM), (3-(4,5-dimethylthiazol-2-yl)-5-(3-carboxymethoxyphenyl)-2-(4-sulfophenyl)-2H-tetrazolium) (MTS) and phenazine methosulfate (PMS) were acquired from Becton, Dickinson and Company (Sparks, MD). All other reagents were analytical grade and used as received.

4.2.1 Synthesis of amine-modified xerogels

Glass microscope slides used as substrates for the xerogels were cut to dimensions of 9 x 25 mm, cleaned via successive 10 min bouts of sonication in water, ethanol, and acetone, and dried in ambient conditions. To facilitate adhesion between subsequent xerogel layers and the glass substrate, the slides were cleaned and oxidized via UV/O_3 for 30 min with a Bioforce TipCleaner (Ames, IA).

Dual-action silver/NO-releasing xerogels were synthesized via a 3-layer approach. The bottom layer consisted of an amine-modified xerogel (serving as the NO-release layer) while the top layer was the $AgNO_3$-doped xerogel (serving as the silver-release layer). A xerogel barrier layer was placed between each to minimize interactions between Ag^+ and the underlying amines. Amine modified xerogels were synthesized from AHAP and BTMOS as previously described.[32] Briefly, BTMOS (378 μL) was prehydrolyzed by adding the silane to ethanol (633 μL), water (190 μL) and 0.5 M HCl (31.7 μL) and reacting for 1 h. Following, 255 μL AHAP was added to the pre-hydrolyzed sol, allowing the silane to crosslink with BTMOS for an additional 1 h. After this time, 45 μL of the resulting amine-modified sol was cast on the glass substrates prepared above, dried for 1 h in ambient conditions and cured at 70 ^oC for 3 d, yielding crack-free, clear AHAP/BTMOS xerogels.

Barrier layers were synthesized from an alkyl-functionalized silane (MTMOS, ETMOS, or PTMOS). Equal volumes of ethanol and the silane (120 μL) were combined and reacted under acidic conditions by adding 16.8 μL H_2O and 7.5 μL 0.5 M HNO_3 and mixing for 2 h. Following, 20, 40 or 60 μL of the sol was cast on the AHAP/BTMOS xerogels prepared above, dried at room temperature for 1 h and cured at 80 ^oC for 24 h.

Silver-releasing xerogels were prepared by including $AgNO_3$ as a dopant within a PTMOS sol. PTMOS (180 μL) and ethanol (219 μL) were mixed briefly prior to the addition of 78.6 μL of $AgNO_3$ in MilliQ water at different concentrations to control the amount of Ag^+ within the sol. Silver nitrate concentrations in the aliquot were 0, 22.8, 57.1, 114.2, or 171.3 mg mL^{-1} resulting in 0 (AG-0), 1 (AG-1), 2.5 (AG-2.5), 5 (AG-5) or 7.5 (AG-7.5) mol% $AgNO_3$ (relative to total moles Si) xerogels, respectively. Following the addition of a 0.5 M HNO_3 catalyst (9.11 μL), the sol was reacted in the dark for 4 h. Aliquots of the sol (144 μL) were then spincoated (2000 rpm; 10 s) onto glass or xerogel substrates. The PTMOS xerogels were dried for 24 h in the dark at room temperature and then cured at 60 ^oC for 48 h. All xerogels were stored over desiccant at room temperature until further use.

4.2.2 N-diazeniumdiolate modification

The secondary amines within the AHAP layer were converted to *N*-diazeniumdiolate NO donors by exposure to high pressure NO gas. Xerogels were pre-purged with argon in a Parr hydrogenation bomb then pressurized to 10 bar NO for 3 d. Following copious purging to remove unreacted NO, the *N*-diazeniumdiolate-modified xerogels were removed and stored at -20 ^oC until further use. This procedure formed NO

donor-modified xerogels (AG-0/NO and AG-(1, 2.5, or 5)/NO from non-silver or silver-containing xerogels, respectively.)

4.2.3 Characterization of silver/NO-releasing xerogels

Nitric oxide-release from the *N*-diazeniumdiolate-modified xerogels was measured using a chemiluminescent nitric oxide analyzer (NOA; Sievers 280i, Boulder, CO). Xerogels were placed in 30 mL deoxygenated phosphate buffered saline (PBS; 37 ^{o}C; pH 7.4). Nitric oxide evolved from the xerogels was carried to the analyzer via a stream of nitrogen supplied via a porous frit submerged in the buffer solution. Measurements were halted when the NO flux from the materials fell below ~20 ppb. The total amount of NO released was determined by integrating the real-time NO flux (vs. time) over the measurement duration.

Release of silver from the xerogels was quantified by submerging the silver-containing xerogels in 10 mL PBS (37 ^{o}C) and transferring each xerogel to new soak solutions at regular time intervals. Silver content within the soak solutions was determined using inductively coupled plasma optical emission spectrometry (Teledyne Leeman Prodigy ICP-OES; Hudson, NH). Standards were prepared using a TraceCert 1000 ppm Ag standard (Fluka; Buchs, Switzerland) at concentrations of 0, 50, 100, 500, and 1000 ppb. Cumulative silver release over the entire soak duration (4 d) was determined by summing the concentrations for each individual time point. Static water contact angles were determined from photographs acquired on a KSV Instruments Cam 200 Optical Contact Angle Meter (Helsinki, Finland).

4.2.4 Adhered viable bacteria assays

The antimicrobial performance of the NO and silver-releasing xerogels was assessed by determining the number of adhered viable bacteria on the substrates after static exposure to *P. aeruginosa* and *S. aureus*. Overnight cultures of *P. aeruginosa* and *S. aureus* were initially grown from frozen stocks, reinnoculated in TSB, and then grown to a concentration of 10^8 cfu mL^{-1}. Following centrifugation, the bacteria were resuspended in PBS (for *P. aeruginosa)* or 0.5% (v/v) TSB in PBS (for *S. aureus)* to reach a final concentration of 10^8 cfu mL^{-1}. Of note, trace TSB was necessary to maintain full survival of *S. aureus* over the experimental duration. In a manner similar to previously developed methods,[28, 33, 34] the xerogels were placed in 4 mL of the 10^8 cfu mL^{-1} bacterial suspensions and gently agitated at 37 ^oC for 3 h. Following exposure, the xerogels were rinsed gently with distilled water to remove loosely adhered bacteria. Bacteria on the face of the glass substrate opposite of the xerogel (i.e., the uncoated portion) were killed by swabbing with ethanol for 30 s. After drying trace ethanol with a laboratory wipe, the substrates were transferred to 4 mL sterile PBS. Adhered bacteria were removed via sonication at 60 KHz for 15 min.[27] Serial 10-fold dilutions of the supernatant were plated on tryptic soy agar, grown overnight, and the resulting colonies (assumed to equal the number of viable adhered bacteria on the xerogel surface) enumerated.

4.2.5 Confocal microscopy

Confocal microscopy was used to quantify bacterial adhesion, intracellular NO uptake, and cell death. A Zeiss 510 Meta inverted laser scanning confocal microscope equipped with a 488 nm Ar excitation laser (30% power; 2.05% intensity) and a 505-530 nm bandpass (BP) filter was used to obtain Syto 9 and DAF2-DA (green) fluorescence

images. A 543 nm HeNe laser (25.3% intensity) and a BP 560—615 nm filter were used during acquisition of PI (red) fluorescence images. All images (both fluorescent and bright field) were acquired with a 20x objective.

For bacterial adhesion studies, xerogels were submerged in suspensions of 10^8 cfu mL^{-1} *P. aeruginosa* for 3 h. Following exposure, the xerogels were removed, rinsed gently in distilled water, and incubated in 10 μM green fluorescent Syto 9 dye for 30 min. The xerogels were then transferred to a glass bottom confocal dish containing 5 mL PBS. The green fluorescent micrographs were digitally thresholded to create binary color images. Bacterial surface coverage was determined by quantifying the relative number of white pixels (from green bacteria) over the image frame. DAF-2 DA (green) and propidium iodide (PI; red) dyes were used to visualize intracellular NO uptake and bacterial membrane damage, respectively. The xerogels were immersed in a 10^8 cfu mL^{-1} suspension of *P. aeruginosa* supplemented with 10 μM DAF-2 DA and 30 μM PI for 1 h, rinsed, and placed in glass bottom confocal dishes containing 5 mL PBS. To improve visualization, monochromatic images were digitally converted from DAF-2 DA and PI fluorescent micrographs following brightness and contrast adjustment. Adjustments were applied to all samples equally.

4.2.6 Xerogel cytotoxicity

The cytotoxic potential of NO and Ag xerogels was assessed against L929 mouse fibroblasts. First, L929 cells were grown in culture flasks containing DMEM and supplemented with 10% (v/v) FBS and 1 wt% penicillin/streptomycin. The flasks were incubated in a humidified 5% CO_2 environment until reaching confluency (80%), removed with trypsin, seeded onto tissue-culture treated 24-well plates, and incubated at

37 ^{o}C for 72 h. After removing the supernatant via aspiration and replacing with 1 mL fresh DMEM, the xerogels were placed face down on the fibroblast cells and incubated at 37 ^{o}C in 5% CO_2 for 24 h. Following aspiration of the supernatant, the wells were rinsed thrice with PBS and replaced by a mixture of DMEM/MTS/PMS (1 mL total at a volume ratio of 105/20/1). The cells were incubated for an additional 90 min. Following this incubation period, 120 μL aliquots of the supernatant were transferred to a microtiter plate. The absorbance of the solutions was measured using a Thermoscientific Multiskan EX plate reader at 490 nm, and compared against blanks (i.e., the DMEM/MTS/PMS mixture) and control AG-0 xerogels.

4.3 Results and discussion

4.3.1 Synthesis and characterization of silver/NO-releasing xerogels

The mild aqueous reaction conditions afforded by the sol-gel method have proven useful for drug delivery applications.[10, 35, 36] We have previously developed NO-releasing materials by incorporating amine-modified silanes into xerogel frameworks, and then converting those amines to *N*-diazeniumdiolate NO donors via reaction with NO gas. Herein, a two-layer approach was used to combine this chemistry with silver release. Amine-modified xerogels were synthesized by co-condensing *N*-6-(aminohexylaminopropyl)trimethoxysilane (AHAP) with isobutyltrimethoxysilane (BTMOS). This silane system, chosen for its stability in physiological buffer and extended NO-release duration,[32, 34, 37] served as the base layer for the dual Ag+/NO-release materials. To fabricate the silver-release layer, $AgNO_3$ was doped within an acid-catalyzed propyltrimethoxysilane (PTMOS) sol at 1, 2.5, or 5 mol% (relative to total Si

content in the sol) and subsequently spincast onto dried AHAP/BTMOS xerogels to yield AG-1, AG-2.5, and AG-5, respectively.

As shown in Figure 4.1 A, cumulative silver release from AG-1 was negligible (~10 ppb over 4 d) unless an additional barrier layer was placed between the AHAP/BTMOS and AG-1 xerogels. In the absence of a barrier layer, we hypothesize that Ag^+ migrates into the AHAP/BTMOS layer where the ion is complexed by amines. Indeed, the tendency of Ag^+ to complex with amines is well-established.[38-40] To minimize undesirable scavenging of Ag^+, ethyltrimethoxysilane (ETMOS) sols were prepared and cast onto the AHAP/BTMOS xerogels as barrier layers. The use of methyltrimethoxysilane and propyltrimethoxysilane were also explored, but ETMOS proved best at spreading evenly over the AHAP/BTMOS substrate while also facilitating even coating by the AG xerogels. As measured via ICP-OES, increasing the ETMOS barrier layer cast volume from 20 to 40 μL resulted in a concomitant increase in silver release from AG-1. When the barrier layer volume was increased to 60 μL, the subsequent change in cumulative silver-release totals was negligible, indicating a leveling-off effect at this volume. Some degree of interaction between Ag^+ in the silver layer and amines in the AHAP/BTMOS layer, then, appears to be inevitable. Cumulative silver release from AG-1 in the absence of an underlying AHAP/BTMOS layer (i.e., the "best-case-scenario" for silver release totals) was ~1.5x greater than release from AG-1 on AHAP/BTMOS with a 40 μL barrier layer. Nonetheless, silver concentrations released from AG-1 with 40 μL barrier layers have proven sufficient to elicit antimicrobial effects.[10] All other xerogel compositions hereafter were fabricated with 40 μL barrier layers separating the AHAP/BTMOS and AG layers. As shown in Figure 4.1B, silver

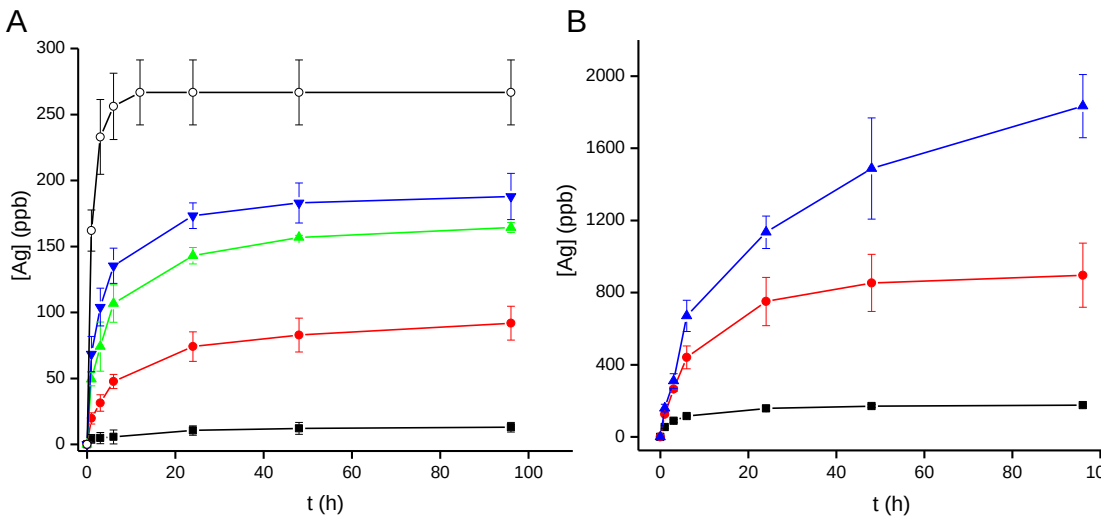

Figure 4.1 (A) Cumulative silver release from AG-1 films with 0 (black), 20 (red), 40 (green), or 60 μL (red) μL barrier layers separating the xerogel from the underlying amine layer. The open-boxed line displays silver-release from AG-1 release in the absence of an underlying AHAP/BTMOS film. (B) Silver release from AG-1 (black), AG-2.5 (red), and AG-5 (blue) on 40 μL barrier layers. Silver was quantified using ICP-OES. Error bars represent the standard deviation of the mean from at least n=3 independently prepared samples.

release totals were tunable by adjusting the mol% of $AgNO_3$ in the PTMOS precursor sols. AG-5 xerogels released ~10-fold more silver than AG-1 xerogels over 4 d, with AG-2.5 xerogels releasing about half that amount. Increasing silver-loading in this manner may prove useful for maximizing the antimicrobial efficacy of these materials.

To ensure that each active release chemistry (i.e., NO and silver) could be controlled independently, the release of silver and NO was evaluated from the materials following *N*-diazeniumdiolate-modification or silver-loading, respectively. Representative NO-release curves from AG-0/NO and AG-1/NO xerogels (Figure 4.2 A) show that the presence of a silver-layer had no discernible effect on real-time NO-release flux. Integrating the curves to determine total amounts of NO indicated a negligible difference in NO-release totals, with AG-0/NO and AG-1/NO xerogels releasing 3.90 ± 0.04 and 3.65 ± 0.05 μmol NO cm^{-2}, respectively. Together, these results suggest that *N*-diazeniumdiolate modification and subsequent decomposition to NO is unaffected by the presence of a silver layer.

Silver release from AG-1, AG-2.5, and AG-5 xerogels was then examined before and after *N*-diazeniumdiolate NO donor. The NO donor formation process (Figure 4.2 B). had negligible effect on the silver release from AG-2.5 and AG-5 xerogels. However, cumulative silver-release totals from AG-1 xerogels after $\geq$ 24 h increased following *N*-diazeniumdiolate modification of the underlying AHAP/BTMOS layer (96 h totals of 176 ± 6 and 247 ± 7 ppb for AG-1 and AG-1/NO, respectively). This effect may be attributed to densification of the AHAP/BTMOS xerogel upon NO exposure. Shin et al. similarly reported the permeability of 40% AHAP/BTMOS xerogels to hydrogen peroxide fell drastically following *N*-diazeniumdiolate formation, despite the

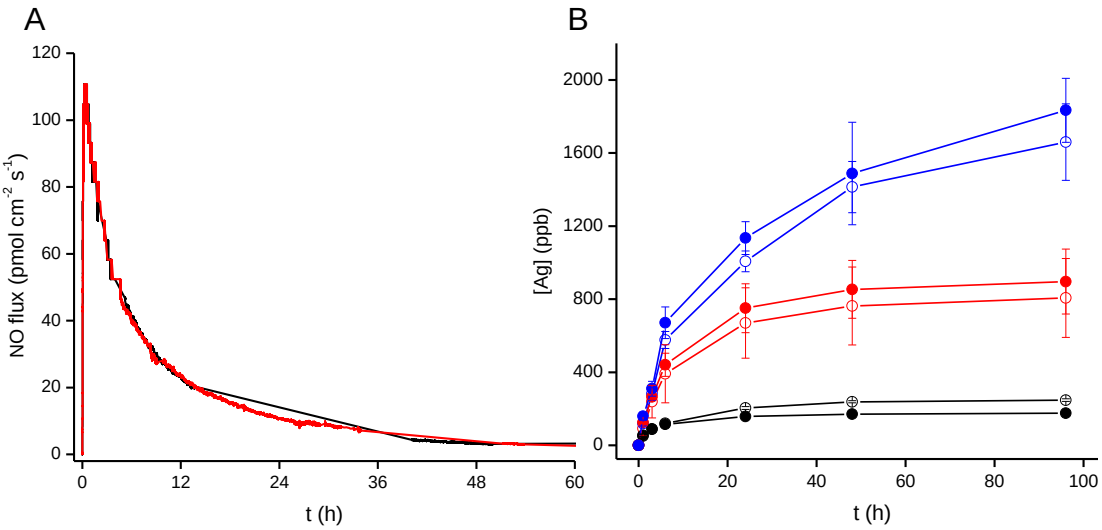

Figure 4.2 (A) Representative NO-release curves from AG-0/NO (black) and AG-1/NO (red) xerogels obtained using chemiluminescence. (B) Silver release from AG-1, AG-2.5, and AG-5 xerogels following N-diazeniumdiolate NO donor formation measured using ICP-OES. Error bars represent the standard deviation of the mean from at least n=3 independently prepared samples.

xerogels being permeable to the small molecule prior to NO donor addition.[41] Similar densification of the *N*-diazeniumdiolate-modified AHAP/BTMOS network herein may impede diffusion of Ag^{+} into the amine-rich AHAP layer, thereby increasing silver release totals. Nonetheless, all bacteria experiments performed herein were evaluated over $\leq$9 h exposure times so that any changes in release from AG-1 and AG-1/NO xerogels after 24 h would not account for differences in antimicrobial effects.

4.3.2 Anti-adhesion and biocidal efficacy of silver/NO-releasing xerogels

The antimicrobial efficacy of AG and AG/NO xerogels was determined under static conditions using 10^{8} cfu mL^{-1} suspensions of *P. aeruginosa* (Gram-negative) and *S. aureus* (Gram-positive), two of the most commonly implicated bacterial strains in orthopedic implant infections.[42, 43] Xerogels were fully submerged in the suspensions upright, allowing the bacteria to adhere to the substrates. Bacteria were removed via sonication and the supernatent was plated on TSA for enumeration.

To start, the AG-0/NO and AG xerogels were exposed to *P. aeruginosa* for 3 h. As shown in Figure 4.3A, the AG-1 xerogels reduced viable (i.e., living) adhered *P. aeruginosa* by 1.1-log relative to controls. Greater silver concentrations released from AG-2.5 and AG-5 killed bacteria more effectively, resulting in a ~3.5 log decrease in viable adhered bacteria (i.e., the limit of detection in our assay). Marini et al. and Stobie et al. have previously reported more complete killing of *S. epidermidis* and *S. aureus* from silver-releasing sol-gel materials.[10, 44] These systems had similar silver-release totals and durations to our AG-1 system. Surprisingly, the AG-1 xerogel only reduced viable *P. aeruginosa* by ~1-log or less despite *P.* aeruginosa being more susceptible to silver (via

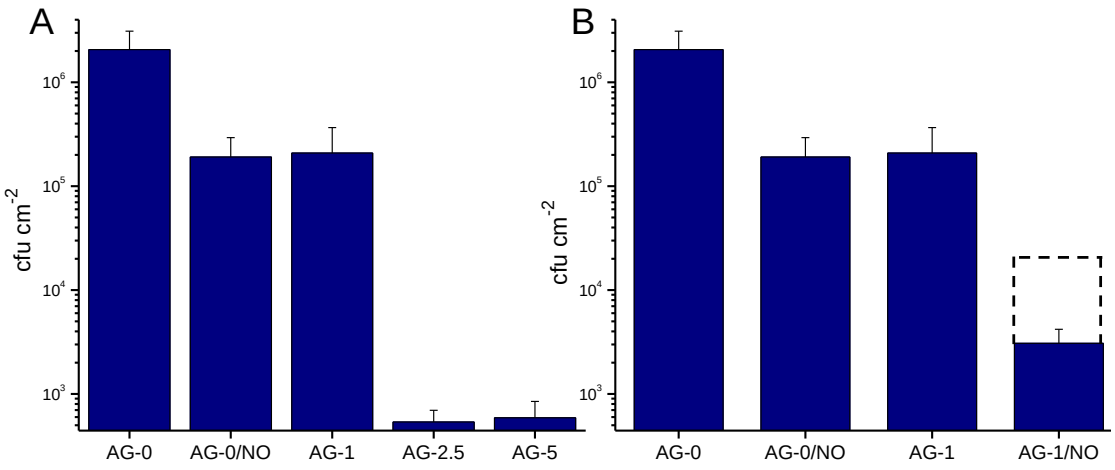

Figure 4.3 (A) Viable adhered colonies on NO- and silver-releasing xerogels after 3 h exposure to 10^8 cfu mL^{-1} *P. aeruginosa* (B) Viable adhered colonies on AG-0, AG-0/NO, AG-1, and AG-1/NO in the same conditions. The traced box represents theoretical additive killing. Error bars represent the standard deviation of the mean from n=3 independent experiments.

silver sulfadiazine) than either *S. aureus* or *S. epidermidis.*[45] We hypothesized that this discrepancy may be related to the highly concentrated (10^8 cfu mL^{-1}) bacteria suspensions used in this work (vs. ~10^6 cfu mL^{-1}). To evaluate the influence of suspension concentration on viable adhesion, the antimicrobial activity of AG-1 xerogels was assessed after diluting the *P. aeruginosa* bacterial suspension to 10^6 or 10^7 cfu mL^{-1}. In both cases, AG-1 resulted in complete killing of *P. aeruginosa.* Following 3 h exposure to 10^7 cfu mL^{-1} of the bacteria, <440 cfu cm^{-2} were found on AG-1 xerogels (i.e., the limit of detection) versus 8.3 x 10^5 cfu cm^{-2} on controls. Likely, excess bacteria in the more concentrated 10^8 cfu mL^{-1} suspensions scavenged some Ag^+ released from the film that would have otherwise interacted with the surface-adhered bacteria. Synergy between NO and Ag^+ would be impossible to detect if one agent caused complete bacterial killing on its own. Thus, 10^8 cfu mL^{-1} concentrations were used for subsequent studies.

AG-1 xerogels were used to study the antimicrobial potential of NO and Ag^+ released in tandem (Figure 4.3B and Table 4.1) because viable bacterial counts on AG-2.5 and AG-5 xerogels were already near the plate counting limit of detection (440 cfu cm^{-2}). Privett et al. reported a fractional bactericidal concentration (FBC) of 0.63 against *P. aeruginosa* when using silver sulfadiazene and PROLI/NO (a rapidly decomposing NO donor) as antimicrobial agents.[22] While this value is technically above the "synergy" threshold of FBC $\leq$ 0.5, Berenbaum has argued that FBC values between 0.5 and 1 should be considered moderately synergistic and still clinically relevant.[46]

Next, AG-0 and AG-1 xerogels with and without *N*-diazeniumdiolate modification were exposed to a 10^8 cfu mL^{-1} suspension of *P. aeruginosa* for 3 h. While AG-0/NO and AG-1 each reduced viable adhered bacteria by 1.1-log individually, the

Table 4.1 Cumulative NO and silver doses delivered from the dual NO- and silver-releasing xerogels following 3 h exposure to *P.* aeruginosa and the resulting log-decrease in viable adhered bacterial colonies.

xerogel	cumulative NO delivered (μmol cm^{-2})	cumulative [Ag] (ppb)	log reduction of viable bacteria
AG-0	0.87 ± 0.13[a]	-	1.1 ± 0.3
AG-1	-	220 ± 9	1.1 ± 0.3
AG-1/NO	0.86 ± 0.09	223 ± 21	2.9 ± 0.2

[a] Values are given as the mean ± standard deviation of at least n=3 independent experiments

combination of the two agents caused a 2.9-log reduction (i.e., a 0.7-log reduction from their summed antimicrobial effects). As shown in Table 4.1, these results could not be attributed to differences in silver or NO delivered over the course of the experiment (Table 4.1), indicating that the combination Ag^+ and NO release causes a greater-than-additive antimicrobial effect against *P. aeruginosa.*

The antifouling and antimicrobial abilities of the xerogels were also assessed against *Staphylococcus aureus* (*S. aureus)*, a Gram-positive pathogen commonly implicated in biofilm formation on orthopedic devices.[7] Figure 4.4A shows adhered viable bacteria on NO and silver-releasing xerogels individually when exposed to a 10^8 cfu mL^{-1} suspension of *S. aureus* for 3 h. While AG-5 caused a 3.5-log reduction in viable adhered *P. aeruginosa*, the same composition only caused a 1.3-log reduction against *S. aureus.* Previous studies have highlighted decreased silver efficacy against *S. aureus*,[47] mostly attributed to its thick peptidoglycan layer in conjunction with the membrane-dependent biocidal mechanisms of Ag^+.[48] Viable adhesion reductions by NO were also lessened for *S. aureus* when compared to *P. aeruginosa.* Nichols et al. demonstrated that reductions in adhered viable *S. aureus* on NO-releasing surfaces were primarily attributed to reduced bacterial adhesion rather than bacterial killing.[28] Significant killing (approaching ~1 log) was not observed until much longer 24 h exposure times.

To overcome these limitations, we assessed the antimicrobial potential of silver and NO-releasing xerogels acting in concert. No synergy between the agents was observed after 3 h (data not shown), despite Privett et al. reporting a synergistic FBC of 0.42 for *S. auereus* when using small molecule donors.[22] This is best explained by the

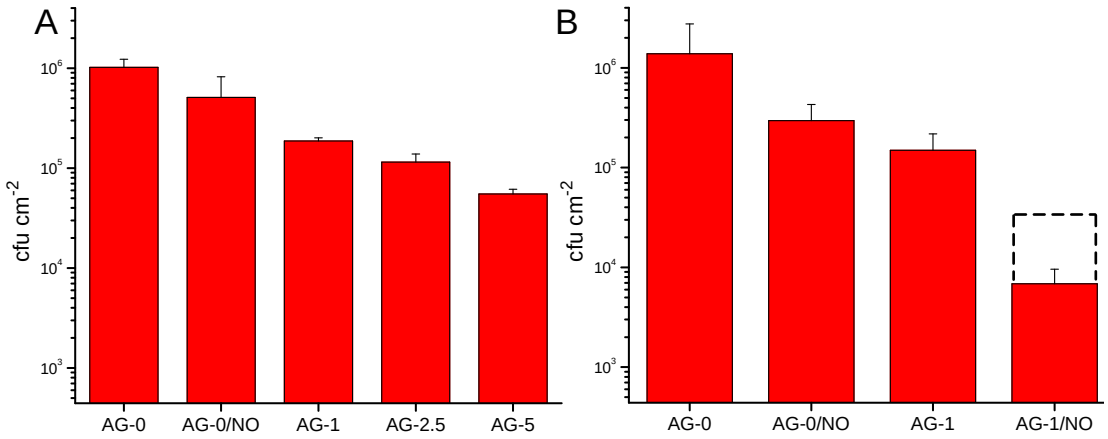

Figure 4.4 (A) Viable adhered colonies on NO- and silver-releasing xerogels after 3 h exposure to 10^8 cfu mL^{-1} *S. aureus*. (B) Viable adhered colonies on AG-0, AG-0/NO, AG-1, and AG-1/NO following an additional 6 h in bacteria-free PBS (9 h total). The traced box represents theoretical additive killing. Error bars represent the standard deviation of the mean for at least n=3 experiments.

larger dosage of each agent required to kill *S. aureus*. Even though silver and NO exhibited less synergy against *P. aeruginosa* than *S. aureus* (as reported by Privett et al.) the overall dosages of the combined agents required for killing were still higher for *S. aureus*. To account this effect on silver/NO-releasing xerogels, we increased the NO and silver-release "dose" by transferring the xerogels to fresh PBS after the initial 3 h bacterial adhesion event, then incubating for an additional 6 h. Following these longer exposure times, a greater-than-additive effect (a further 0.7-log reduction) was observed from the combination of NO and silver-release, with a 2.4-log killing observed for the two agents in tandem (Figure 4.4B and Table 4.2). Overall, these results support the promise of dual-action NO/silver releasing xerogels for killing adhered bacteria while minimizing undesirable silver accumulation.

Despite potential synergy, it is unclear whether reductions in adhered viabile bacteria on the xerogel surfaces were the result of decreased bacterial adhesion, increased bacterial killing, or a combination of both. Previous evidence suggests that NO's action (at least over the exposure durations used herein) results from reduced bacterial adhesion rather than bacterial killing.[27, 28] Nablo et al. reported that NO-release at similar fluxes caused a ~10-fold reduction in *P. aeruginosa* surface coverage,[26] consistent with the 1-log reduction in viable adhered bacteria observed in Figure 4.3. Hetrick et al. examined bacterial killing on NO-releasing AHAP/BTMOS xerogels using live/dead fluorescent probes, and found that NO did not begin to damage *P. aeruginosa* membranes until 7 h of continuous exposure.[27]

This hypothesis was explored through additional bacterial adhesion studies. The xerogels were incubated in Syto 9 (a fluorescent nucleic acid stain for both live

Table 4.2 Cumulative NO and silver doses delivered from the NO- and silver-releasing xerogels during a 9 h exposure to *S. aureus* a and the resulting log-decrease in viable adhered bacterial colonies.

xerogel	cumulative NO delivered (µmol cm^{-2})	cumulative [Ag] (ppb)	log reduction in viable adhered bacteria
AG-0	1.76 ± 0.16[a]	-	0.7 ± 0.2
AG-1	-	306 ± 13	1.0 ± 0.2
AG-1/NO	1.70 ± 0.15	334 ± 12	2.4 ± 0.3

[a] Values are given as the mean ± standard deviation of at least n=3 independent experiments

and dead cells) following 3 h exposure to 10^8 cfu mL^{-1} *P. aeruginosa*. Of note, fluorescent microscopy was utilized instead of bright field microscopy because of optical interference caused by salt aggregates on the silver-loaded films. A similar issue was reported by Stobie et al. for low-temperature $AgNO_3$-doped sol-gels.[10] As shown in Figure 4.5 and Table 4.3, bacterial coverage on control surfaces was approximately 30%. Silver-releasing xerogels (AG-1) reduced the adhesion slightly (30% lower coverage relative to the control xerogels), consistent with previous findings that silver does reduce the extent of bacterial adhesion.[49, 50] Compared to silver release at these concentrations, NO-releasing xerogels proved more effective at reducing bacterial adhesion. For both AG-0/NO and AG-1/NO xerogels the overall surface bacteria coverage was reduced by ~90% vs. controls (i.e., a 1-log reduction), confirming that the 1.1-log reduction of viable *P. aeruginosa* adhesion on AG-0/NO xerogels (Figure 4.3) results from reduced bacterial adhesion rather than bacterial killing. In contrast, AG-1 xerogels only reduced bacterial adhesion by ~30% relative to controls despite a 1.1-log reduction in adhered viable bacteria. This result suggests that the bulk of silver's mechanism of action must occur through bacterial killing.

Confocal microscopy was also utilized to interrogate the antimicrobial mechanisms of each agent and gain an understanding of the greater-than-additive effect observed from tandem NO and Ag^+ release. Bacterial membrane damage (indicative of cell death) was probed using propidium iodide (PI) while intracellular levels were observed using green fluorescent DAF-2 DA. The DAF-2 DA molecule permeates bacterial cell membranes where it is then hydrolyzed by bacterial esterases to produce the membrane-impermeable fluorescent probe DAF2.[51] Following reaction with NO and

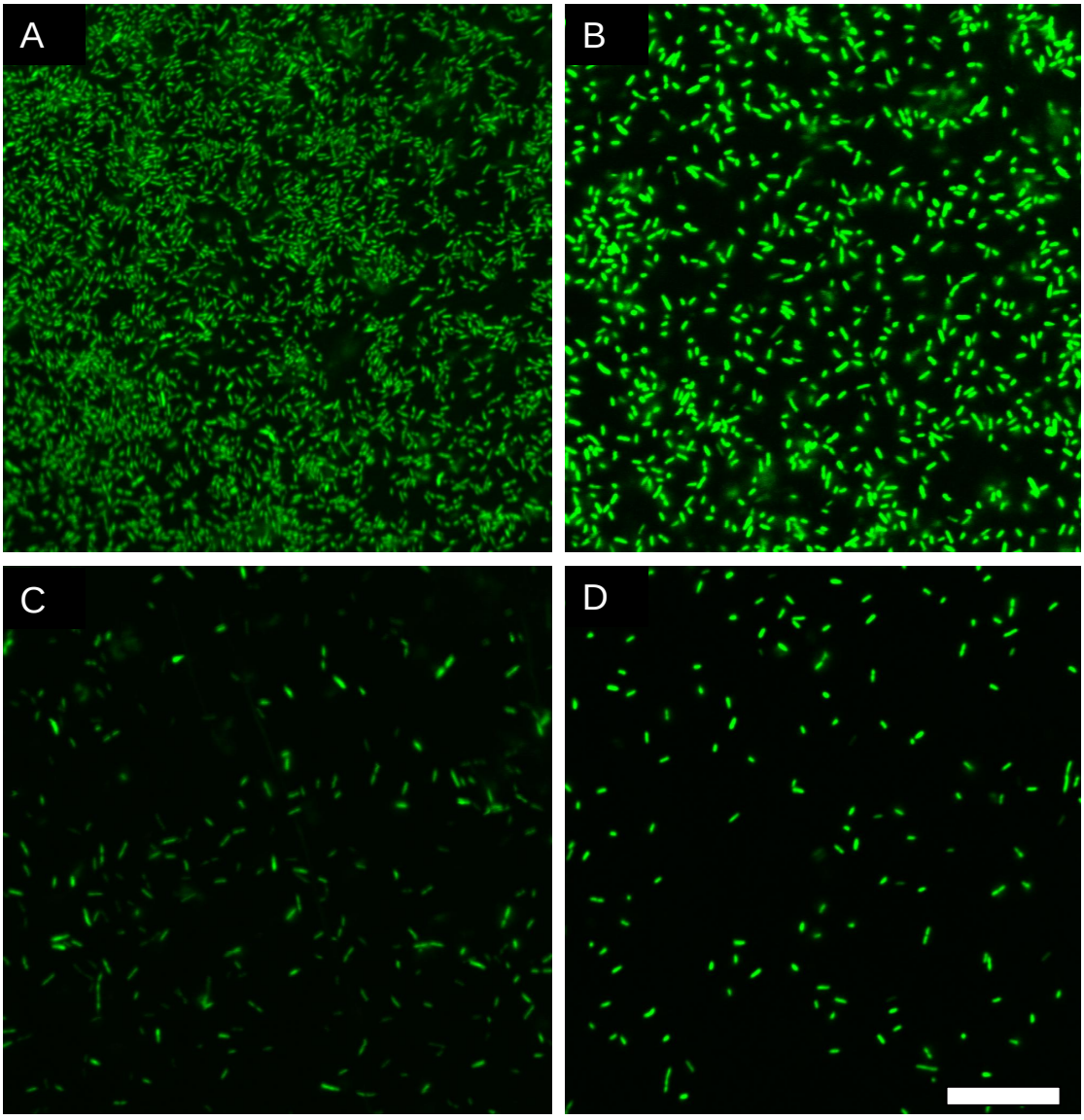

Figure 4.5 Fluorescent images of *P. aeruginosa* on (A) AG-0 (B) AG-1 (C) AG-0/NO, and (D) AG-1/NO visualized using the Syto 9 fluorescent probe. Scale bar = 20 μm.

Table 4.3 Bacterial surface coverage on NO- and silver-releasing xerogels following 3 h immersion in 10^8 cfu mL^{-1} *P. aeruginosa*.

xerogel	% bacterial surface coverage	contact angle (^{o})
AG-0	30.1 ± 2.4[a]	92.8 ± 1.7
AG-0/NO	2.6 ± 0.4	92.6 ± 1.0
AG-1	20.6 ± 3.2	91.0 ± 3.6
AG-1/NO	2.5 ± 0.4	85.1 ± 0.7

[a] Values are given as the mean ± standard deviation from at least n=3 locations on each xerogel

associated nitrosative intermediates, the DAF2 probe fluoresces green and is thus an indicator of high intracellular NO concentrations.[51] Propidium iodide is membrane-impermeable, only entering cells once membrane damage has occurred (i.e., via the presence of an exogenous antimicrobial), indicating cell death.

Xerogels were incubated in 10^8 cfu mL^{-1} *P. aeruginosa* supplemented with DAF2-DA and PI and transferred to sterile PBS. The confocal micrographs show intracellular NO uptake within bacteria adhered to both the AG-0/NO and AG-1/NO xerogels (Figure 4.6). However, the absence of a strong PI fluorescence signal from AG-0/NO indicates that associated cell membrane damage had not yet occurred. In a related study that evaluated the antimicrobial action of NO-releasing nanoparticles against bacteria, Hetrick et al. showed that NO uptake preceded bacterial membrane damage.[27] Taken together, this observation supports our hypothesis that reductions in viable adhered bacteria on NO-releasing xerogels (without silver) are primarily caused by reduced bacterial adhesion. In contrast, PI fluorescence from cells adhered to the AG-1 xerogels shows that nearly all of the bacteria are membrane-compromised despite thorough *P. aeruginosa* adhesion. The antifouling capabilities of the silver-releasing xerogels must primarily occur through bacterial killing rather than the prevention of bacterial adhesion. Bacteria adhered on the AG-1/NO xerogels exhibited bright DAF2-DA and PI-associated fluorescence, indicating that significant membrane damage and NO uptake is occurring. For AG-1/NO xerogels, we observed only a few bacterial cells exhibiting both green and red fluorescence simultaneously; instead, the fluorescence observed from the bacteria appears to be biphasic (i.e., either red or green), despite nearly all cells being red on AG-1 xerogels. Two hypotheses could explain this observation: 1) low levels of exogenously

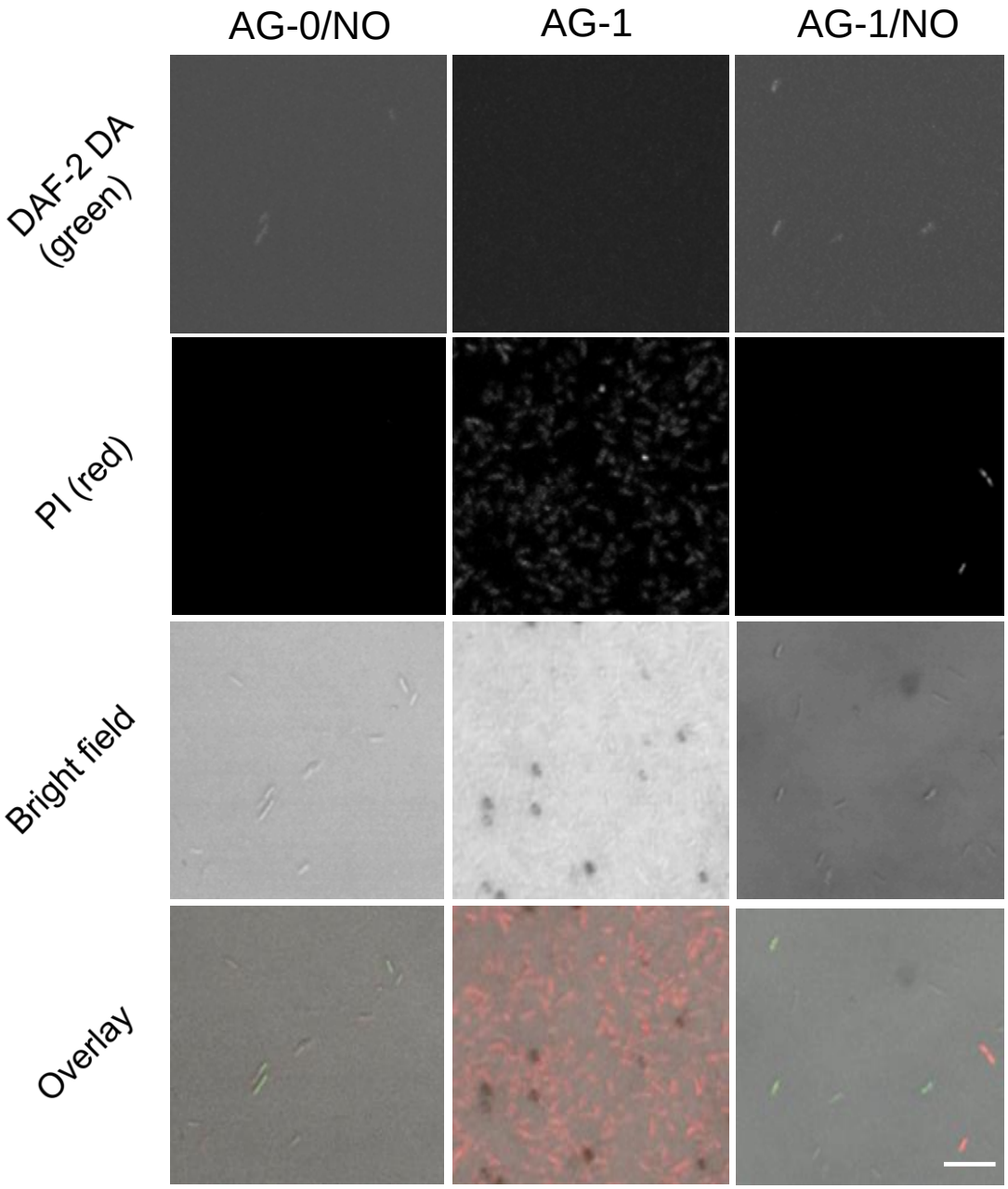

Figure 4.6 Representative confocal micrographs of AG-0/NO, AG-1, and AG-1/NO xerogels for visualizing intracellular NO uptake (DAF-2 DA) and cell death (PI). Fluorescent images showing DAF-2 DA and PI were converted to grey scale for improved visualization. Full-color images are provided in the overlays. Scale bar = 10 μm.

supplied NO have a protective effect against oxidative stress induced by Ag^+ ions (some bacteria generate NO for this purpose)[52]; and/or 2) excessive membrane disruption results in leaking of the DAF2-DA and PI probes from the bacteria. The first hypothesis seems unlikely given the greater-than-additive antimicrobial effect of the two agents in tandem against *P. aeruginosa*. The second mechanism is thus more plausible. Indeed, both PI and DAF-2 have been reported to "leak" through highly compromised membranes, especially when transferred to fresh, dye-free media, as was the case in our experiments.[27, 53]

Collectively, the above bacterial experiments above lead to a hypothesis for the greater-than-additive antimicrobial effects observed against *P. aeruginosa* and *S. aureus* from dual-action NO/silver-releasing xerogels. Individually, NO-release reduces bacterial adhesion to the xerogels while silver kills adhered bacteria. When combined, the anti-adhesive effects of NO are transferred to the silver-releasing xerogels. Silver release from these dual-action surfaces causes significant bacterial membrane damage, inducing oxidative stress cascades that produce reactive intermediates such as superoxide.[54] With the membranes already compromised, NO is able to enter the bacterium more readily, reacting with oxidative intermediates to enhance killing.[54]

4.3.3 Cytotoxicity of silver/NO-releasing xerogels

The silver and NO-releasing xerogels synthesized herein exhibited a greater-than-additive antimicrobial effect towards *P. aeruginosa* and *S. aureus*. However, cytotoxicity has been previously observed for each agent individually at concentrations similar to those herein.[37, 55, 56] The toxicity of these materials against L929 mouse fibroblasts was thus assessed to ensure that no ensuing "toxic synergy" resulted. As shown in Figure 4.7,

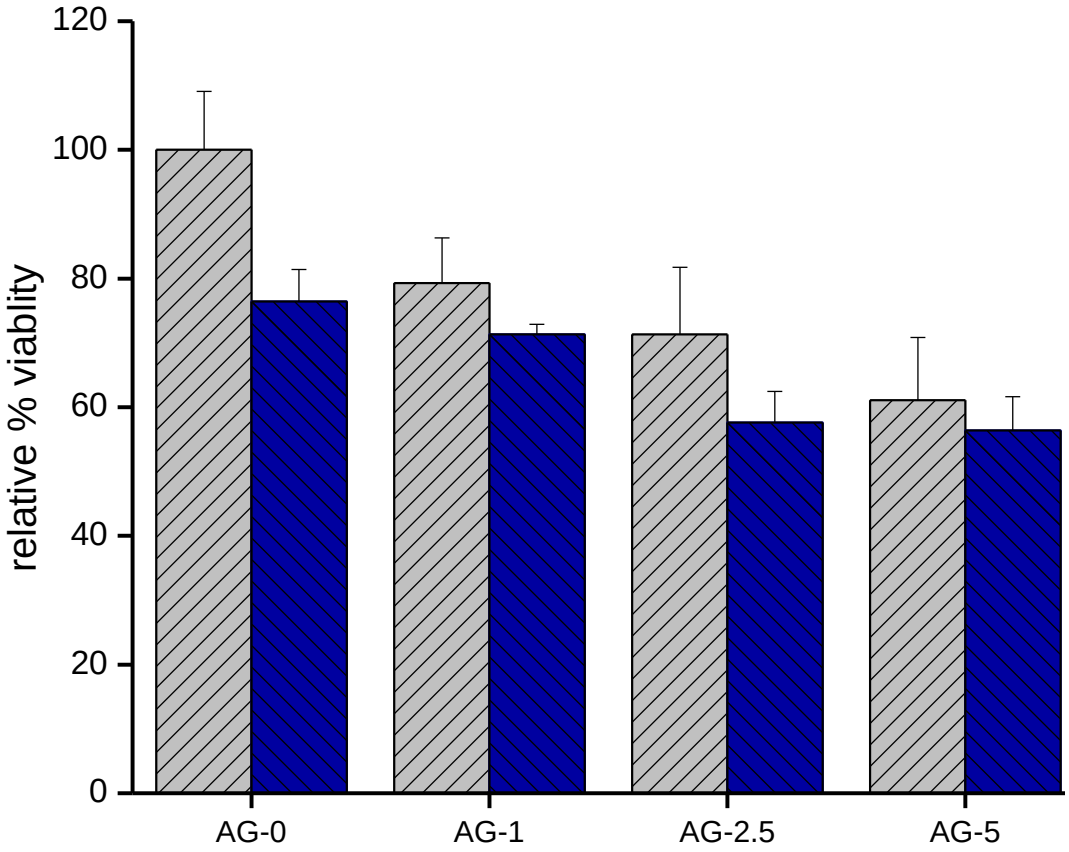

Figure 4.7 Cytotoxicity of AG-0, 1, 2.5, and 5 films without (grey bar) and with (blue bar) NO-release capability against L929 fibroblasts. Cells are normalized to non-NO-releasing AG-0 xerogels. Error bars represent the standard deviation of the mean from n=3 independent experiments.

AG xerogels reduced fibroblast viability with increasing silver content (21—39% vs. AG-0 controls), while the percentage of viable cells declined 24.4% for AG-0/NO xerogels. When contrasting the toxicity of AG-1, AG-2.5, and AG-5 xerogels with their NO-releasing counterparts, cell viability is only reduced by 7.9, 13, and 4.9%, respectively, indicating that the toxic effects are less-than-additive. We hypothesize that this phenomenon arises from protective mechanisms against oxidative stress in mammalian cells. Much of NO's toxicity occurs indirectly via reaction with superoxide to form toxic oxidative intermediates such as peroxynitrite.[57, 58] Hidalgo et al. observed upregulation of superoxide dismutase by L929 fibroblasts in response to oxidative stress incurred by $AgNO_3$.[56] This enzyme scavenges superoxide ions, mitigating toxic effects of NO that occur through oxidative intermediates.[59] These mechanisms may protect fibroblasts from any combined toxicity due to Ag^+ and NO.

4.4 Conclusions

Dual-action silver/NO-releasing xerogels synthesized via the sol-gel method exhibited a greater-than-additive antimicrobial effect against common biofilm-forming pathogens, with no greater-than-additive increase in toxicity. These differences were not attributable to changes in NO-release or silver-release following $AgNO_3$ loading or *N*-diazeniumdiolate formation, respectively. Considering the lower efficacy of both NO and Ag^+ alone against *S. aureus*, this strategy may be useful for improving the antimicrobial potential of silver-releasing materials against Gram-positive species. The ensuring broad-spectrum action antimicrobial action should minimize the likelihood of bacterial

resistance. Overall, this dual-action strategy should prove effective at maximizing antimicrobial activity while minimizing other harmful consequences.

REFERENCES

1. Schierholz, J. M.; Beuth, J., "Implant infections: A haven for opportunistic bacteria." *J. Hosp. Infect.* **2001**, *49*, 87-93.

2. Gristina, A. G., "Implant failure and the immuno-incompetent fibro-inflammatory zone." *Clin. Orthop. Relat. R.* **1994**, 106-18.

3. Toole, G. O.; Kaplan, H. B.; Kolter, R., "Biofilm formation as microbial development." *Annu. Rev. Microbiol.* **2000**, *54*, 49-79.

4. Stewart, P. S.; Costerton, J. W., "Antibiotic resistance of bacteria in biofilms." *Lancet* **2001**, *358*, 135-8.

5. Epstein, A. K.; Pokroy, B.; Seminara, A.; Aizenberg, J., "Bacterial biofilm shows persistent resistance to liquid wetting and gas penetration." *Proc. Nat. Acad. Sci USA* **2010**, *108*, 995-1000.

6. Zimmerli, W., "Infection and musculoskeletal conditions: Prosthetic-joint-associated infections." *Best. Prac. Res. Cl. Rh.* **2006**, *20*, 1045-1063.

7. Costerton, J. W., "Bacterial biofilms: A common cause of persistent infections." *Science* **1999**, *284*, 1318-1322.

8. Hetrick, E. M.; Schoenfisch, M. H., "Reducing implant-related infections: Active release strategies." *Chem. Soc. Rev.* **2006**, *35*, 780-9.

9. Stickler, D. J., "Biomaterials to prevent nosocomial infections: Is silver the gold standard?" *Curr. Opin Infect. Dis.* **2000**, *13*, 389-393.

10. Stobie, N.; Duffy, B.; McCormack, D. E.; Colreavy, J.; Hidalgo, M.; McHale, P.; Hinder, S. J., "Prevention of Staphylococcus epidermidis biofilm formation using a low-temperature processed silver-doped phenyltriethoxysilane sol-gel coating." *Biomaterials* **2008**, *29*, 963-969.

11. Trop, M.; Novak, M.; Rodl, S.; Hellbom, B.; Kroell, W.; Goessler, W., "Silver-coated dressing acticoat caused raised liver enzymes and argyria-like symptoms in burn patient." *J. Traum. Accute Care Surg.* **2006**, *60*, 648-652.

12. Marambio-Jones, C.; Hoek, E. M. V., "A review of the antibacterial effects of silver nanomaterials and potential implications for human health and the environment." *J. Nanopart. Res.* **2010**, *12*, 1531-1551.

13. Silver, S., "Bacterial resistances to toxic metal ions - a review." *Gene* **1996**, *179*, 9-19.

14. Silver, S., "Bacterial silver resistance: Molecular biology and uses and misuses of silver compounds." *FEMS Microbiol. Rev.* **2003**, *27*, 341-353.

15. Silver, S.; Phung, L. T.; Silver, G., "Silver as biocides in burn and wound dressings and bacterial resistance to silver compounds." *J. Ind. Microbiol. Biot.* **2006**, *33*, 627-34.

16. Wan, A. T.; Conyers, R. A.; Coombs, C. J.; Masterton, J. P., "Determination of silver in blood, urine, and tissues of volunteers and burn patients." *Clin. Chem.* **1991**, *37*, 1683-7.

17. Hardes, J.; Ahrens, H.; Gebert, C.; Streitbuerger, A.; Buerger, H.; Erren, M.; Gunsel, A.; Wedemeyer, C.; Saxler, G.; Winkelmann, W.; Gosheger, G., "Lack of toxicological side-effects in silver-coated megaprostheses in humans." *Biomaterials* **2007**, *28*, 2869-2875.

18. Eliopoulos, G. M.; Eliopoulos, C. T., "Antibiotic combinations: Should they be tested?" *Clin. Microbiol. Rev.* **1988**, *1*, 139-156.

19. Cottarel, G.; Wierzbowski, J., "Combination drugs, an emerging option for antibacterial therapy." *Trends Biotechnol.* **2007**, *25*, 547-555.

20. Berenbaum, M., "A method for testing for synergy with any number of agents." *J. Infect. Dis.* **1978**, *137*, 122-130.

21. Li, P.; Li, J.; Wu, C.; Wu, Q.; Li, J., "Synergistic antibacterial effects of β-lactam antibiotic combined with silver nanoparticles." *Nanotechnology* **2005**, *16*, 1912.

22. Privett, B. J.; Deupree, S. M.; Backlund, C. J.; Rao, K. S.; Johnson, C. B.; Coneski, P. N.; Schoenfisch, M. H., "Synergy of nitric oxide and silver sulfadiazine against gram-negative, gram-positive, and antibiotic-resistant pathogens." *Mol. Pharm.* **2010**, *7*, 2289-2296.

23. Logghe, C.; Van Ossel, C.; D'hoore, W.; Ezzedine, H.; Wauters, G.; Haxhe, J., "Evaluation of chlorhexidine and silver-sulfadiazine impregnated central venous catheters for the prevention of bloodstream infection in leukaemic patients: A randomized controlled trial." *J. Hosp. Infect.* **1997**, *37*, 145-156.

24. MacMicking, J.; Xie, Q.-w.; Nathan, C., "Nitric oxide and macrophage function." *Annu. Rev. Immunol.* **1997**, *15*, 323-350.

25. Nablo, B. J.; Chen, T. Y.; Schoenfisch, M. H., "Sol-gel derived nitric-oxide releasing materials that reduce bacterial adhesion." *J. Am. Chem. Soc.* **2001**, *123*, 9712-3.

26. Nablo, B. J.; Schoenfisch, M. H., "Poly(vinyl chloride)-coated sol-gels for studying the effects of nitric oxide release on bacterial adhesion." *Biomacromolecules* **2004**, *5*, 2034-2041.

27. Hetrick, E. M.; Schoenfisch, M. H., "Antibacterial nitric oxide-releasing xerogels: Cell viability and parallel plate flow cell adhesion studies." *Biomaterials* **2007**, *28*, 1948-1956.

28. Nichols, S. P.; Schoenfisch, M. H., "Nitric oxide flux-dependent bacterial adhesion and viability at fibrinogen-coated surfaces." *Biomater. Sci. 10.1039/C3BM60130G [Available online July 17, 2013]*.

29. Cai, W.; Wu, J.; Xi, C.; Meyerhoff, M. E., "Diazeniumdiolate-doped poly(lactic-*co*-glycolic acid)-based nitric oxide releasing films as antibiofilm coatings." *Biomaterials* **2012**, *33*, 7933-7944.

30. Holt, J.; Hertzberg, B.; Weinhold, P.; Storm, W.; Schoenfisch, M.; Dahners, L., "Decreasing bacterial colonization of external fixation pins via nitric oxide release coatings." *J. Orthop. Trauma* **2011**, *25*, 432-437.

31. Nablo, B. J.; Prichard, H. L.; Butler, R. D.; Klitzman, B.; Schoenfisch, M. H., "Inhibition of implant-associated infections via nitric oxide release." *Biomaterials* **2005**, *26*, 6984-6990.

32. Marxer, S. M.; Rothrock, A. R.; Nablo, B. J.; Robbins, M. E.; Schoenfisch, M. H., "Preparation of nitric oxide (NO)-releasing sol-gels for biomaterial applications." *Chem. Mater.* **2003**, *15*, 4193-4199.

33. Riccio, D. A.; Dobmeier, K. P.; Hetrick, E. M.; Privett, B. J.; Paul, H. S.; Schoenfisch, M. H., "Nitric oxide-releasing S-nitrosothiol-modified xerogels." *Biomaterials* **2009**, *30*, 4494-4502.

34. Nablo, B. J.; Schoenfisch, M. H., "Antibacterial properties of nitric oxide-releasing sol-gels." *J. Biomed. Mater. Res. A* **2003**, *67*, 1276-83.

35. Radin, S.; Ducheyne, P., "Controlled release of vancomycin from thin sol-gel films on titanium alloy fracture plate material." *Biomaterials* **2007**, *28*, 1721-1729.

36. Adams, C. S.; Antoci, V.; Harrison, G.; Patal, P.; Freeman, T. a.; Shapiro, I. M.; Parvizi, J.; Hickok, N. J.; Radin, S.; Ducheyne, P., "Controlled release of vancomycin from thin sol-gel films on implant surfaces successfully controls osteomyelitis." *J. Orthopaed. Res.* **2009**, *27*, 701-709.

37. Nablo, B. J.; Schoenfisch, M. H., "In vitro cytotoxicity of nitric oxide-releasing sol-gel derived materials." *Biomaterials* **2005**, *26*, 4405-4415.

38. Bruehlman, R. J.; Verhoek, F. H., "The basic strengths of amines as measured by the stabilities of their complexes with silver ions." *J. Am. Chem. Soc.* **1948**, *70*, 1401-1404.

39. Manna, A.; Imae, T.; Iida, M.; Hisamatsu, N., "Formation of silver nanoparticles from a N-Hexadecylethylenediamine silver nitrate complex." *Langmuir* **2001**, *17*, 6000-6004.

40. Stokes, R. H.; Walton, H. F., "Metal-amine complexes in ion exchange." *J. Am. Chem. Soc.* **1954**, *76*, 3327-3331.

41. Shin, J. H.; Marxer, S. M.; Schoenfisch, M. H., "Nitric oxide-releasing sol-gel particle/polyurethane glucose biosensors." *Anal. Chem.* **2004**, *76*, 4543-9.

42. Brouqui, P.; Rousseau, M.; Stein, A.; Drancourt, M.; Raoult, D., "Treatment of Pseudomonas aeruginosa-infected orthopedic prostheses with ceftazidime-ciprofloxacin antibiotic combination." *Antimicrob. Agents. Ch.* **1995**, *39*, 2423-2425.

43. Kalmeijer, M. D.; van Nieuwland-Bollen, E.; Bogaers-Hofman, D.; Baere, G. A. J.; Kluytmans, J. A., "Nasal carriage of Staphylococcus aureus is a major risk factor for surgical-site infections in orthopedic surgery." *Infect. Cont. Hosp. Ep.* **2000**, *21*, 319-323.

44. Marini, M.; De Niederhausern, S.; Iseppi, R.; Bondi, M.; Sabia, C.; Toselli, M.; Pilati, F., "Antibacterial activity of plastics coated with silver-doped organic-inorganic hybrid coatings prepared by sol-gel processes." *Biomacromolecules* **2007**, *8*, 1246-1254.

45. Privett, B. J.; Broadnax, A. D.; Bauman, S. J.; Riccio, D. A.; Schoenfisch, M. H., "Examination of bacterial resistance to exogenous nitric oxide." *Nitric Oxide-Biol. Ch.* **2012**, *26*, 169-173.

46. Berenbaum, M. C., "Minor synergy and antagonism may be clinically important." *J Antimicrob. Chemoth.* **1987**, *19*, 271-273.

47. Jung, W. K.; Koo, H. C.; Kim, K. W.; Shin, S.; Kim, S. H.; Park, Y. H., "Antibacterial activity and mechanism of action of the silver ion in Staphylococcus aureus and Escherichia coli." *Appl. Environ. Microb.* **2008**, *74*, 2171-2178.

48. Rai, M.; Yadav, A.; Gade, A., "Silver nanoparticles as a new generation of antimicrobials." *Biotechnol. Adv.* **2009**, *27*, 76-83.

49. Triandafillu, K.; Balazs, D. J.; Aronsson, B. O.; Descouts, P.; Tu Quoc, P.; van Delden, C.; Mathieu, H. J.; Harms, H., "Adhesion of Pseudomonas aeruginosa strains to untreated and oxygen-plasma treated poly(vinyl chloride) (PVC) from endotracheal intubation devices." *Biomaterials* **2003**, *24*, 1507-1518.

50. Balazs, D. J.; Triandafillu, K.; Wood, P.; Chevolot, Y.; van Delden, C.; Harms, H.; Hollenstein, C.; Mathieu, H. J., "Inhibition of bacterial adhesion on PVC

endotracheal tubes by RF-oxygen glow discharge, sodium hydroxide and silver nitrate treatments." *Biomaterials* **2004**, *25*, 2139-2151.

51. Kojima, H.; Nakatsubo, N.; Kikuchi, K.; Kawahara, S.; Kirino, Y.; Nagoshi, H.; Hirata, Y.; Nagano, T., "Detection and imaging of nitric oxide with novel fluorescent indicators: Diaminofluoresceins." *Anal. Chem.* **1998**, *70*, 2446-2453.

52. Gusarov, I.; Shatalin, K.; Starodubtseva, M.; Nudler, E., "Endogenous nitric oxide protects bacteria against a wide spectrum of antibiotics." *Science* **2009**, *325*, 1380-1384.

53. Levelt, C. N.; Eichmann, K., "Streptavidin-tricolor is a reliable marker for nonviable cells subjected to permeabilization or fixation." *Cytometry* **1994**, *15*, 84-86.

54. Park, H.-J.; Kim, J. Y.; Kim, J.; Lee, J.-H.; Hahn, J.-S.; Gu, M. B.; Yoon, J., "Silver-ion-mediated reactive oxygen species generation affecting bactericidal activity." *Water. Res.* **2009**, *43*, 1027-1032.

55. Asharani, P.; Wu, Y. L.; Gong, Z.; Valiyaveettil, S., "Toxicity of silver nanoparticles in zebrafish models." *Nanotechnology* **2008**, *19*, 255102.

56. Hidalgo, E.; Domínguez, C., "Study of cytotoxicity mechanisms of silver nitrate in human dermal fibroblasts." *Toxicol. Lett.* **1998**, *98*, 169-179.

57. Radi, R.; Beckman, J. S.; Bush, K. M.; Freeman, B. A., "Peroxynitrite oxidation of sulfhydryls. The cytotoxic potential of superoxide and nitric oxide." *J. Biol. Chem.* **1991**, *266*, 4244-4250.

58. Beckman, J. S.; Koppenol, W. H., "Nitric oxide, superoxide, and peroxynitrite: The good, the bad, and ugly." *Am. J Physiol.-Cell Ph.* **1996**, *271*, C1424-C1437.

59. Beckman, J. S.; Beckman, T. W.; Chen, J.; Marshall, P. A.; Freeman, B. A., "Apparent hydroxyl radical production by peroxynitrite: Implications for endothelial injury from nitric oxide and superoxide." *Proc. Natl. Acad. Sci USA* **1990**, *87*, 1620-1624.

Chapter 5:

Nitric Oxide-Releasing Poly(Amido Amine) Dendrimer-Doped Polyurethanes

5.1 Introduction

The earliest report of a nitric oxide (NO)-releasing coating utilized gaseous NO (via a high pressure cylinder) infused into a semi-permeable polymeric membrane.[1] In an effort to create NO-releasing coatings that may be used clinically, researchers have since utilized chemical NO donors (i.e., *N*-diazeniumdiolates and *S*-nitrosothiols) to controllably store and release the small, therapeutic radical.[2-8] Release of NO from *S*-nitrosothiols involves multiple simultaneous mechanisms including light, temperature, and copper-mediated decomposition.[9-11] In contrast, *N*-diazeniumdiolates decompose upon protonation of the secondary amine that coordinates two equivalents of NO.[12] Since decomposition is proton-dependent, NO release from *N*-diazeniumdiolate-based coatings may be tuned by adjusting water uptake into the material.[8]

In the simplest method to develop NO-releasing coatings, NO donors are dispersed within a dissolved polymer solution and cast on a substrate to yield a dried polymer film containing the NO source.[8, 13] In this manner, NO-releasing polymers have been prepared from small molecule *N*-diazeniumdiolate NO donors,[5] fine sol-gel powders,[4] and silica nanoparticles.[14] The simplicity of this approach has been applied to other types of materials as well; for example, PROLI/NO and silica nanoparticles have

been incorporated within electrospun fibrous mats.[15, 16] These fibers feature controllable diameters and large surface areas.[17] In the context of biomaterial implants, the rough topography and high degree of porosity of the fiber mats promote integration into the native host tissue by allowing cell infiltration.[18] As such, electrospun nanofiber mats are able to promote wound healing and mitigate certain aspects of the foreign body response (FBR).[18, 19]

Despite the clinical promise of NO-releasing films and nanofibers synthesized from *N*-diazeniumdiolates, these polymer dispersions leave several areas for improvement. First, the NO donors typically must be hydrophobic to remain within a polymer, limiting options for tuning NO release.[8] Second, NO-release durations are often too short in duration for certain clinical applications (e.g., the one-week release above ~1 pmol cm^{-2} s^{-1} needed to significantly reduce the localized inflammatory response to implants).[20]

Recently, our laboratory has developed NO-releasing dendrimers capable of releasing large NO payloads (> 1 μmol mg^{-1}) with a range of NO-release kinetics (~0.5 h to ~4.8 h).[21-23] The high density of primary amines on these dendrimers allows for conversion to secondary amines that may be used to form *N*-diazeniumdiolate NO donors. In this chapter, NO-releasing PAMAM dendrimers were explored as dopants within polyurethane dispersions to make both films and electrospun fibers. The ability to tune NO release kinetics was evaluated by incorporating different secondary amine functionalities on the dendrimer. Furthermore, the use of dendrimers featuring more than one secondary amine moiety was studied as a means to adjust NO release and dendrimer hydrophobicity.

5.2 Materials and methods

Acrylonitrile (ACN), 1,2-epoxy-9-decene (ED), and styrene oxide (SO) were purchased from Sigma-Aldrich (Milwaukee, WI). Tecoplast TP-470-000 and Tecoflex SG-80A (TPU) were gifts from Thermedics (Woburn, MA). Anhydrous *N*,*N*-dimethylformamide, anhydrous tetrahydrofuran (THF), and 5.4 M sodium methoxide were purchased from Fisher Scientific (Fairlawn, NJ). Nitric oxide calibration gas (26.85 ppm), nitrogen and argon gasses were acquired from Airgas National Welders (Durham, NC). Nitric oxide gas (pure) was obtained from Praxair (Bethlehem, PA). Tecoplast TP-470-000 (TP470) and Tecoflex SG-80A (TPU) were gifts from Thermedics (Woburn, MA). L929 fibroblast cells were obtained from the UNC tissue culture facility (Chapel Hill, NC). Dulbecco's modified essential media (DMEM), (3-(4,5-dimethylthiazol-2-yl)-5-(3-carboxymethoxyphenyl)-2-(4-sulfophenyl)-2H-tetrazolium) (MTS) and phenazine methosulfate (PMS) were acquired from Becton, Dickinson and Company (Sparks, MD). All other reagents were analytical grade and used as received.

5.2.1 Synthesis of secondary amine-functionalized PAMAM dendrimers

Secondary-amine functionalized poly(amido amine) dendrimers were prepared as previously described.[21] Briefly, ED-, SO-, or 50 mol% ACN/50 mol% SO (hereafter referred to as ACN/SO) modified dendrimers were prepared by first dissolving 25 mg of G4-PAMAM in THF (750 μL) and methanol (700 μL), while ACN-modified dendrimers were prepared by first dissolving 100 mg of the G4-PAMAM the dendrimer in methanol (1 mL). The desired functionality was added at a 1:1 molar ratio relative to the total number of primary amines on the dendrimer (i.e., 64 for G4-PAMAM) and allowed to

react in a sealed vial for 5 d at room temperature. Following removal of the unreacted precursors at reduced pressure, the dendrimers were dissolved again in the same solvent mixtures described above to yield G4-ED, G4-SO, G4-ACN, and G4-ACN/SO dendrimers (structures shown in Figure 5.1).

Proton nuclear magnetic resonance (^{1}H NMR) spectra for each dendrimer were obtained with a Bruker 400 MHz spectrometer. Representative ^{1}HNMR data of G4 PAMAM dendrimers modified with ACN, ED, and SO (referred to as G4-ACN, G4-ED, G4-SO, and G4-ACN/SO) are as follows. G4-ACN: ^{1}HNMR (400 MHz, CD_3OD, δ) 2.82 – 2.80 (t, NH*CH_2CH_2*CN), 2.29 (s, NCH_2*CH_2*C(O)NH). G4-ED: ^{1}HNMR (400 MHz, CD_3OD, δ) 5.77 – 5.71 (m, CH_2C*H*=CH_2), 4.93 – 4.83 (q, CH_2CH=C*H_2*), 2.30 (s, NCH_2*CH_2*C(O)NH). G4-SO: ^{1}HNMR (400 MHz, CD_3OD, δ) 7.27 – 7.18 (m, CH_2CH(OH)*Ph*), 2.29 (s, NCH_2*CH_2*C(O)NH). G4-ACN/SO: ^{1}HNMR (400 MHz, CD_3OD, δ) 7.27 – 7.18 (m, CH_2CH(OH)*Ph*), 2.82 – 2.80 (t, NH*CH_2CH_2*CN), 2.30 (s, NCH_2*CH_2*C(O)NH).

5.2.2 N-diazeniumdiolate addition to secondary amine-functionalized PAMAM dendrimers

Following synthesis of the secondary amine-functionalized PAMAM dendrimers, excess solvent was removed *in vacuo*. G4-SO, G4-ED, and G4-ACN/SO dendrimers were then dissolved in a solution of methanol (500 μL) and THF (750 μL), while G4-ACN dendrimers were dissolved in 100 mL methanol. One molar equivalent of a 5.4 M sodium methoxide solution (relative to the total number of primary amines in the PAMAM-NH_2 dendrimers precursors used initially) was added to each dendrimer

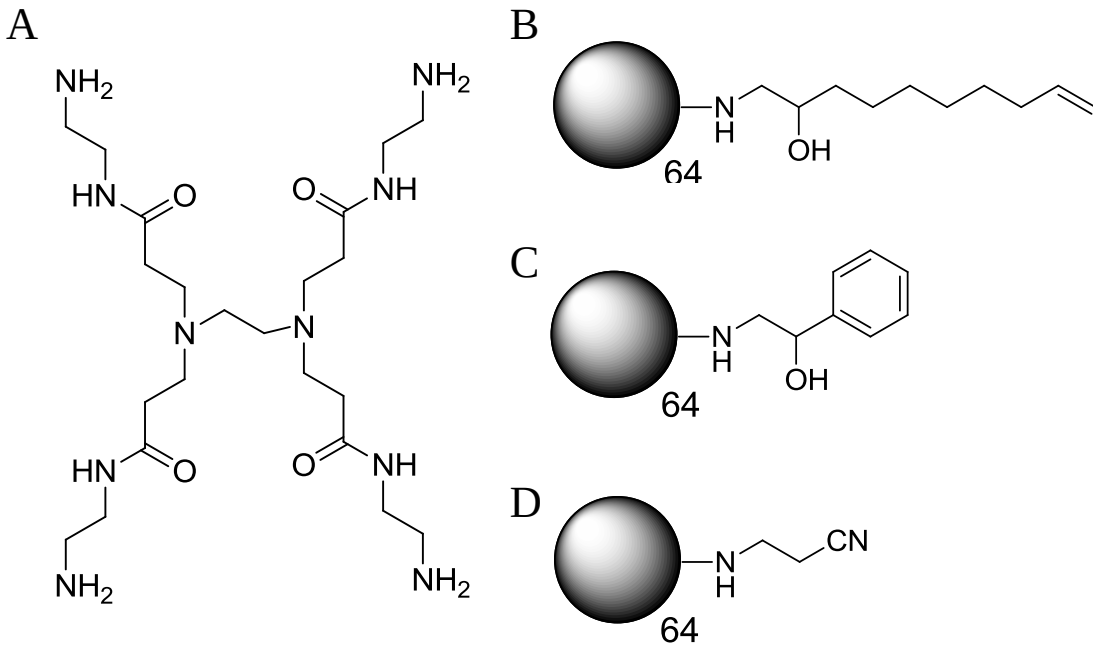

Figure 5.1 Structures of the 2^{o} amines formed on (A) PAMAM from (B) 1,2-expoy-9-decene (ED), (C) styrene oxide (SO), and (D) acrylonitrile (ACN). The PAMAM structure provided for reference is G0 (4 primary amines).

solution. Vials were placed in a 500 mL Parr reaction vessel, purged copiously with argon and held under high pressure NO gas (10 bar) for 3 d to convert the secondary amines within to *N*-diazeniumdiolate NO donors. Following additional argon purges to remove excess NO, the dendrimer solutions were removed from the vessel. Excess solvent was removed by placing the dendrimers under vacuum overnight. The *N*-diazeniumdiolate-functionalized PAMAM dendrimers were dissolved in 450 μL anhydrous methanol, yielding 94.1, 85.9, 68.8, and 77.3 mg mL^{-1} solutions of G4-ED, G4-SO, G4-ACN, and G4-ACN/SO, respectively. The dendrimers were sealed and stored at -20 ^{o}C until further use.

For the leaching assays used in this work, G4-PAMAM dendrimers were modified with rhodamine B isothiocyanate (RITC). Exactly 100 mg G4-PAMAM was dissolved in 1 mL methanol. Triethylamine and RITC were added to the solution at 1:1 and 1:64 molar ratios relative to the molar amount of G4-PAMAM (i.e., so that each dendrimer, on average, only contained one RITC moiety). The reaction was allowed to proceed for 24 h in the dark. Following removal of the solvent, the product mixture was dissolved in water, dialyzed against water for 3 d and lyophilized. The resulting G4-PAMAM-RITC dendrimers were then modified with ED, ACN, SO, or ACN/SO in a manner identical to that described above. To avoid photobleaching, care was taken to shield the G4-PAMAM-RITC dendrimers from light during storage and handling.

5.2.3 Synthesis and characterization of NO-releasing PAMAM-doped polyurethane films

Glass slides cut to dimensions of 9 x 12.5 mm were used as substrates for the PAMAM dendrimer-doped polyurethane films. Prior to casting, the slides were

roughened using 400-grit silicon carbide (to facilitate adhesion of the films to the substrate) and cleaned by successive 10 min bouts of ultrasonication in MilliQ water, ethanol, and acetone for 10 min. They were then dried in the ambient.

Polyurethane solutions were prepared using two different polyurethanes having different water uptake properties: TP470 (water uptake = 0.04 mg H_2O mg^{-1} polyurethane)[14] and TPU (water uptake = 0.20 mg H_2O mg^{-1} polyurethane)[14] were prepared by dissolving dissolution in THF at a concentration of 40 mg mL^{-1}. Following, 433 μL of the polyurethane solution was mixed with 586 μL THF and 1.9, 3.8 or 5.8 mg of the *N*-diazeniumdiolate modified dendrimers were added to make polyurethane solutions with 10, 18, or 25 wt% (relative to the total polyurethane mass) of the *N*-diazeniumdiolate modified dendrimer, respectively. To ensure dissolution of the dendrimer within the polyurethane solution, the mixture was ultrasonicated (120 KHz) for 20 min. To fabricate the NO-releasing dendrimer-doped polyurethane films, 15 layers of the G4-PAMAM-doped polyurethane solutions were cast (60 μL per layer) onto the substrates, allowing 10 min drying time between each layer. For polyurethane films utilizing an upper barrier layer, a final 30 μL aliquot of 40 mg mL^{-1} TP470 solution was cast on the films after addition of the NO-releasing layer. For polyurethane films that utilized an adhesion layer (i.e., polyurethane films synthesized from G4-ACN and G4-ACN/SO), four 30 μL aliquots of a 75:25 w/w 40 mg mL^{-1} TP470:TPU were cast prior to the NO-releasing G4-PAMAM dendrimer layers. After casting all layers, the films were dried on the benchtop for 30 min, in a nitrogen environment overnight, and then under vacuum for 24 h to ensure complete removal of the solvent.

5.2.4 Preparation of NO-releasing G4-PAMAM-doped electrospun fibers

Electrospun fibers doped with NO-releasing G4-PAMAM dendrimers were prepared according to previously described methods.[15, 16] Briefly, a 6 kV voltage was applied to a 22 gauge blunt-tip needle held 15 cm from a grounded steel collector plate covered in aluminum foil. A syringe containing an NO-releasing G4-PAMAM dendrimer/TP470 solution was affixed to the needle, and the polymer solution loaded within was ejected at a rate of 0.015 mL min^{-1} towards the collector using a Kent Scientific Genie Plus syringe pump (Torrington, CT). Polyurethane solutions were prepared by first dissolving 1360 mg TP470 in a 3:1:1 ratio of THF:DMF:methanol (v:v:v). Following, a 200 μL aliquot of each NO-releasing G4-PAMAM dendrimer (in methanol) was added to 800 μL of the TP470 solution such that final dendrimer concentration was 5 wt% relative to the total mass of TP470 in the polymer solution.

5.2.5 Materials characterization

Nitric oxide release from G4-PAMAM dendrimers and G4-PAMAM-doped films and fibers was measured at 37 ^{o}C in 30 mL PBS according to previously described methods using a Sievers Model 280i Chemiluminescent Nitric Oxide Analyzer (Boulder, CO).[3, 24, 25] For G4-PAMAM dendrimers, approximately 0.3-0.6 mg of the dendrimer sample was used. Measurement ceased when the NO release fell to below 10 ppb mg^{-1}. For G4-PAMAM-doped films, the measurement was halted at < 1 pmol cm^{-2} s^{-1}. For fibers, 20-40 mg of the fiber mat was placed in the sample flask. A small metal clip was placed atop the mat to ensure it remained submerged during measurement.

Fluorescently tagged dendrimers were utilized to quantify leaching of each dendrimer from its respective scaffold. Briefly, the G4-PAMAM-RITC dendrimers prepared above were modified with the secondary amine functionality of interest (e.g., -

ED, -SO, or –ACN) and *N*-diazeniumdiolate-modified to yield G4-ED-RITC, G4-SO-RITC, G4-ACN-RITC, or G4-ACN/SO-RITC. For leaching assays, the G4-PAMAM-doped films or fibers were prepared as described above, but a portion of the G4-PAMAM dendrimers was replaced with G4-PAMAM-RITC dendrimers having the same secondary amine modifier. For film leaching assays, the G4-PAMAM-RITC dendrimers comprised 25% of the overall dendrimer mass. For fiber leaching assays, the RITC-tagged dendrimers comprised 50% of the overall dendrimer mass. After drying, each film was submerged in 2 mL PBS (37 ^{o}C), and then transferred to fresh PBS after 1, 4, or 7 d. After the specified duration, films were removed from the soak solutions. Calibration standards were prepared at concentrations correlating with 0—50% leaching in 2 mL PBS. To facilitate dissolution of the dendrimers, 50 μL 1.0 M HCl was added to all calibration standards and soak solutions. Fluorescent leaching assays for electrospun fibers were performed in a similar manner, with approximately ~10 mg of the electrospun fiber mat placed in 2 mL PBS and incubated for 1 week. The fluorescent intensity was measured using a BMG PolarStar Omega fluorescence plate reader (Ortenberg, Germany). Typical limits of detection were ~0.1-0.3% (w/w) for films and ~1% (w/w) for fibers.

The preliminary cytotoxic potential of the G4-PAMAM dendrimer doped films was assessed against L929 mouse fibroblasts. First, L929 cells were cultured in DMEM (37 ^{o}C, 5% CO_2) supplemented with 10% (v/v) FBS and 1 wt% penicillin/streptomycin until reaching confluency. The cells were then trypsinized and seeded onto 24-well plates. After incubation for 3 d at 37 ^{o}C, the supernatant was aspirated and replaced with 1 mL fresh DMEM. The G4-PAMAM-doped polyurethanes were then placed face-down

on the fibroblast cells and incubated at 37 ^{o}C in 5% CO_2 for an additional 24 h. After removing the substrates, excess media was removed via aspiration and each well was rinsed three times with PBS. DMEM/MTS/PMS (105/20/1 v:v:v) was added (1 mL) to each well, and the cells were incubated for an additional 90 min. Aliquots (120 μL) of the supernatant were then transferred to a microtiter plate and the absorbance was measured at 490 nm using a Thermoscientific Multiskan EX plate reader. Absorbance values were compared against blank wells (i.e., the DMEM/MTS/PMS mixture) and controls (i.e., TP470/TPU polyurethane films containing no G4-PAMAM dendrimers) to determine % viability of the cells.

5.3. Results and discussion

5.3.1 Synthesis of NO-releasing G4-PAMAM dendrimers

The G4-PAMAM dendrimers were synthesized according to previously published protocol for poly(propylene imine) (PPI) dendrimers.[21] Of note, PAMAM dendrimers were chosen as the scaffold for this work instead of PPI as PAMAM exhibits less dose-dependent toxicity against mammalian cells.[26] The NO-release properties were controlled by manipulating the functionality (e.g., ED, SO, ACN, or ACN/SO) used to form the secondary amine on the dendrimers. Following exposure to NO, the conversion efficiency of secondary amines to *N*-diazeniumdiolates between the different systems spanned a range from 12.5—19.4%, with *N*-diazeniumdiolate formation and subsequent NO release being lowest for the G4-SO dendrimers (Table 5.1). Of note, ^{1}H NMR confirmed that the total number of secondary amine functionalities on each dendrimer precursor were similar for all systems (71-77.5%). Thus, the lower conversion efficiency in the G4-SO system was attributable to the *N*-diazeniumdiolate formation process.

Increased steric hindrance by the –SO functionality likely reduces accessibility of base (sodium methoxide) to the secondary amine required for *N*-diazeniumdiolate formation.[21]

Nitric oxide-release durations (t_d) and half-lives ($t_{1/2}$) were longest for G4-ACN dendrimers. Lu et al. proposed that this effect was caused by cationic stabilization of the *N*-diazeniumdiolate by a protonated imidate formed at the ACN moiety (Table 5.1). As this stabilization is lacking in G4-ED and G4-SO dendrimers, NO release was markedly faster for these dendrimers as indicated by a shorter NO-release half-life and large maximum instantaneous NO release ($[NO]_m$). Combining ACN- and SO-modifiers in a 50:50 ratio on one PAMAM scaffold (G4-ACN/SO) resulted in a material with hybrid NO-release kinetics influenced by the –SO and –ACN dendrimers individually. G4-ACN/SO dendrimers exhibited a large initial burst of NO (similar to G4-SO dendrimers) followed by much slower, sustained NO release (similar to G4-ACN dendrimers). Tuning the composition of the dendrimer scaffold in this manner may prove useful for tailoring kinetics towards specific applications when doped within films (e.g., large fluxes for killing bacteria,[27] or low sustained fluxes for mitigating the FBR[20]) and indicates the versatility of dendritic scaffolds as NO-releasing macromolecules.

5.3.2 Synthesis and characterization of NO-releasing G4-PAMAM-doped polyurethane films

Following synthesis of the NO-releasing G4-PAMAM dendrimers, the water uptake properties of the polyurethane were varied to determine the polymer attributes necessary to maximize NO-release durations and totals (i.e., to improve the therapeutic potential of these membranes) while minimizing dendrimer leaching (i.e., to avoid cytotoxicity). Using G4-ED dendrimers as a dopant, TP470:TPU polymers were

Table 5.1 Nitric oxide-release characterization of *N*-diazeniumdiolate-modified G4-PAMAM dendrimers. All values were determined using chemiluminescent nitric oxide analysis.

dendrimer	t[NO][a] µmol mg^{-1}	t[NO][b] µmol µmol^{-1}	$[NO]_m$[c] ppb mg^{-1}	$t_{1/2}$ (h)[d]	t_d (h)[e]	conversion efficiency %
G4-ED	0.90 ± 0.2[g]	20.9 ± 4.3	3500 ± 1100	0.55 ± 0.05	8.4 ± 3.3	16.4 ± 3.4
G4-SO	0.73 ± 0.26	16.1 ± 5.7	4150 ± 1600	0.7 ± 0.3	10.6 ± 0.5	12.5 ± 4.5
G4-ACN	1.05 ± 0.06	18.5 ± 1.1	1000 ± 10	3.7 ± 0.9	20.9 ± 4.3	14.4 ± 0.8
G4-ACNSO	1.4 ± 0.2	27.8 ± 3.6	5100 ± 1900	1.5 ± 0.2	19.4 ± 2.5	19.4 ± 2.5

[a] Total µmol nitric oxide released per mg dendrimer
[b] Total µmol NO released per µmol dendrimer
[c] Maximum instantaneous release rate
[d] half-life
[e] duration of release above 10 ppb mg^{-1}
[f] percentage of *N*-diazeniumdiolate NO donors based off of total number of primary amines
[g] Values are given as the mean ± standard deviation of at least n=3 dendrimer preparations

combined in 100:0, 75:25, 50:50, 25:75, and 0:100 ratios (w/w). The G4-ED dendrimer system was chosen for this study due to its hydrophobicity. In this manner, leaching values should be more indicative of the polymer composition than the dendrimer. It was hypothesized that the negligible water uptake of the TP470 polyurethane (0.04 mg H_2O mg^{-1} TP470) would result in increased retention of the dendrimers within the polyurethane scaffold when compared to the TPU polyurethane (0.20 mg H_2O mg^{-1} TPU). As shown in Figure 5.2, dendrimer leaching was substantial at TP470:TPU ratios of 25:75 and 0:100, owing to increased swelling of the polyurethane network following water uptake. Furthermore, NO-release from 10 wt% G4-ED polyurethanes using either 100:0 or 75:25 TP470:TPU ratios revealed that NO release totals from 100:0 TP470 (0.28 μmol cm^{-2}) were markedly lower than those from 75:25 TP470:TPU polyurethanes (0.54 μmol cm^{-2}). Increasing TPU content further in the polyurethane mixture had no discernible effect on NO-release totals, suggesting that water uptake was not altered. Identical experiments performed using 10 wt% G4-ACN/SO dendrimers revealed considerable dendrimer leaching for 50:50 TP470:TPU polyurethanes (20 wt% leached after 7 d). Extensive swelling of the polyurethane matrix was visually evident, indicating that the G4-ACN/SO dopant contributed to swelling by virtue of the more hydrophilic -ACN modifier (vs. the sizable alkyl chain on -ED). These results suggested an optimum TP470:TPU ratio of 75:25 to maximize NO-release while minimizing leaching events that may cause toxicity.

While the 10 wt% G4-ED doped polyurethanes exhibited maximum flux values (29.1 pmol cm^{-2} s^{-1}) sufficient for reducing adhesion of several Gram-negative –positive bacteria strains by 1-log, the short duration (~25 h) likely renders the material inadequate

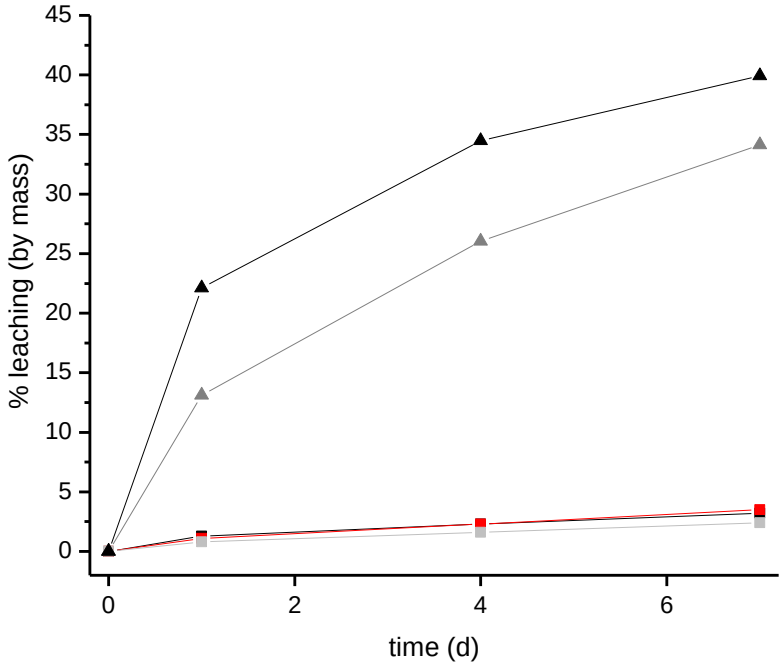

Figure 5.2 Dendrimer leaching from 10 wt% G4-ED doped polyurethanes as a function of time for TP470:TPU ratios of 100:0 (grey square), 75:25 (black square), 50:50 (red square), 25:75 (grey triangle) and 0:100 (black triangle). Leaching was determined through RITC-tagged dendrimers measured using fluorometry. Error bars represent the standard deviation of n=3 measurements from n=1 film.

for long-term applications, such as more biocompatible implants that mitigate the foreign body response. For instance, *in vitro* NO release durations of 7—14 d durations have been observed for films prepared from *S*-nitrosothiol-based polymer dispersions.[20] These materials reduce the inflammatory response for up to 7 d post-implantation, while those releasing NO for shorter durations exhibit no such effect.[20] To increase NO-release durations, concentrations of G4-ED dendrimer within the polyurethane were increased to 18 and 25 wt%. Unfortunately, substantial leaching of the dendrimer occurred from these systems (e.g., 18.9% of the total dendrimer mass after 1 week when using 25 wt% G4-ED). Again, the leaching was attributed to swelling of the polyurethane network for 25 wt% G4-ED dendrimers doped into 75:25 TP470:TPU polyurethanes. The expansion of the polymer network that occurs when the polyurethane fills with water likely provides a route for the otherwise hydrophobic G4-ED dendrimers to diffuse from the polymer matrix. Cytotoxicity studies revealed complete killing of L929 fibroblasts cells (24 h exposure) at these dendrimer concentrations. To remedy leaching and toxicity that occurs when large masses of dendrimers are doped within these polyurethanes, a thin hydrophobic barrier layer was used to inhibit water uptake and swelling. A 30 μL layer aliquot of a 40 mg mL^{-1} TP470 solution was cast on the 25 wt% G4-ED polymer films. Leaching totals at 1 week from the polyurethane network decreased to 2.5%. Increasing the concentration of G4-ED doped within the polyurethane to 25 wt% increased the total dose of NO delivered to 1.1 ± 0.2 μmol cm^{-2}. The duration of physiologically-relevant (> 1 pmol cm^{-2} s^{-1}) NO increased to 3.2 ± 0.7 d (representative NO-release curves shown in Figure 5.3).

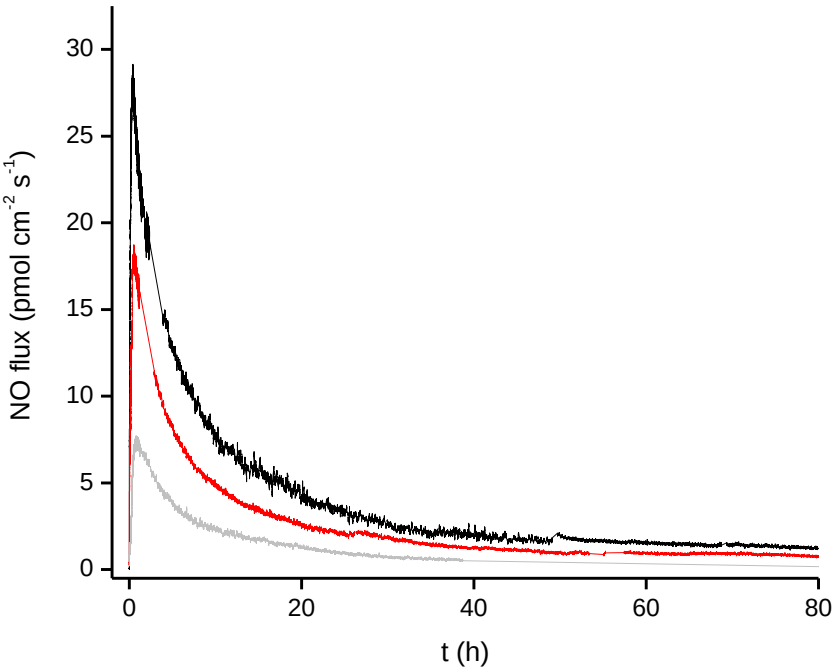

Figure 5.3 Real-time nitric oxide release from 75:25 TP470:TPU polyurethanes containing 10 (light grey), 18 (red), and 25 (black) wt% G4-ED. Measurements were acquired through chemiluminescent nitric oxide analysis.

Of the NO-releasing G4-PAMAM dendrimers employed herein, the G4-ED dendrimer featured the shortest NO-release half-life and duration. Doping a dendrimer with a longer NO-release duration (e.g., G4-ACN or G4-ACN/SO) within a 75:25 TP470:TPU matrix at 25 wt% would likely increase the NO-release duration from the resulting film.[5] However, significant leaching was observed even in the presence of a barrier layer when preparing 25 wt% films from G4-ACN and G4-ACN/SO. Swelling of G4-ACN and G4-ACN/SO-doped polyurethanes resulted in "lifting" or detachment of the polymer from the substrate. To remedy this, an "adhesive layer" was applied to the substrate (i.e., 75:25 TP470:TPU containing no dendrimer) prior to casting the G4-ACN or G4-ACN/SO polyurethanes. This layer prevented delamination of the polyurethane and subsequently reduced leaching (Figure 5.4). Of note, it was hypothesized that the addition of the bulky, hydrophobic styrene oxide in G4-ACN/SO would reduce dendrimer leaching by increasing hydrophobic-hydrophobic interactions between the polyurethane and the dendrimer. While the G4-ACN/SO dendrimers did leach ~50% less than G4-ACN dendrimers both with and without an adhesive layer, the data in Figure 5.4 clearly demonstrates that swelling of the polymer matrix impacts leaching to a much greater extent.

Table 5.2 shows the NO-release characteristics of 25 wt% G4-ED, G4-SO, G4-ACN, or G4-ACN/SO doped within a 75TP470:25TPU polyurethane. The NO-release from all 25 wt% systems is sufficient for reducing adhesion of Gram-negative and Gram-positive bacteria,[7, 27] reducing platelet adhesion,[3] reducing collagen capsule thickness[7, 20], reducing collagen capsule thickness *in vivo*,[20] and reducing inflammation *in vivo*.[27] Furthermore, G4-ACN and G4-ACN/SO-doped polyurethanes release NO at levels that

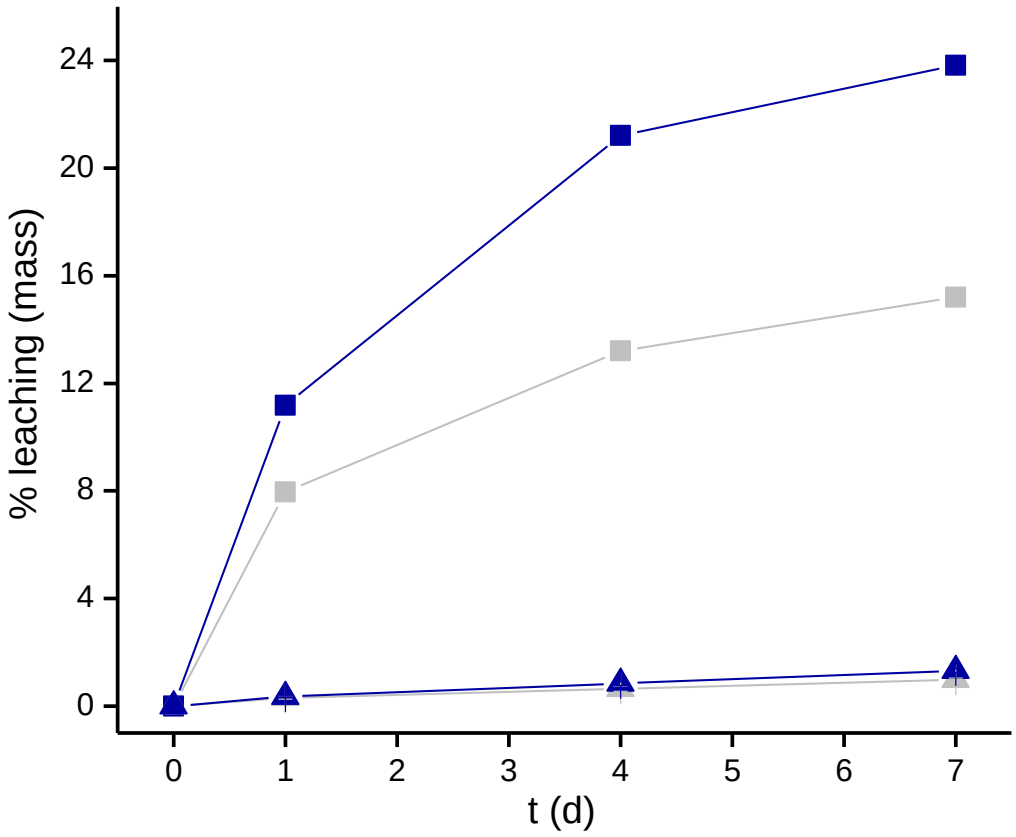

Figure 5.4 Cumulative leaching from G4-ACN/SO (grey) and G4-ACN (blue) with (triangle) and without (square) an adhesion layer. Leaching was determined through RITC-tagged dendrimers and fluorometry. Error bars represent the standard deviation of the mean (n=3 measurements of n=1 film per data point).

Table 5.2 Nitric oxide-release characterization of *N*-diazeniumdiolate-modified dendrimers doped within 75TP470:25TPU polyurethanes (25 wt%) and coated with TP470 barrier layers (30 μL; 40 mg mL^{-1}). Adhesion layers (75TP470:25TPU) were used for G4-ACN and G4-ACN/SO systems.

dendrimer dopant (25 wt%)	**$[NO]_m$ pmol cm^{-2} s^{-1}**	**t[NO] μmol cm^{-2}**	**$t_{1/2}$ (h)**	**t_d (d)**	**% leaching (7 d; wt%)**
G4-ED	27.0 ± 2.0[a]	1.1 ± 0.2	14 ± 2	3.2 ± 0.7	2.5 ± 0.3
G4-SO	14.1 ± 1.2	1.1 ± 0.3	20 ± 3	3.4 ± 0.2	3.0 ± 0.4
G4-ACN[b]	4.4 ± 0.04	1.6 ± 0.4	69 ± 13	6.9 ± 0.9	1.3 ± 0.2
G4-ACN/SO[b]	17.2 ± 6.4	2.0 ± 0.7	50 ± 14	8.8 ± 3.2	1.0 ± 0.2

[a] Values are given as mean ± standard deviation for n=3 samples
[b] n=2

significantly inhibit *S. aureus* and *E. coli* biofilm formation over 7 d.[28] Consistent with the NO-release characteristics of the *N*-diazeniumdiolate-modified G4-PAMAM precursors themselves, the release durations from the 25 wt% G4-SO and G4-ED films were much shorter than the G4-ACN and G4-ACN/SO films. To the best of our knowledge, the duration (8.8 ± 3.2 d) and half-life (50 ± 14 h) of NO release from 25 wt% G4-ACN/SO is the longest to date for an *N*-diazeniumdiolate-based film formed from a polyurethane dispersion, and the second-longest to date for any *N*-diazeniudiolate surface formulation. Cai et al. achieved a 10 d duration > 1 pmol cm^{-2} s^{-1} by doping a small molecule NO donor (*N*-diazeniumdiolate-modified dibutylhexyldiamine; 20 wt%) into a poly(lactic-co-glycolic) acid matrix coated with silicon rubber.[28] In that configuration, the amine-based NO donor was geographically concentrated at the center of the film so that the internal pH surrounding the *N*-diazeniumdiolate increased. Thus, the proton-driven decomposition of the *N*-diazeniumdiolate slows dramatically. Slow hydrolysis of the poly(lactic-co-glycolic) scaffold produced lactic and glycolic acids, supplementing the internal matrix with protons. In return, NO release continues, albeit slowly. Despite the slightly longer NO release kinetics using this approach, our strategy may prove more useful for long-term implants and coatings in that it does not rely on degradation of the polymer to achieve NO release.

As shown in Table 5.2, a slight amount of dendrimer leaching (<3 wt%) occurred from the G4-PAMAM dendrimer-doped polyurethanes after immersion in PBS (pH 7.4; 37 ^{o}C). To probe the connection between leaching and toxicity (if any), the G4-PAMAM-doped polyurethanes were incubated atop L929 fibroblasts for 24 h (Figure 5.5). The G4-ACN/SO-doped polyurethanes did not exhibit any cytotoxicity, in alignment with our

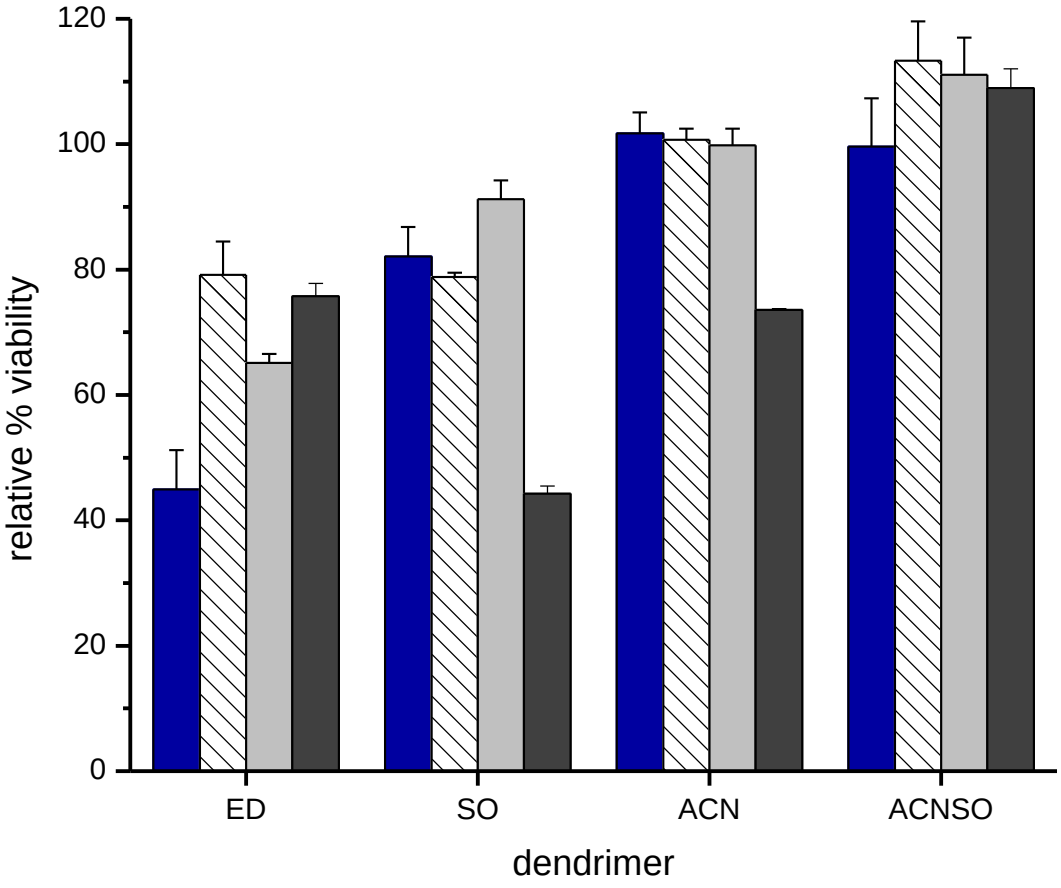

Figure 5.5 Cytotoxicity of L929 fibroblasts following 24 h exposure to G4-ED, G4-SO, G4-ACN, or G4-ACNSO-doped polyurethanes. Films are either 10 wt% dendrimer; no barrier layer (blue), 10 wt% dendrimer; with barrier layer (white stripe), 20 wt% dendrimer (light grey) or 30 wt% dendrimer (dark grey). Error bars represent the standard deviation of the mean from triplicate measurements of n=1 film.

findings that amphiphilic dendrimers are not toxic towards mammalian cells.[29] In contrast, G4-SO (30 wt%) and G4-ED (10 wt%; no barrier layer) systems displayed significant toxicity towards the L929 fibroblasts. Our results clearly indicate that the polymer composition, barrier layer, and dendrimer must be carefully selected to minimize toxicity from polyurethane films.

5.3.3 Synthesis and characterization of NO-releasing G4-PAMAM-doped electrospun polyurethane fibers

Electrospun fibers have potential application as wound dressings,[30] tissue engineering scaffolds,[31] and sensors.[32] Several overlapping advantages may exist for electrospun fibers and NO release. For example, both strategies promote tissue integration,[18] improve the wound-healing response,[19] and reduce collagen capsule thickness.[18, 33] As such, we hypothesize that NO-releasing electrospun fiber mats may further reduce the foreign body response to tissue-based implants. Electrospun fiber mats synthesized in our laboratory to date have utilized NO-releasing polymer dispersions of PROLI/NO or silica nanoparticles.[15, 16] While not expected to cause toxicity, electrospun fibers doped with PROLI/NO and G4-PAMAM leach most of their contents when submerged in phosphate buffer,[6] thus limiting the extended NO-release durations afforded by the polyurethane matrix itself. The NO-releasing G4-PAMAM dendrimers may remain entrapped within the electrospun fiber mats more readily than particles or PROLI/NO due to improved partitioning. Furthermore, the properties of the G4-PAMAM dendrimers synthesized herein would result in fibers with tunable NO-release totals and durations.

Koh et al. demonstrated that electrospun fibers synthesized from TP470 exhibited less swelling in aqueous solution than those made from TPU or other more hydrophilic polyurethanes.[14] Thus, TP470 was chosen as the polymer for the fibers explored herein. Each dendrimer was dissolved within a viscous TP470 solution (12% w/v) at an overall concentration of 5 wt% relative to the total amount of TP470. G4-PAMAM-doped fibers with nanometer dimensions were produced following extrusion of the dendrimer-doped polymer through a needle tip and application of a high voltage electric field (Figure 5.6). No significant differences in fiber diameters were observed between the different G4-PAMAM systems (Table 5.3). Using TP470 with silicon nanoparticles, Koh et al. similarly reported that fiber diameter was influenced more by kinematic viscosity (i.e., a property of the polymer solution itself) than by the dopant included within. Having independent control of fiber diameter (separate from the dopant) in this manner may prove useful in future experiments aimed to evaluate the role of NO-release and electrospun fibers in tissue.

Compared to fibers doped with *N*-diazeniumdiolate-modified silica particles that leach 35-100% of their contents within 7 d, the NO-releasing G4-PAMAM-doped fibers herein leached only 7—16% over the same period (Table 5.3). Predictably, the most hydrophilic dendrimer (G4-ACN) leached the most. Styrene oxide-modified dendrimers (G4-ACN/SO) leached only half of this amount, consistent with observations above for G4-ACN and G4-ACN/SO films. Nitric oxide release totals (Table 5.4) from the fibers were similar to those reported for NO-releasing silica particle-doped mats. However, the NO-release durations for the 5wt% G4-ACN and G4-ACN/SO dendrimers are the longest reported for *N*-diazeniumdiolate-based NO donors within an electrospun

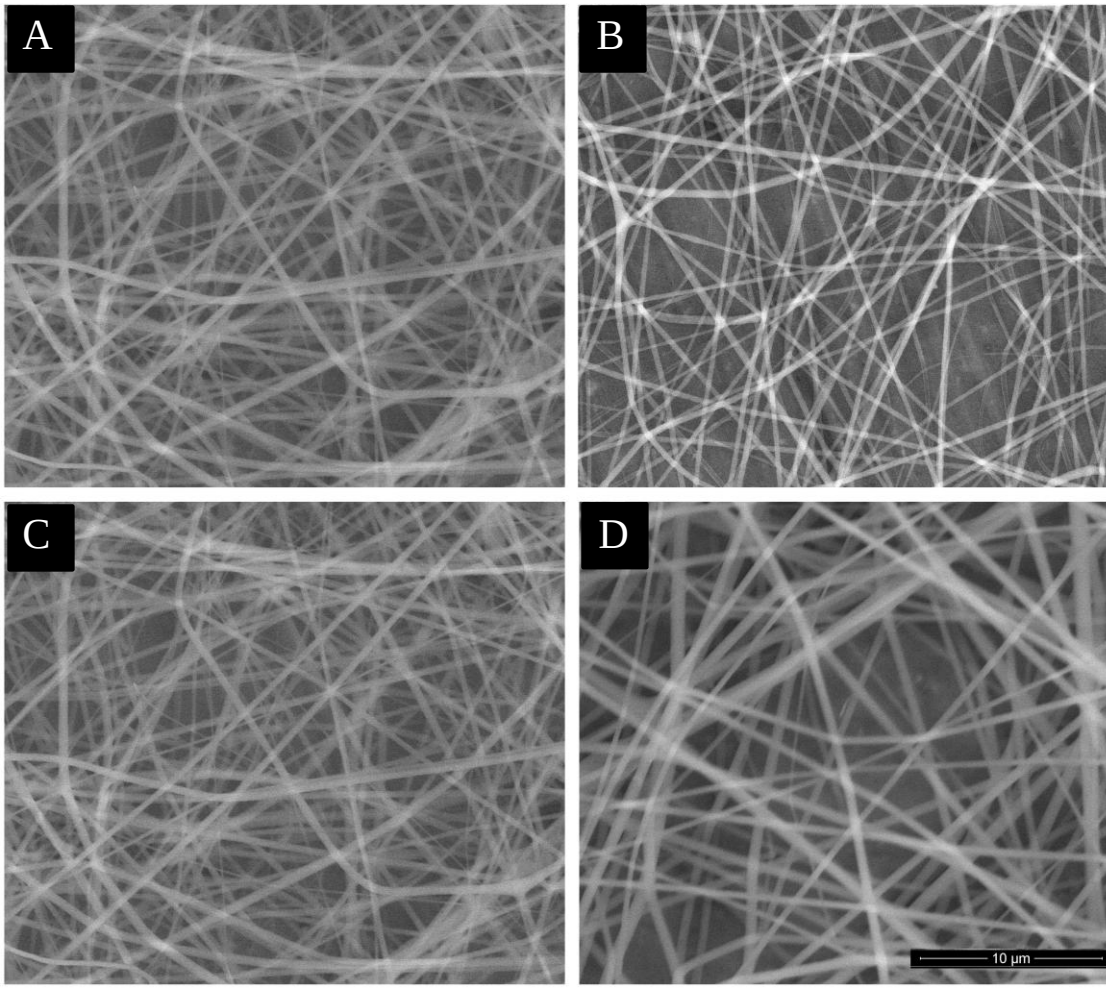

Figure 5.6 Electrospun TP470 fibers doped with 5 wt% (A) G4-ED, (B) G4-SO, (C) G4-ACN, or (D) G4-ACN/SO viewed using SEM. Scale bar = 10 μm.

Table 5.3 Fiber diameters and dendrimer leaching from NO-releasing G4-PAMAM-doped electrospun TP470 fibers. Dendrimers were doped at a concentration of 5 wt% relative to the TP470 polyurethane. Fiber diameters were determined from SEM and leaching was measured through RITC-tagged dendrimers measured using fluorometry.

dendrimer dopant	**fiber diameter (nm)**[a,b]	**% leaching**[c]
G4-ED	470 ± 110	7.2 ± 0.5
G4-SO	440 ± 130	11.3 ± 0.6
G4-ACN	480 ± 120	16.2 ± 1.6
G4-ACN/SO	490 ± 150	9.6 ±1.8

[a] Values are given as the mean ± standard deviation from n=50 random locations on the fiber mat
[b] Diameters were measured using imageJ software.
[c] Values are given as the mean ± standard deviation from n=3 fiber samples.

Table 5.4 Nitric oxide release properties from G4-PAMAM-doped electrospun TP470 fibers determined via chemiluminescence. Dendrimers were doped at a concentration of 5 wt% relative to the TP470 polyurethane.

dendrimer dopant	ppb mg[a]	nmol mg^{-2}	half-life (h)	duration (h)
G4-ED	52.6 ± 12.9	19 ± 2	0.9 ± 0.1	17 ± 4
G4-SO	17.5 ± 7.7	12 ± 0.7	1.7 ± 0.5	17 ± 3
G4-ACN	13.2 ± 4.4	27 ± 5	4.6 ± 1.2	42 ± 14
G4-ACN/SO	51.9 ± 12.3	34 ± 4	2.1 ± 0.1	38 ± 11

[a] Values are given as the mean ± standard deviation of n=3 fiber samples.

fiber mat. Overall, the results indicate that facile surface modification of dendrimer scaffolds may be used control dopant-polymer partitioning (i.e., reducing leaching via hydrophobic groups) and extend NO-release kinetics.

5.4 Conclusions

Preparing NO-donor/polymer dispersions represents one of the simplest approaches to fabricate NO-releasing coatings. However, controlling NO-release kinetics (i.e., to enable low NO flux anti-FBR coatings or higher NO flux anti-bacterial coatings) while also minimizing NO-donor leaching is difficult because strategies that modulate NO release rate may often influence leaching of the dopant from the polymer. In this chapter, NO-releasing PAMAM dendrimers were used as polymer dopants. The tunable surface hydrophobicity, NO-release kinetics and sizable NO payloads of PAMAM dendrimers enabled tailored NO-release kinetics while limiting donor leaching from polyurethanes. Future work should explore the potential for covalent dendrimer-polymer attachment, instead of the hydrophobic-hydrophobic interactions explored herein, to completely eliminate NO donor leaching.

REFERENCES

1. Ramamurthi, A.; Lewis, R. S., "Measurement and modeling of nitric oxide release rates for nitric oxide donors." *Ann. Biomed. Eng.* **1997**, *10*, 408-413.

2. Riccio, D. A.; Schoenfisch, M. H., "Nitric oxide release: Part I. Macromolecular scaffolds." *Chem. Soc. Rev.* **2012**, *41*, 3731-41.

3. Riccio, D. A.; Dobmeier, K. P.; Hetrick, E. M.; Privett, B. J.; Paul, H. S.; Schoenfisch, M. H., "Nitric oxide-releasing S-nitrosothiol-modified xerogels." *Biomaterials* **2009**, *30*, 4494-4502.

4. Shin, J. H.; Marxer, S. M.; Schoenfisch, M. H., "Nitric oxide-releasing sol-gel particle/polyurethane glucose biosensors." *Anal. Chem.* **2004**, *76*, 4543-9.

5. Batchelor, M. M.; Reoma, S. L.; Fleser, P. S.; Nuthakki, V. K.; Callahan, R. E.; Shanley, C. J.; Politis, J. K.; Elmore, J.; Merz, S. I.; Meyerhoff, M. E., "More lipophilic dialkyldiamine-based diazeniumdiolates: Synthesis, characterization, and application in preparing thromboresistant nitric oxide release polymeric coatings." *J. Med. Chem.* **2003**, *46*, 5153-61.

6. Reynolds, M. M.; Frost, M. C.; Meyerhoff, M. E., "Nitric oxide-releasing hydrophobic polymers: preparation, characterization, and potential biomedical applications." *Free Radical Bio. Med.* **2004**, *37*, 926-936.

7. Hetrick, E. M.; Schoenfisch, M. H., "Antibacterial nitric oxide-releasing xerogels: Cell viability and parallel plate flow cell adhesion studies." *Biomaterials* **2007**, *28*, 1948-1956.

8. Mowery, K. A.; Schoenfisch, M. H.; Saavedra, J. E.; Keefer, L. K.; Meyerhoff, M. E., "Preparation and characterization of hydrophobic polymeric films that are thromboresistant via nitric oxide release." *Biomaterials* **2000**, *21*, 9-21.

9. Singh, R. J.; Hogg, N.; Joseph, J.; Kalyanaraman, B., "Mechanism of nitric oxide release from S-nitrosothiols." *J. Biol. Chem.* **1996**, *271*, 18596-18603.

10. Liu, L.; Hausladen, A.; Zeng, M.; Que, L.; Heitman, J.; Stamler, J. S., "A metabolic enzyme for S-nitrosothiol conserved from bacteria to humans." *Nature* **2001**, *410*, 490-494.

11. Stubauer, G.; Giuffrè, A.; Sarti, P., "Mechanism of S-nitrosothiol formation and degradation mediated by copper ions." *J. Biol. Chem.* **1999**, *274*, 28128-28133.

12. Keefer, L. K., "Fifty years of diazeniumdiolate research. From laboratory curiosity to broad-spectrum biomedical advances." *ACS Chem. Biol.* **2011**, *6*, 1147-1155.

13. Wu, Y.; Meyerhoff, M. E., "Nitric oxide-releasing/generating polymers for the development of implantable chemical sensors with enhanced biocompatibility." *Talanta* **2008**, *75*, 642-650.

14. Koh, A.; Riccio, D. A.; Sun, B.; Carpenter, A. W.; Nichols, S. P.; Schoenfisch, M. H., "Fabrication of nitric oxide-releasing polyurethane glucose sensor membranes." *Biosens. Bioelectron.* **2011**, *28*, 17-24.

15. Coneski, P. N.; Nash, J. A.; Schoenfisch, M. H., "Nitric oxide-releasing electrospun polymer microfibers." *ACS Appl. Mater. Interfaces* **2011**, *3*, 426-432.

16. Koh, A.; Carpenter, A. W.; Slomberg, D. L.; Schoenfisch, M. H., "Nitric oxide-releasing silica nanoparticle-doped polyurethane electrospun fibers." *ACS. Appl. Mater. Interfaces DOI: 10.1021/am402044s [Available online August 5, 2013]*.

17. Doshi, J.; Reneker, D. H., "Electrospinning process and applications of electrospun fibers." *J. Electrostat.* **1995**, *35*, 151-160.

18. Cao, H.; McHugh, K.; Chew, S. Y.; Anderson, J. M., "The topographical effect of electrospun nanofibrous scaffolds on the in vivo and in vitro foreign body reaction." *J. Biomed. Mater. Res. A* **2010**, *93*, 1151-9.

19. Khil, M. S.; Cha, D. I.; Kim, H. Y.; Kim, I. S.; Bhattarai, N., "Electrospun nanofibrous polyurethane membrane as wound dressing." *J. Biomed. Mat. Res. B* **2003**, *67*, 675-679.

20. Nichols, S. P.; Koh, A.; Brown, N. L.; Rose, M. B.; Sun, B.; Slomberg, D. L.; Riccio, D. A.; Klitzman, B.; Schoenfisch, M. H., "The effect of nitric oxide surface flux on the foreign body response to subcutaneous implants." *Biomaterials* **2011**, *33*, 6305-6312.

21. Lu, Y.; Sun, B.; Li, C.; Schoenfisch, M. H., "Structurally diverse nitric oxide-releasing poly(propylene imine) dendrimers." *Chem. Mater.* **2012**, *23*, 4227-4233.

22. Stasko, N. A.; Fischer, T. H.; Schoenfisch, M. H., "S-nitrosothiol-modified dendrimers as nitric oxide delivery vehicles." *Biomacromolecules* **2008**, *9*, 834-841.

23. Stasko, N. A.; Schoenfisch, M. H., "Dendrimers as a scaffold for nitric oxide release." *J. Am. Chem. Soc.* **2006**, *128*, 8265-8271.

24. Coneski, P. N.; Schoenfisch, M. H., "Nitric oxide release: Part III. Measurement and reporting." *Chem. Soc. Rev.* **2012**, *41*, 3753-8.

25. Carpenter, A. W.; Slomberg, D. L.; Rao, K. S.; Schoenfisch, M. H., "Influence of scaffold size on bactericidal activity of nitric oxide-releasing silica nanoparticles." *ACS Nano* **2011**, *5*, 7235-44.

26. Shao, N.; Su, Y.; Hu, J.; Zhang, J.; Zhang, H.; Cheng, Y., "Comparison of generation 3 polyamidoamine dendrimer and generation 4 polypropylenimine dendrimer on drug loading, complex structure, release behavior, and cytotoxicity." *Int. J. Nanomedicine* **2011**, *6*, 3361.

27. Nichols, S. P.; Schoenfisch, M. H., "Nitric oxide flux-dependent bacterial adhesion and viability at fibrinogen-coated surfaces." *Biomater. Sci. 10.1039/C3BM60130G [Available online July 17, 2013]*.

28. Cai, W.; Wu, J.; Xi, C.; Meyerhoff, M. E., "Diazeniumdiolate-doped poly(lactic-co-glycolic acid)-based nitric oxide releasing films as antibiofilm coatings." *Biomaterials* **2012**, *33*, 7933-7944.

29. Jain, K.; Kesharwani, P.; Gupta, U.; Jain, N. K., "Dendrimer toxicity: Let's meet the challenge." *Int. J. Pharm.* **2010**, *394*, 122-142.

30. Khil, M.-S.; Cha, D.-I.; Kim, H.-Y.; Kim, I.-S.; Bhattarai, N., "Electrospun nanofibrous polyurethane membrane as wound dressing." *J. Biomed. Mat. Res. B* **2003**, *67*, 675-679.

31. Xie, J.; MacEwan, M. R.; Schwartz, A. G.; Xia, Y., "Electrospun nanofibers for neural tissue engineering." *Nanoscale* **2010**, *2*, 35-44.

32. Aussawasathien, D.; Dong, J.-H.; Dai, L., "Electrospun polymer nanofiber sensors." *Synthetic Met.* **2005**, *154*, 37-40.

33. Nichols, S. P.; Koh, A.; Storm, W. L.; Shin, J. H.; Schoenfisch, M. H., "Biocompatible materials for continuous glucose monitoring devices." *Chem. Rev.* **2013**, *113*, 2528-49.

Chapter 6:

Summary and Future Directions

6.1 Summary

The preceding chapters have detailed new designs in NO-releasing antimicrobial coatings for enhancing the utility and function of biomedical implants. In Chapter 1, the circumstances that cause bacterial colonization on implants and strategies for bacterial adhesion were described to provide some perspective on non-fouling interfaces. Particular attention was given to "passive" and "active" antimicrobial coatings, and the strengths and limitations of each.

In Chapter 2, the synthesis of NO-releasing xerogels from *N*-diazeniumdiolate-modified silane precursors was developed using the sol-gel method. Prior to this approach, the route to NO-releasing xerogels first required synthesis of an amine-modified silica network with subsequent exposure to high pressures of NO gas (≥5 bar). This process limited the analytical utility of these xerogels as glucose sensor membranes and also required the substrate to be placed under high pressure NO—a requirement that may be impractical for some medical devices. Both the size of the nitric oxide payload and the kinetics of its release were tunable by varying the identity and concentration of the precursor NO donor within the xerogel. To further illustrate the clinical utility of this method, AEAP/NO-PTMOS xerogels were developed as outer sensor membranes for glucose sensors.

In Chapter 3, passive and active antimicrobial strategies were combined to create antifouling surfaces. Nitric oxide-releasing xerogels were spraycoated with a mixture of

silica and a fluorosilane to provide the microscale roughness and low-surface energy required for superhydrophobicity. By adjusting the thickness of the superhydrophobic layer, NO-release durations were tuned from 59—105 h, suggesting that these coatings may also have utility in controlled drug release applications. The antimicrobial properties of these interfaces were measured using 10^8 cfu mL^{-1} *P. aeruginosa.* Individually, NO-release and superhydrophobicity each reduced viable adhered bacteria by ~1-log. Xerogels that were both superhydrophobic and released NO decreased viable adhesion by ~2-log, suggesting an additive antifouling effect for the two strategies. The biocidal capabilities of the NO-release layer were demonstrated by incubating the xerogels in PBS for an additional 12 h where an additional ~1.8-log reduction in bacteria was observed. As the superhydrophobic coating itself was shown to be non-toxic, combining superhydrophobicity with NO release maximized the antifouling potential of these coatings without negatively affecting cell toxicity.

In Chapter 4, the synthesis of xerogels that release silver and NO simultaneously was described to study potential antimicrobial synergy. The xerogels were synthesized using a multi-layer approach. While the NO-releasing layer was fabricated using an amine-modified AHAP xerogel, the silver-releasing layer consisted of an alkylsilane loaded with silver nitrate. Release of each agent from its respective layer was independently controllable (i.e., silver loading did not alter NO release, and the *N*-diazeniumdiolate formation process did alter silver release). The antibacterial potential of these xerogels was assessed against *P. aeruginosa* and *S. aureus,* common Gram-negative and Gram-positive bacteria implicated in orthopedic infections.[1, 2] Against both bacterial strains, a greater-than-additive bactericidal effect was observed when the two agents were

released simultaneously. Through confocal microscopy experiments, we found that NO's action could primarily be attributed to reduced adhesion. Silver's mechanism of action was primarily through cellular killing. We hypothesized that membrane damage caused by silver allowed NO to permeate the cell more readily, where it could react with oxidative stressors (e.g., those that resulted from Ag^{+} treatment) to form potent antimicrobials such as peroxynitrite. Despite the greater-than-additive killing effect observed against bacteria, no such effect was observed on L929 mouse fibroblasts. These materials may be important tools for limiting the toxicity and bioaccumulation of silver-releasing materials that are widespread in clinical care.

In Chapter 5, NO-releasing poly(amido amine) (PAMAM) dendrimers were used as dopants within polyurethane films and nanofibers. By altering the modifier that forms secondary amines on the dendrimer (necessary for *N*-diazeniumdiolate formation), materials with a range of NO surface fluxes and durations were achieved. Polyurethanes with acrylonitrile (ACN)-modified G4-PAMAM dendrimers released low levels of NO (max flux 3—10 pmol cm^{-2} s^{-1}) for up to 8.8 d with low toxicity to L929 fibroblast cells. By incorporating hydrophobic modifiers (e.g., styrene oxide (SO)) on the exterior of ACN-modified dendrimers, leaching of the macromolecules from both films and fibers was reduced while retaining the longer release characteristics of the ACN systems. As films, the sustained NO release from these materials hold promise as antibiofilm coatings,[3] while the fibers may be utilized to create sensor membranes or antimicrobial wound dressings.[4, 5]

6.2 Future directions

Chemists have developed a broad-array of biomedical device coatings that prevent the adhesion of microbial pathogens or kill adhered microbes.[6] Despite their promise, the inherent limitations present with some types of antimicrobial coatings could be overcome by rationally combining different drug-release or surface-modification strategies. In this section, new techniques for effective antimicrobial materials are introduced. In addition, surfaces that hold promise for others types of fouling will be suggested.

6.2.1 Silver/NO-releasing wound dressings

Silver-releasing wound dressings are used extensively to treat infection-prone wounds such as burns and diabetic ulcers.[7, 8] Unfortunately, these materials exhibit toxicity towards karatinocyte and fibroblast cells, both of which are critical to the body's wound-healing response.[7, 9] Large concentrations of silver may accumulate systemically from these treatments. In a case report from 2006, a burn patient developed severe argyria-like symptoms (i.e., graying of the skin and elevated silver concentrations in the liver and plasma) following treatment with silver sulfadiazine-doped wound dressings.[10] Therapies are needed that reduce silver toxicity without compromising its antimicrobial efficacy. In Chapter 4, dual-action silver/NO-releasing xerogels were shown to exhibit greater-than-additive killing of surface-adhered *P. aeruginosa* and *S. aureus*. Translating this drug-release combination to wound dressings would alleviate some of the pitfalls associated with silver release by lowering the overall dose of the metal required for an identical antimicrobial effect.

The benefits of a silver/NO-releasing dressing may extend beyond reduced toxicity. In vivo, NO regulates wound healing and is an essential factor for collagen deposition by fibroblasts.[11] Exogenous NO has been employed as a treatment to promote wound healing.[12, 13] Hydrogels that release NO enhance extracellular matrix production by fibroblasts. Likewise, NO-releasing nanoparticles accelerate the wound healing process by promoting angiogenesis.[13] Exogenous NO therapies are particularly efficacious for the two clinical populations treated most with silver-releasing wound dressings: diabetics and burn victims.[14, 15]

Polyurethane electrospun fibers would be ideal polymer scaffolds for fabricating silver/NO-releasing wound dressings.[16, 17] Khil et al. observed improved epithelialization and tissue organization at wounds treated with electrospun polyurethane nanofiber mats. These results were attributed to the high oxygen permeability of polyurethanes along with their ability to trap moisture at wound sites, lending credence to their potential as wound dressings.[16, 17] To incorporate both NO and silver-release capabilities to such fibers, poly(amido amine) dendrimers may be used as macromolecular scaffolds for the effective storage of these agents. Generation 4 PAMAM dendrimers are able to solubilize transition metal cations such as silver through complexes formed at the internal 3^{o} amines of the dendrimers.[18] Balogh et al. reported that silver-doped dendrimers prepared in this manner were bactericidal against *S. aureus, E. coli, and P. aeruginosa.* Post-functionalizing silver-containing dendrimers with *N*-diazeniumdiolate NO donors may result in an effective silver/NO-releasing macromolecular scaffold that could be included within electrospun polyurethane fiber mats. If the chemistries used for *N*-diazeniumdiolate synthesis and silver-loading prove to be incompatible, a two-agent

system (i.e., a mixture of *N*-diazeniumdiolate-modified dendrimers and silver-loaded dendrimers) could be loaded into the electrospun fibers instead. The resulting material should lower the doses of silver necessary for a specific bactericidal effect while also encouraging potent wound-healing properties through NO release.

6.2.2 Quaternary ammonium (QA)-functionalized superhydrophobic surfaces

An ideal antifouling surfaces for medical devices would reduce bacterial adhesion, kill bacteria that do adhere, and have a mechanism of action that operates indefinitely.[19] Passive antifouling surfaces (e.g., PEGylated and superhydrophobic membranes) resist adhesion, but their inability to kill bacteria still allows for biofilm growth. Materials that actively release biocidal agents (e.g., NO or Ag^{+}) are able to resist adhesion and kill bacteria, but their antimicrobial duration is finite. Polycationic QA-functionalized surfaces represent a strategy that merges the benefits of each. The presence of long, hydrophobic alkyl chains and a dense cationic surface charge disrupts the membranes of adhered bacteria without exhibiting marked toxicity to mammalian cells.[20, 21] As the biocide is permanently affixed to the surface, such materials could theoretically kill bacteria indefinitely. In practice, the utility of QA-functionalized coatings is limited for biomedical applications. Bacteria killed by the QA-groups remain adhered, masking the substrate from further bacteria.[22] The Klibanov group examined this phenomenon by spraying aerosolized bacteria (~$5x10^{6}$ cfu mL^{-1} E. coli) onto QA-modified brush polymers. After four sprays of the bacteria suspension, the bacterial killing ability of the coating declined by nearly 45%.[22] The authors demonstrated that the coating could be regenerated by washing with a surfactant, but such a step would be impractical for implantable medical devices.

The development of QA-functionalized surfaces that also resist adhesion would improve the long-term utility of these materials. A superhydrophobic QA-functionalized surface should both reduce bacterial adhesion (through the superhydrophobic component) and kill bacteria (through the QA component). Fewer adhered bacteria would translate to fewer masked QA moieties on the surface, ultimately extending their biocidal efficacy. Furthermore, the self-cleaning properties of superhydrophobic coatings may serve to "regenerate" the surface through removal of dead bacteria.

In Chapter 3 of this dissertation, a superhydrophobic material was coated on NO-releasing xerogels. Silica particles were reacted in the presence of a fluorinated sol-gel material to create the surface roughness and low surface energy needed for superhydrophobicity. In the future, superhydrophobic QA-modified coatings could be created by exchanging the silane components in this sol-gel with a QA-modified silane (Scheme 6.1). First, QA-modified silanes of varying chain lengths may be synthesized via an established nucleophilic aliphatic substitution reaction to create a library of QA silane precursors. The effect of alkyl chain length, alkyl chain density, and charge density can be explored by adjusting either the identity or the relative concentration of the QA silane precursors. Each of these features will likely affect both contact angle and bactericidal efficacy. Quaternary ammonium species with longer alkyl chains (10-16 carbons)[23-26] have proven more effective at killing bacteria. Longer alkyl chains will likely provide the low surface energy necessary for superhydrophobicity. Oosterhof et al. reported hydrophobic contact angles (100^{o}) on smooth substrates modified with a commercially available 18-carbon QA silane.[27] The same fluorosilane membranes used to create the superhydrophobic materials in Chapter 3 feature a static water contact angle of

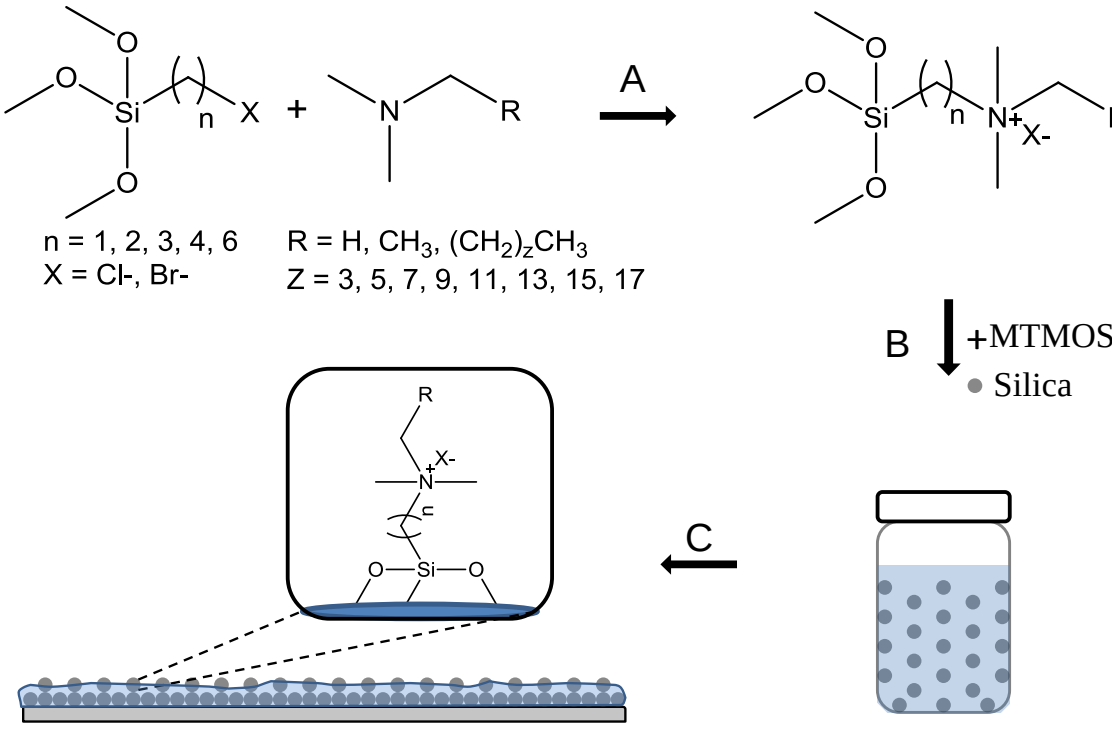

Scheme 6.1 Proposed synthesis of QA-modified surfaces. (**A**) An alkyl halide-functionalized silane and tertiary amine are reacted via nucleophilic aliphatic substitution to yield QA-modified silanes. (**B**) QA-modified silanes are co-condensed with linker silanes and silica colloids, before (**C**) application to a substrate to yield superhydrophobic QA-modified surfaces.

105^{o} when cast on smooth surfaces.[28] In preliminary experiments, a commercially available QA silane featuring two 10-carbons chains pendant from the quaternary ammonium (*N*,*N*-didecyl-*N*-methyl *N*-(3-trimethoxysilylpropyl) ammonium chloride; DDMTS) was incorporated into a silica-particle doped sol at concentrations of 0, 10, or 20 mol% (balance MTMOS). As shown in Figure 6.1A, increasing the mol% of DDTMS within the membrane caused a concomitant increase in the intensity of a characteristic QA X-ray photoelectron spectroscopy (XPS) peak at ~400 eV (Figure 1A).[23] The water contact angle of the particle-doped 20 mol% DDTMS composite was 149^{o} (Figure 6.1B), indicating near-superhydrophobic behavior. To optimize the anti-wetting properties of these materials, longer-chained QAs or fluorosilanes should be incorporated into the composite. Subsequent bacteria testing should be two-pronged, with focus given to waterborne and airborne assays.[29] The benefits of the self-cleaning superhydrophobic layer could be proved through repeated aerosolized bacteria challenges or pre-immersion in a suspension of proteins to model the fouling events that mask the bactericidal action of QA moieties.

6.2.3 Superhydrophobic materials for ultrasound-triggered NO release

The superhydrophobic NO-releasing xerogels described in Chapter 3 were synthesized by applying a thin superhydrophobic membrane onto an existing (non-superhydrophobic) NO-releasing xerogel. In contrast, Yohe et al. synthesized releasing 3-dimensional (3D) superhydrophobic fiber meshes where a cancer drug was doped *within* the superhydrophobic material.[30] When the mats were submerged in water, entrapped air prevented diffusion of the drug payload out into the surroundings. Water was forced into

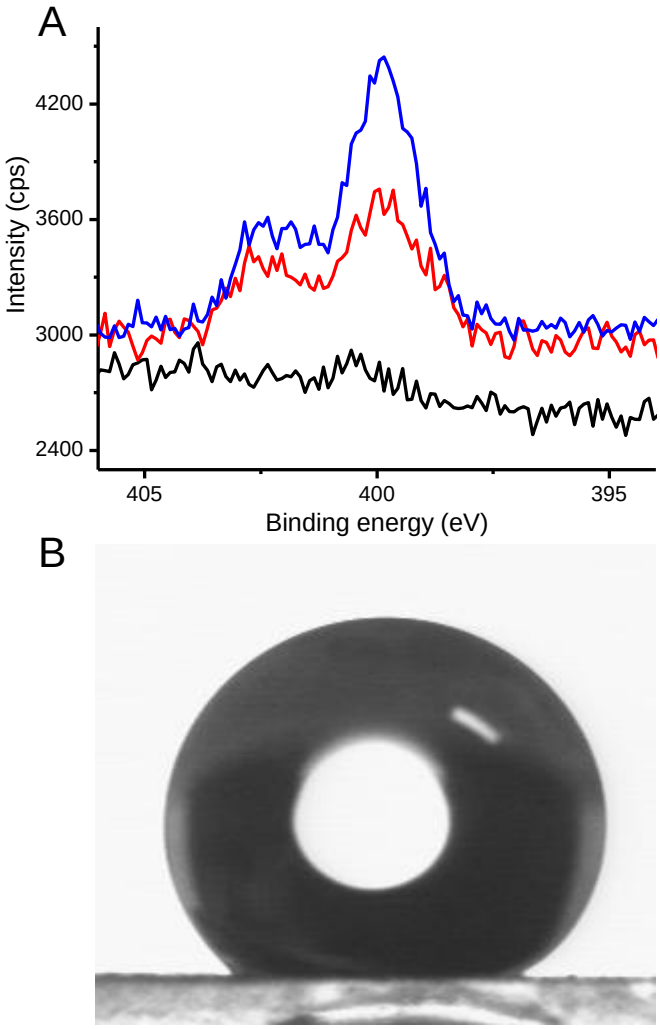

Figure 6.1 (A) Xray photoelectron spectra of 0 (black), 10 (red), and 20 mol% (blue) DDTMS (balance MTMOS) silica composites (B) A water droplet (contact angle 149^{o}) on a 20 mol% DDTMS (balance MTMOS) silica composite.

the mat by applying ultrasound, effectively creating a controlled external trigger for drug-release.

Triggered release of antimicrobial agents such as NO may prove useful for delaying implant associated infections that manifest weeks or months after surgery.[31] Nitric oxide is also involved in biofilm dispersal,[32] so this technique may be useful for disrupting mature biofilms that develop on the implant. An NO-releasing material with ultrasound-triggered-release could be prepared by using the *N*-diazeniumdiolate-modified silane precursors employed in Chapter 2. By incorporating these precursors into a silica-fluorosilane sol and applying the membrane as a thick coating on a surface, the *N*-diazeniumdiolate NO donors would be distributed throughout the entirety of the superhydrophobic silica network. With reduced water uptake into the material, proton-dependent decomposition of the NO donors would slow, but could later be triggered by applying ultrasound much like the fiber mats prepared by Yohe and coworkers. Such a material might improve patient care by eradicating infections that form after device implantation.

6.2.4 Superhydrophobic coatings as mold-resistant materials

The work presented here has focused on coatings that resist the adhesion of virulent bacteria on implanted devices. However, some of these materials may prove useful for resisting adhesion and colonization of other medically-relevant microbes. Specifically, the spray-on superhydrophobic coatings presented could be used to combat fungal growth (i.e., mold) that proliferates on the surfaces of building materials.[33] Mold spores colonize moist surfaces, forming vegetative mycelia and growing through extension of hyphae until releasing more spores into the air that further colonize new

surfaces.[33-35] In the hospital setting, spores from pathogenic fungi (e.g., *Aspergillus spp.)*[36] cause infections in immunocompromised patients (e.g., patients with AIDS, or those taking immunosuppressive medications following organ transplants).[37, 38] Unfortunately, morbidity and mortality rates for these infections are high despite antifungal treatments.[36]

Measures that reduce the number of airborne spore counts in hospitals have been directly linked to a decreased incidence of nosocomial fungal infections.[39] Biocidal paints are often used for this purpose, and their mechanism mirrors those developed for implantable biomaterials (i.e., active release of biocides or surface-grafted QA moieties).[40] The anti-wetting properties of superhydrophobic surfaces should prevent mold-growth by limiting the water accessibility needed for fungal replication and survival.[41-43] Moreover, the self-cleaning properties of superhydrophobic materials should allow for easy removal of spores that do adhere.[44]

In preliminary experiments, an accelerated growth model (ASTM D5590)[45] was employed to measure *Aspergillus niger* fungal growth on card stock paper spraycoated with the 30 mol% 17FTMS (balance MTMOS)/silica superhydrophobic composites used in Chapter 3. In this assay, the substrates were placed on nutrient agar, inoculated with ~$4x10^5$ fungal spores, and incubated in the dark for 1 week at 25 ^oC at 93% relative humidity. The fungal inoculum is placed outside the perimeter of the substrate, such that it grows from the outside of the substrate towards the center. Of note, the conditions used in this assay are extremely favorable for mold growth. Controls were either uncoated, MTMOS-coated, or 17FTMS/MTMOS-coated cardstock substrates. While all controls had significant fungal coverage, the superhydrophobic materials displayed almost no

fungal growth (Figure 6.2). These preliminary results demonstrate the promise of superhydrophobic materials for resisting fungal growth. It is hypothesized that the anti-fungal abilities of these materials are partially attributable to low water availability on superhydrophobic surfaces. Mold-forming fungi only grow on surfaces when the water vapor pressure (Water activity; A_w) at the surface-air interface is sufficiently high.[46] The minimum A_w capable of supporting growth is specific to each fungus. If superhydrophobic materials are antifungal by virtue of having an intrinsically low A_w, less growth would be expected for water-loving fungi. Future experiments should evaluate this hypothesis using fungi implicated in nosocomial infections (i.e., *Aspergillus fumigatus, Aspergillus terreus, Fusarium moniliforme,* and *Scedosporium prolificans*).

6.3 Conclusions

The work presented here highlights the importance of implant coatings that resist microbial adhesion and/or kill adhered bacteria. As NO released from a surface is capable of doing both, particular focus was given to this species. Methods were developed utilizing NO to maximize the antifouling capabilities of surfaces while minimizing associated cellular toxicity. These techniques should guide the development of new antimicrobial surfaces, especially those that combine multiple antimicrobial strategies to overcome the limitations of another. While combating infection is critical, others problems also plague clinical devices, such as inadequate wound healing, the foreign body response, and excessive inflammation. Concerns about these issues and infection almost never exist apart from each other, and the next-generation of biomedical coatings must be able to address each. Given NO's ability to improve all of these implant-related

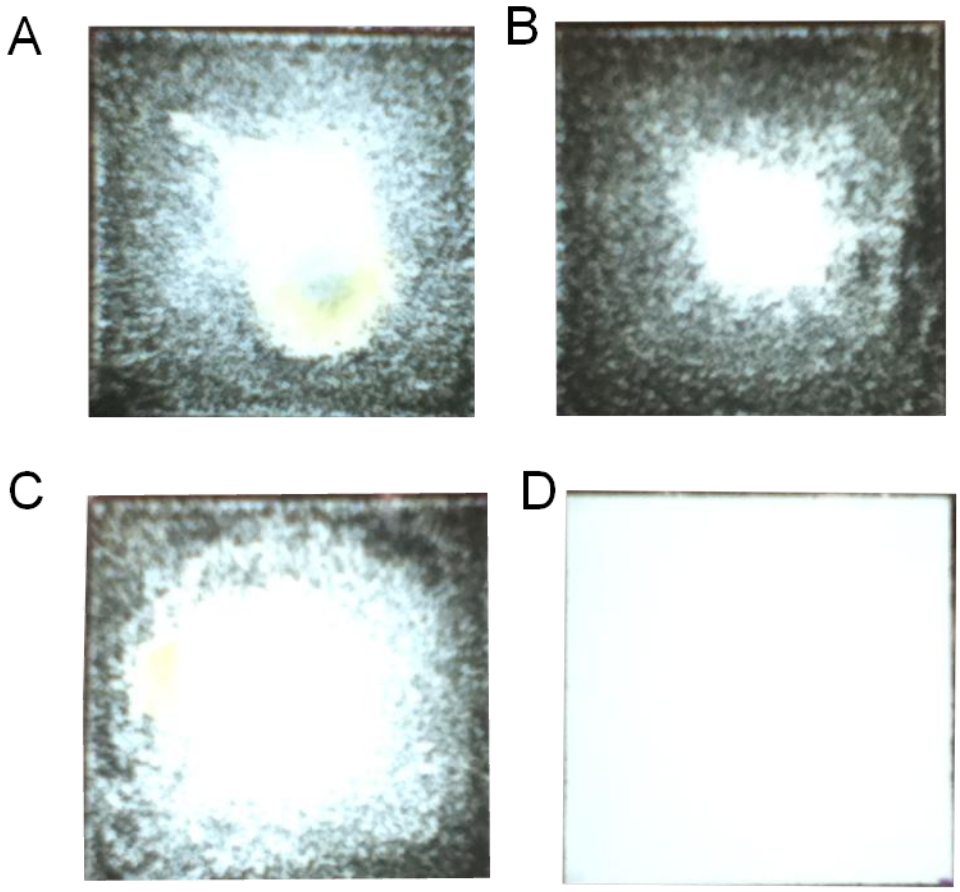

Figure 6.2 *Aspergillus niger* growth on (A) uncoated (B) MTMOS-coated (C) 30 mol% 17FTMS (balance MTMOS)-coated and (D) superhydrophobic card stock. White areas represent the card stock substrate, and black areas are the spore-laden mycelia of the fungus. Each image displays the full area of the substrate (3 cm x 3 cm).

pitfalls, the materials synthesized here may guide future developments of superior anti-fouling coatings.

REFERENCES

1. Brouqui, P.; Rousseau, M.; Stein, A.; Drancourt, M.; Raoult, D., "Treatment of Pseudomonas aeruginosa-infected orthopedic prostheses with ceftazidime-ciprofloxacin antibiotic combination." *Antimicrob. Agents. Ch.* **1995**, *39*, 2423-2425.

2. Kalmeijer, M. D.; van Nieuwland-Bollen, E.; Bogaers-Hofman, D.; Baere, G. A. J.; Kluytmans, J. A., "Nasal carriage of Staphylococcus aureus is a major risk factor for surgical-site infections in orthopedic surgery." *Infect. Cont. Hosp. Ep.* **2000**, *21*, 319-323.

3. Cai, W.; Wu, J.; Xi, C.; Meyerhoff, M. E., "Diazeniumdiolate-doped poly(lactic-*co*-glycolic acid)-based nitric oxide releasing films as antibiofilm coatings." *Biomaterials* **2012**, *33*, 7933-7944.

4. Koh, A.; Carpenter, A. W.; Slomberg, D. L.; Schoenfisch, M. H., "Nitric oxide-releasing silica nanoparticle-doped polyurethane electrospun fibers." *ACS. Appl. Mater. Interfaces DOI: 10.1021/am402044s [Available online August 5, 2013]*.

5. Nichols, S. P.; Koh, A.; Storm, W. L.; Shin, J. H.; Schoenfisch, M. H., "Biocompatible materials for continuous glucose monitoring devices." *Chem. Rev.* **2013**, *113*, 2528-49.

6. Hetrick, E. M.; Schoenfisch, M. H., "Reducing implant-related infections: Active release strategies." *Chem. Soc. Rev.* **2006**, *35*, 780-9.

7. Ip, M.; Lui, S. L.; Poon, V. K.; Lung, I.; Burd, A., "Antimicrobial activities of silver dressings: an in vitro comparison." *J. Med. Microbiol.* **2006**, *55*, 59-63.

8. Melaiye, A.; Youngs, W. J., "Silver and its application as an antimicrobial agent." *Expert Opin. Ther. Pat.* **2005**, *15*, 125-130.

9. Poon, V. K.; Burd, A., "In vitro cytotoxity of silver: implication for clinical wound care." *Burns* **2004**, *30*, 140-147.

10. Trop, M.; Novak, M.; Rodl, S.; Hellbom, B.; Kroell, W.; Goessler, W., "Silver-coated dressing acticoat caused raised liver enzymes and argyria-like symptoms in burn patient." *J. Traum. Accute Care Surg.* **2006**, *60*, 648-652.

11. Schäffer, M. R.; Tantry, U.; Gross, S. S.; Wasserkrug, H. L.; Barbul, A., "Nitric oxide regulates wound healing." *J. Surg. Res.* **1996**, *63*, 237-240.

12. Masters, K. S. B.; Leibovich, S. J.; Belem, P.; West, J. L.; Poole-Warren, L. A., "Effects of nitric oxide releasing poly(vinyl alcohol) hydrogel dressings on dermal wound healing in diabetic mice." *Wound. Repair. Regen.* **2002**, *10*, 286-294.

13. Han, G.; Nguyen, L. N.; Macherla, C.; Chi, Y.; Friedman, J. M.; Nosanchuk, J. D.; Martinez, L. R., "Nitric oxide-releasing nanoparticles accelerate wound healing by promoting fibroblast migration and collagen deposition." *Am. J. Pathol.* **2012**, *180*, 1465-1473.

14. Luo, J.-D.; Wang, Y.-Y.; Fu, W.-L.; Wu, J.; Chen, A. F., "Gene therapy of endothelial nitric oxide synthase and manganese superoxide dismutase restores delayed wound healing in type 1 diabetic mice." *Circulation* **2004**, *110*, 2484-2493.

15. Zhu, H.; Ka, B.; Murad, F., "Nitric oxide accelerates the recovery from burn wounds." *World J. Surg.* **2007**, *31*, 624-631.

16. Khil, M.-S.; Cha, D.-I.; Kim, H.-Y.; Kim, I.-S.; Bhattarai, N., "Electrospun nanofibrous polyurethane membrane as wound dressing." *J. Biomed. Mat. Res. B* **2003**, *67*, 675-679.

17. Zahedi, P.; Rezaeian, I.; Ranaei-Siadat, S.-O.; Jafari, S.-H.; Supaphol, P., "A review on wound dressings with an emphasis on electrospun nanofibrous polymeric bandages." *Polym. Advan. Technol.* **2009**, *21*, 77-95.

18. Balogh, L.; Swanson, D. R.; Tomalia, D. A.; Hagnauer, G. L.; McManus, A. T., "Dendrimer-silver complexes and nanocomposites as antimicrobial agents." *Nano Lett.* **2001**, *1*, 18-21.

19. Stickler, D. J., "Biomaterials to prevent nosocomial infections: Is silver the gold standard?" *Curr. Opin Infect. Dis.* **2000**, *13*, 389-393.

20. Murata, H.; Koepsel, R. R.; Matyjaszewski, K.; Russell, A. J., "Permanent, non-leaching antibacterial surfaces: How high density cationic surfaces kill bacterial cells." *Biomaterials* **2007**, *28*, 4870-4879.

21. Denyer, S. P., "Mechanisms of action of antibacterial biocides." *Int. Biodeter. Biodegr.* **1995**, *36*, 227-245.

22. Mukherjee, K.; Rivera, J. J.; Klibanov, A. M., "Practical aspects of hydrophobic polycationic bactericidal "paints"." *Appl. Biochem. Biotech.* **2008**, *151*, 61-70.

23. Carpenter, A. W.; Worley, B. V.; Slomberg, D. L.; Schoenfisch, M. H., "Dual action antimicrobials: Nitric oxide release from quaternary ammonium-functionalized silica nanoparticles." *Biomacromolecules* **2012**, *13*, 3334-3342.

24. Kourai, H.; Horie, T.; Takeichi, K.; Shibasaki, I., "The antimicrobial characteristics of quaternary ammonium salts and their alkyl chain length." *J. Antibact. Antifung. Agents* **1980**, *8*, 9-17.

25. Gilbert, P.; Al-taae, A., "Antimicrobial activity of some alkyltrimethylammonium bromides." *Lett. Appl. Microbiol.* **1985**, *1*, 101-104.

26. Chen, C. Z.; Beck-Tan, N. C.; Dhurjati, P.; van Dyk, T. K.; LaRossa, R. A.; Cooper, S. L., "Quaternary ammonium functionalized poly(propylene imine) dendrimers as effective antimicrobials: structure-activity studies." *Biomacromolecules* **2000**, *1*, 473-480.

27. Oosterhof, J. J. H.; Buijssen, K. J. D. A.; Busscher, H. J.; Van Der Laan, B. F. A. M.; Van Der Mei, H. C., "Effects of quaternary ammonium silane coatings on mixed fungal and bacterial biofilms on tracheoesophageal shunt prostheses." *Appl. Environ. Microb.* **2006**, *72*, 3673-3677.

28. Shin, J. H.; Privett, B. J.; Kita, J. M.; Wightman, R. M.; Schoenfisch, M. H., "Fluorinated xerogel-derived microelectrodes for amperometric nitric oxide sensing." *Anal. Chem.* **2008**, *80*, 6850-6859.

29. Tiller, J. C.; Lee, S. B.; Lewis, K.; Klibanov, A. M., "Polymer surfaces derivatized with poly(vinyl-N-hexylpyridinium) kill airborne and waterborne bacteria." *Biotechnol. Bioeng.* **2002**, *79*, 465-71.

30. Yohe, S. T.; Kopechek, J. a.; Porter, T. M.; Colson, Y. L.; Grinstaff, M. W., "Triggered drug release from superhydrophobic meshes using high-intensity focused ultrasound." *Adv. Healthc. Mater.* **2013**, 1-5.

31. Hope, P.; Kristinsson, K. G.; Norman, P.; Elson, R., "Deep infection of cemented total hip arthroplasties caused by coagulase-negative staphylococci." *J. Bone Joint Surg. Br.* **1989**, *71*, 851-855.

32. Barraud, N.; Hassett, D. J.; Hwang, S.-H.; Rice, S. A.; Kjelleberg, S.; Webb, J. S., "Involvement of nitric oxide in biofilm dispersal of Pseudomonas aeruginosa." *J. Bacteriol.* **2006**, *188*, 7344-7353.

33. Gravesen, S.; Nielsen, P. A.; Iversen, R.; Nielsen, K. F., "Microfungal contamination of damp buildings--examples of risk constructions and risk materials." *Environ. Health. Persp.* **1999**, *107*, 505-508.

34. Meis, J. F., "Moulds and man." *J. Antimicrob. Chemoth.* **2009**, *63*, i21-i22.

35. Small, B. M., "Creating mold-free buildings: A key to avoiding health effects of indoor molds." *Arch. Environ. Health* **2003**, *58*, 523-527.

36. Perloth, J.; Choi, B.; Spellberg, B., "Nosocomial fungal infections: epidemiology, diagnosis, and treatment." *Med. Mycol.* **2007**, *45*, 321-346.

37. Husain, S.; Alexander, B. D.; Munoz, P.; Avery, R. K.; Houston, S.; Pruett, T.; Jacobs, R.; Dominguez, E. A.; Tollemar, J. G.; Baumgarten, K.; Yu, C. M.; Wagener, M. M.; Linden, P.; Kusne, S.; Singh, N., "Opportunistic mycelial fungal infections in organ transplant recipients: emerging importance of non-Aspergillus mycelial fungi." *Clin. Infect. Dis.* **2003**, *37*, 221-229.

38. Hardin, B. D.; Kelman, B. J.; Saxon, A., "Adverse human health effects associated with molds in the indoor environment." *J. Occup. Environ. Med.* **2003**, *45*, 470-478.

39. Loo, V.G.; Bertrand, C.; Dixon, C.; Vityé, D.; DeSalis, B.; McLean, A.; Brox, A.; Robson, H. G., "Control of construction-associated nosocomial aspergillosis in an antiquated hematology unit." *Infect. Cont. Hosp. Ep.* **1996**, 360-364.

40. Ravikumar, T.; Murata, H.; Koepsel, R. R.; Russell, A. J., "Surface-active antifungal polyquaternary amine." *Biomacromolecules* **2006**, *7*, 2762-2769.

41. Pitt, J.; Christian, J., "Water relations of xerophilic fungi isolated from prunes." *Appl. Microbiol.* **1968**, *16*, 1853-1858.

42. Kang, C. K.; Woodburn, M.; Pagenkopf, A.; Cheney, R., "Growth, sporulation, and germination of Clostridium perfringens in media of controlled water activity." *Appl. Microbiol.* **1969**, *18*, 798-805.

43. Magan, N.; Lacey, J., "Effect of temperature and pH on water relations of field and storage fungi." *T. Brit. Mycol. Soc.* **1984**, *82*, 71-81.

44. Fürstner, R.; Barthlott, W.; Neinhuis, C.; Walzel, P., "Wetting and self-cleaning properties of artificial superhydrophobic surfaces." *Langmuir* **2005**, *21*, 956-961.

45. Adan, O. C. G.; Samson, R. A., Fundamentals of mold growth in indoor environments and strategies for healthy living. In *The fungal resistance of interior finishing materials*, Wageningen Academic Publishers: 2011; pp 335-352.

46. Vinnere Pettersson, O.; Leong, S.-l. L., Fungal xerophiles (osmophiles). In *eLS*, John Wiley & Sons, Ltd: 2001.